

**People's Democratic Republic of Algeria**  
**Ministry of Higher Education and Scientific Research**  
**University M'Hamed BOUGARA – Boumerdes**



**Institute of Electrical and Electronic Engineering**  
**Department of Electronics**

Thesis Presented in Partial Fulfilment of the Requirements of the Degree of

**Doctorate**

**In Electrical and Electronic Engineering**

Entitled

**FPGA-Based Intelligent Dual-Axis  
Solar Tracking Control System**

By

***BENZEKRI Azzouz***

**Before the examining board composed of**

<b><i>AKSAS Rabia</i></b>	<b>Professor, ENP</b>	<b>President</b>
<b><i>AZRAR Arab</i></b>	<b>Professor, UMBB</b>	<b>Supervisor</b>
<b><i>LARBES Chérif</i></b>	<b>Professor, ENP</b>	<b>Examiner</b>
<b><i>DAHIMENE Abdelhakim</i></b>	<b>MCA, UMBB</b>	<b>Examiner</b>

---

---

## **Acknowledgments**

---

---

I express my sincere gratitude to my supervisor **Professor Arab AZRAR** for allowing me to conduct this research under his auspices despite his busy agenda. I am especially grateful for his confidence, the freedom he gave me to do this work, his assistance, support and encouragements throughout the course of this work.

I am deeply grateful to **Professor Rabia. AKSAS** for agreeing to chair the jury. My warmest thanks go to **Professor Cherif. LARBES** and **Dr Abdelhakim DAHIMENE** for accepting to participate in the defense of this thesis.

I am grateful to **Amira** for her support and kindness.

---

---

## Abstract

---

---

*This thesis describes the design process of an FPGA-based sensor-driven intelligent controller applied to a dual-axis sun tracking system. Fuzzy control based on fuzzy logic theory is used as a solution for the FPGA implementation of a digital controller for this industrial application. The real-time controller determines when and how much to tune the driving motors to minimize the misalignment of the solar panel surface with the sun's incident rays during the day in order to harvest maximum power from the solar panel mounted on a tracker.*

*To achieve such a digital controller, we developed an FPGA-based heterogeneous computing platform with the capability of partitioning the overall controller between two concurrent subsystems: (1) a hardware subsystem made up of a pair of fuzzy-like PD-type controllers implemented on the programmable fabric of the FPGA using the (Very-High Speed Integrated Circuit) Hardware Description Language (VHDL), and (2) a software subsystem, a soft processor Nios® II-based supervisory control system implemented using the system-on-a-programmable (SoPC) approach. This hardware/software codesign implemented in a single chip makes the connections between the two subsystems work with low power and low latency resulting in an optimal efficiency and performance.*

*An experimental structure is constructed in the laboratory. The controller allows this structure to perform an approximate three-dimensional hemispheroidal rotation to track the sun's movement during the day to improve the overall efficiency of the solar panel.*

*Integrating the whole digital controller in a single chip accelerates development time while maintaining design flexibility. Moreover, it reduces the circuit board costs with a single-chip solution, and simplifies product testing. Compared with traditional design approach using programmed logic (microprocessor- microcontroller- and DSP-based systems), the proposed solution uses a single low-cost FPGA device while enabling higher degrees of flexibility and concurrency.*

*The digital controller developed with Altera Quartus II 9.1 sp2 Web Edition software development suite tools is simulated and realized on a Cyclone-II EP2C35F672C6 FPGA platform to verify its feasibility and functionality.*

**Keywords:** *FPGA; SoPC; Fuzzy logic module; Nios® II; Sun tracker.*

## ملخص المنشورة

تصف هذه المنشورة تصميم منهج على أساس استعمال المنطقة القابلة للبرمجة في الميدان (FPGA) لقيادة ذكية لكشاف في نظام ملاحقة ذو قطبين للشمس. إن المراقب الآني يحدد الوقت و بكم يضبط محرك القيادة لتقليص انحراف اللوح الضوئي مع الأشعة الشمسية الواردة للاستخلاص الأعظم للطاقة. لانجاز مثل هذا المراقب الرقمي، صممنا نظام غير متجانس مرتكز على المنطقة القابلة للبرمجة في الميدان (FPGA) مبني على نظامين فرعيين: (1) مشتق متناسب متحكم ضبابي أنجز على عناصر المنطقة القابلة للبرمجة في الميدان (FPGA) باستعمال لغة VHDL، (2) جمع البيانات باستعمال معالج «Nios® II» بتطبيق طريقة (SoPC). لقد استعمل نظام التطوير (Quartus II) من إنتاج شركة (Altera) لتحقيق هذه المراقبة، إن إدماج هذا المراقب في جهاز واحد يقلص عدد الوحدات، التكلفة و مدة التطوير، مع تحسين الموثوقية. المراقب يحاكي و ينجز على بطاقة المنطقة القابلة للبرمجة في الميدان (FPGA) من نوع ((Cyclone II EP2C35) للتأكد من صحة و إمكانية تشغيله.

**كلمات مفتاح:** FPGA، SoPC، متحكم ضبابي، Nios® II، ملاحق الشمس

---

---

## Résumé

---

---

*Cette thèse décrit le processus de conception d'un contrôleur intelligent à base de FPGA appliqué à un système de poursuite du soleil à double axe. Le contrôleur à base de logique floue détermine en temps réel quand et de combien faudrait-il ajuster les moteurs d'entraînement pour minimiser le désalignement de la surface du panneau solaire avec les rayons du soleil pendant la journée afin de récolter le maximum de puissance du panneau solaire monté sur un suiveur.*

*Pour atteindre un tel objectif de commande numérique, nous avons développé une plate-forme informatique hétérogène à base de FPGA avec la possibilité de cloisonner le contrôleur global entre deux sous-systèmes simultanés: (1) un sous-système de matériel informatique constitué d'une paire de logique floue comme régulateurs de type PD mis en œuvre sur FPGA en utilisant le langage VHDL, et (2) un système de contrôle de surveillance à base II processeur Nios® mis en œuvre en utilisant l'approche SoPC. Cette conception matériel / logiciel mise en œuvre dans une seule puce rend les connexions entre les deux sous-systèmes fonctionnent avec une faible puissance et de faible latence résultant en une efficacité et des performances optimales.*

*L'intégration du contrôleur numérique en une seule puce accélère le temps de développement tout en maintenant la flexibilité de conception. En outre, il réduit les coûts avec une solution mono-puce, et simplifie les tests de produits. Par rapport à l'approche traditionnelle de conception utilisant la logique programmée (microprocesseur et microcontrôleur et de DSP), la solution proposée utilise un dispositif de FPGA à faible coût unique tout en permettant des degrés de flexibilité et de concurrence plus élevés.*

*Le contrôleur numérique développé avec le logiciel de développement d'Altera le Quartus II Edition 9.1 sp2 est simulé et réalisé sur une plate-forme Cyclone II FPGA EP2C35F672C6 pour vérifier sa faisabilité et sa fonctionnalité.*

**Mots Clés:** *FPGA; SoPC; Logique Floue; Nios® II; Suiveur.*

---

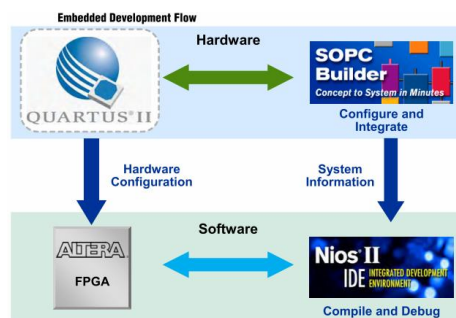
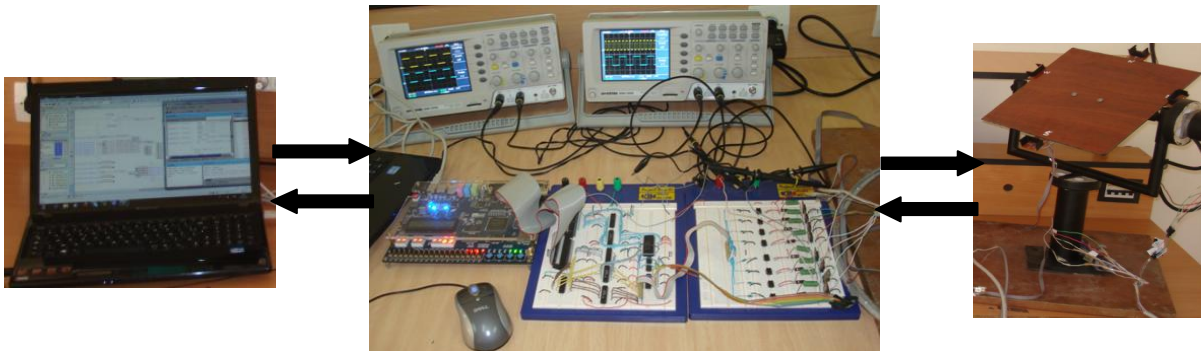
---

## Graphical Abstract

---

---

- ◆ A brand new methodology to implement intelligent embedded systems using SoPC approach
- ◆ Both simulation and physical implementation of the digital controller
- ◆ Implementation in the FPGA functions commonly realized by analog discrete components.
- ◆ Partitioning the digital controller between SoPC and non-SoPC simplifies design complexity while increasing design flexibility and reusability.
- ◆ The FLC module designed and implemented in VHDL is seamlessly integrated in the overall system using SoPC approach
- ◆ The target device on the DE2 board is the Altera EP2C35F672C6 FPGA of Cyclone II family



---

---

## **Table of Contents**

---

---

Acknowledgement.....i

Abstract.....ii

Graphical Abstract.....v

Table of Contents.....vi

List of Figures.....xi

List of Tables.....xiv

List of Abbreviations.....xiv

### **Chapter 1 Introduction**

---

**1 Introduction.....1**

**2 Renewable Energies.....2**

    2.1 Hydro source of Energy.....2

    2.2 Wind Source of Energy.....3

    2.3 Biomass Source of Energy.....3

    2.4 Geothermal Source of Energy.....3

    2.5 Solar Energy.....3

**3 Sun Tracker Types .....5**

**4 Sun Tracker Driving Modes.....6**

**5 Computing Platforms.....7**

    5.1 ASIC Solution.....7

    5.2 Software-Programmed Logic.....8

    5.3 Reconfigurable Logic or Programmable Hardware.....8



---

5.4	Implementation of Fuzzy Controllers.....	9
<b>6</b>	<b>Structure of the Sun Tracking System.....</b>	<b>10</b>
<b>7</b>	<b>Objectives of the Thesis.....</b>	<b>11</b>
<b>8</b>	<b>Organization of the Thesis.....</b>	<b>13</b>

**Chapter 2      Literature Review**

---

<b>1</b>	<b>Introduction.....</b>	<b>14</b>
<b>2</b>	<b>Open Loop Tracking Strategies.....</b>	<b>15</b>
<b>3</b>	<b>Closed Loop Tracking Strategies.....</b>	<b>18</b>
<b>4</b>	<b>FPGA Based Tracking Strategies.....</b>	<b>21</b>
<b>5</b>	<b>Fuzzy Control Tracking Strategies.....</b>	<b>24</b>

**Chapter 3      Fuzzy Logic**

---

<b>1</b>	<b>Introduction.....</b>	<b>26</b>
<b>2</b>	<b>Fuzzy Sets.....</b>	<b>27</b>
2.1	Operations with Fuzzy Sets.....	28
2.2	Properties of Fuzzy Sets.....	30
<b>3</b>	<b>Membership Functions.....</b>	<b>32</b>
3.1	Piecewise Linear Membership Function.....	33
3.1.1	Triangular Membership Function.....	33
3.1.2	Trapezoidal Membership Function.....	33
3.2	Features of the Membership Function.....	34
3.2.1	Core.....	34
3.2.2	Support.....	34
3.2.3	Boundary.....	34
3.2.4	Height.....	34
3.3	Structure of Membership Functions.....	35

---

3.4	Number and Degree of Overlapping of Membership Functions.....	36
3.5	Linguistic Variables and Values.....	36
<b>4</b>	<b>Fuzzy IF-THEN Rules.....</b>	<b>37</b>
<b>5</b>	<b>Properties of Fuzzy Rules.....</b>	<b>38</b>
5.1	Completeness.....	39
5.2	Consistency.....	39
5.3	Continuity.....	40
<b>6</b>	<b>Fuzzy Logic Controller.....</b>	<b>40</b>
6.1	Fuzzification Interface.....	41
6.2	Fuzzy Knowledge Base.....	41
6.3	Fuzzy Inference Mechanism.....	42
6.3.1	Fuzzy Implication.....	42
6.3.2	Aggregation of Fuzzy Conclusions.....	43
6.4	Defuzzification Interface.....	45
6.4.1	Maxima Methods.....	46
6.4.1.1	First of Maxima (FOM).....	46
6.4.1.2	Last of Maxima (LOM).....	47
6.4.1.3	Middle of Maxima (MOM).....	47
6.4.2	Distribution Methods.....	47
6.4.2.1	Max-Membership Method.....	48
6.4.2.2	Weighted Average Method.....	48
6.4.2.3	Center of Gravity (COG).....	49
6.4.2.4	Center of Gravity for Singleton (COGS).....	49

---

**Chapter 4**      **FPGA Technology**

---

<b>1</b>	<b>Introduction.....</b>	<b>51</b>
<b>2</b>	<b>History and Evolution of Programmable Logic devices.....</b>	<b>52</b>
<b>3</b>	<b>Architecture of FPGAs.....</b>	<b>54</b>
3.1	Logic Element.....	55
3.2	Logic Array Block.....	55

---

3.3	Adaptive Logic Module.....	56
3.4	Integrated Functional Blocks.....	57
3.4.1	Embedded RAM Blocks.....	57
3.4.2	Embedded Multiplier Blocks.....	58
3.4.3	Gigabit Transceivers.....	60
3.4.4	Embedded Processor Cores.....	60
<b>4</b>	<b>FPGA Programming Technologies.....</b>	<b>61</b>
4.1	SRAM-Based FPGA.....	61
4.2	Antifuse-Based FPGA.....	61
4.3	Flash-Based FPGA.....	61
<b>5</b>	<b>Applications of FPGAs.....</b>	<b>62</b>
<b>6</b>	<b>The Nios® II and SoPC Builder.....</b>	<b>62</b>
6.1	The Nios® II Processor.....	62
6.2	The SoPC Builder.....	65

---

**Chapter 5      Design of the Fuzzy Logic Module**

---

<b>1</b>	<b>Introduction.....</b>	<b>68</b>
<b>2</b>	<b>Structure of the Fuzzy Logic Module.....</b>	<b>69</b>
<b>3</b>	<b>Fuzzy Logic Controller Design Flow.....</b>	<b>69</b>
<b>4</b>	<b>The Azimuth Fuzzy Logic Controller.....</b>	<b>71</b>
4.1	Input/Output Membership Functions.....	72
4.2	Construction of Rule Base.....	74
<b>5</b>	<b>The Elevation Fuzzy Logic Controller.....</b>	<b>77</b>

---

**Chapter 6      Hardware/Software Codesign Implementation**

---

<b>1</b>	<b>Introduction.....</b>	<b>79</b>
<b>2</b>	<b>FPGA Hardware Design Flow (SoPC Approach).....</b>	<b>80</b>
<b>3</b>	<b>Implementation of the Intelligent Sun Tracking Controller.....</b>	<b>82</b>

---

3.1	Off-Chip Hardware Module.....	83
3.1.1	Sun Finder Unit.....	83
3.1.2	Data Acquisition Unit.....	85
3.1.3	Bidirectional Voltage Level Translation Unit.....	88
3.1.4	Motors Driving Unit.....	88
3.2	On-Chip Hardware Module.....	91
3.2.1	On-Chip non-SoPC Builder Subsystem.....	91
3.2.1.1	The clock divider module.....	91
3.2.1.2	Implementation of the Fuzzy Logic Module.....	92
3.2.1.3	Stepper Motor Sequence Generator.....	93
3.2.2	On-chip SoPC Builder Subsystem.....	95
3.2.3	Building the Embedded System in the SoPC Builder.....	96
3.2.4	Integrating the SoPC and non-SoPC Builder.....	
	Subsystems in Quartus II Project.....	99
3.2.5	Firmware Development.....	101
<b>4</b>	<b>Real-Time Experiment.....</b>	<b>102</b>
4.1	Operational Cycle Time.....	103
4.2	Simulation.....	104
<b>Chapter 7</b>	<b><u>Conclusions</u>.....</b>	<b>106</b>
	<b><u>References</u>.....</b>	<b>109</b>

---

---

## List of Figures

---

---

<b>Figure-1.1</b>	(left) A dam to energize a hydroelectric power station. (right) Airflows..... used to run wind turbines.....	2
<b>Figure-1.2</b>	Wood chip bio fuel a renewable alternative source of energy.....	3
<b>Figure-1.3</b>	(a) Multi-crystalline-based solar panel. (b) Single crystal-based solar panel. (c) Amorphous-based solar panel.....	4
<b>Figure 1.4</b>	Structure of a dual-axis sun tracker.....	6
<b>Figure-1.5</b>	High-level representation of the FPGA-based intelligent dual-axis sun tracking system.....	10
<b>Figure-1.6</b>	Pictorial representation of the FPGA-based intelligent dual-axis sun..... Tracking system.....	12
<b>Figure-3.1</b>	Membership function for crisp and fuzzy sets.....	27
<b>Figure-3.2</b>	Graphical representation of complement, union and intersection ..... of fuzzy operations.....	29
<b>Figure-3.3</b>	Graphical representation of fuzzy union and intersection.....	30
<b>Figure-3.4</b>	Fuzzy membership function for speed.....	32
<b>Figure-3.5</b>	Asymmetric triangular and trapezoidal membership functions.....	33
<b>Figure-3.6</b>	Features of a membership function.....	34
<b>Figure-3.7</b>	Graphical representation of a fuzzy variable with 5 fuzzy sets.....	35
<b>Figure-3.8</b>	Structure of a generic Mamdani type Fuzzy Logic Controller.....	41
<b>Figure-3.9</b>	Graphical representation of Max-Min and Max-Prod inference.....	

	methods with crisp inputs with two inputs and two rules.....	44
<b>Figure-3.10</b>	Example of defuzzification for two-rule fuzzy inference.....	45
<b>Figure-3.11</b>	First, Last and Middle of maxima defuzzification methods.....	47
<b>Figure-3.12</b>	Max-membership defuzzification method.....	48
<b>Figure-3.13</b>	Weighted average defuzzification method.....	48
<b>Figure-4.1</b>	Generic structure of a CPLD.....	53
<b>Figure-4.2</b>	Generic structure of an early FPGA.....	54
<b>Figure-4.3</b>	Block diagram of the Altera logic element.....	55
<b>Figure-4.4</b>	Block diagram of a Cyclone II LAB [78].....	56
<b>Figure-4.5</b>	High-level block diagram of the Altera Stratix-V ALM [79].....	57
<b>Figure-4.6</b>	An M4K RAM embedded memory block in a Cyclone FPGA [78].....	58
<b>Figure-4.7</b>	Architecture of an embedded multiplier block in a Cyclone FPGA [78].....	59
<b>Figure-4.8</b>	Architecture of an embedded multiplier block in a Cyclone FPGA [78].....	59
<b>Figure-4.9</b>	The 3 flavors of the Nios® II soft core processor [79].....	63
<b>Figure-4.10</b>	Screenshot of a SoPC Builder system.....	66
<b>Figure-4.11</b>	System interconnect fabric with multiple mastering components [85].....	67
<b>Figure 5.1</b>	Operational block diagram of the intelligent dual-axis sun tracking ..... fuzzy logic module.....	69
<b>Figure-5.2</b>	Sun tracking fuzzy logic module with errors and rate of change of error..... Generator.....	70
<b>Figure-5.3</b>	Incident angle of sunrays with solar panel surface.....	71
<b>Figure-5.4</b>	(a) MFs of the angular error $E_{EW}$ in degrees. (b) MFs of $cE_{EW}$ ..... in degrees/sec (c) Singleton membership functions of the output..... variable 'U' in number of steps.....	73
<b>Figure-5.5</b>	(a) MFs of the angular error $E_{NS}$ in degrees. (b) MFs of $cE_{NS}$ ..... in degrees/sec (c) Singleton membership functions of the output .....	

	variable 'U' in number of steps.....	78
<b>Figure-6.1</b>	A Typical microprocessor-based system, (left) traditional method..... (right) SoPC approach.....	80
<b>Figure-6.2</b>	FPGA-Based Hardware/Software Design Flow using SoPC Approach.....	81
<b>Figure-6.3</b>	The overall fuzzy control based dual-axis sun tracking system ..... block diagram implemented in the Cyclone II FPGA.....	83
<b>Figure-6.4</b>	The Off-Chip hardware functional block diagram.....	84
<b>Figure-6.5</b>	Circuit diagram of the sensing and data acquisition unit.....	86
<b>Figure-6.6</b>	Flow chart for the data acquisition subroutine.....	87
<b>Figure-6.7</b>	The motor driver power stage unit to energize the two actuators .....	89
<b>Figure-6.7b</b>	One branch (out of 8) of the driver power stage unit.....	90
<b>Figure-6.8</b>	The On-Chip hardware module .....	91
<b>Figure-6.9</b>	VHDL code of the clock divider custom hardware module.....	92
<b>Figure-6.10</b>	Detailed view of the FL module in Quartus II and the RTL Viewer... ..	93
<b>Figure-6.11</b>	Unipolar stepper motor windings and full-step sequence.....	94
<b>Figure-6.12</b>	VHDL code for a stepper motor full-step sequence generator.....	94
<b>Figure-6.13</b>	SoPC-based intelligent sun tracking controller optimized in an FPGA.....	97
<b>Figure-6.14</b>	Top-Level schematic for the FPGA-Based FLC design process for a..... dual-axis sun tracking system .....	100
<b>Figure-6.15</b>	PC running Quartus II and Altera Monitor Program software.....	101
<b>Figure-6.16</b>	Hardware setup of the FPGA Based intelligent dual-axis..... sun tracking systems.....	102
<b>Figure-6.17</b>	The operational cycle time .....	104
<b>Figure-6.18</b>	Behavioral simulation window in the Quartus II simulator.....	105

---

---

## List of Tables

---

---

<b>Table 3.1</b>	The NxM set of fuzzy if-then rules in matrix form.....	39
<b>Table-5.1</b>	The 7x7 fuzzy rule-base matrix used in the fuzzy-like PD-type.....	
	FLC for the vertical pivot shaft (east-West).....	74
<b>Table-5.2</b>	The 5x5 fuzzy rule-base matrix used in the fuzzy-like PD-type .....	
	FLC for the horizontal pivot shaft (North-South).....	78



---

---

## List of Abbreviations

---

ADC	Analog to Digital Converter
ALE	Address Latch Enable
ALM	Adaptive Logic Module
AMP	Altera Monitor Program
ARM	<b>A</b> dvanced <b>R</b> ISC (Reduced Instruction Set Computer) <b>M</b> achine
ASIC	Application Specific Integrated Circuit
ASSP	Application Specific Standard Product
CLB	Configurable Logic Block
CMOS	Complementary Metal Oxide Semiconductor
COG	Center of Gravity
COGS	Center of Gravity for Singleton
CPLD	Complex Programmable Logic Device
DCT	Discrete Cosine Transform
DMIPS	Dhrystone Million Instructions Per Second
DOM	Degree of Membership
DSC	Digital Signal Controller
DSP	Digital Signal Processor
EOC	End of Conversion
EEPROM	Electrically Erasable Programmable Read Only Memory
EPROM	Erasable Programmable Read Only Memory
FFT	Fast Fourier Transform
FIFO	First IN First OUT
FIR	Finite Impulse Response
FLC	Fuzzy Logic Controller
FOM	First Of Maximum
FPD	Field Programmable Device
FPGA	Field Programmable Gate Array
GPIO	General Purpose Input/Output
GUI	Graphical User Interface
HDL	Hardware Description Language
HPS	Hard Processor System
IBM	International Business Machine
IC	Integrated Circuit
IOB	Input Output Block
IOE	Input Output Element
IP	Intellectual Property
JTAG	Joint Test Action Group
LAB	Logic Array Block
LCD	Liquid Crystal Display

---

LDR	Light Dependent Resistor
LE	Logic Element
LOM	Last of Maxima
LUT	Look Up Table
MCU	Micro Controlling Unit
MF	Membership Function
MIPS-ISA	Microprocessor without Interlocking Pipe Stages – Instruction Set Architecture
MMI	Monolithic Memories Inc
MMU	Memory Management Unit
MOM	Middle of Maxima
MSI	Medium Scale Integration
NIOS	Netware Input-Output Subsystem
OTP	One-Time Programmable
PAL	Programmable Array Logic
PC	Personal Computer
PCB	Printed Circuit Board
PD	Proportional Derivative
PI	Proportional Integral
PIA	Programmable Interconnect Array
PID	Proportional Integral Derivative
PLA	Programmable Logic Array
PLD	Programmable Logic Device
PROM	Programmable Read Only Memory
RAM	Random Access Memory
RISC	Reduced Instruction Set Computer
ROM	Read Only Memory
RTL	Register Transfer Logic
SDRAM	Synchronous Dynamic Random Access Memory
SoC	System on Chip
SoPC	System on Programmable Chip
SPI	Serial Peripheral Interface
SPLD	Simple Programmable Logic Device
SRAM	Static Random Access Memory
SSI	Small Scale Integration
TTL	Transistor Transistor Logic
UART	Universal Asynchronous Receiver Transmitter
USB	Universal Serial Bus
VHDL	(Very High Speed Integrated Circuit) <b>H</b> ardware <b>D</b> escription <b>L</b> anguage

---

---

**Chapter 1**

---

---

**Introduction**

---

---

**1 Introduction**

Since the beginning of the Industrial Revolution, coal, crude oil and natural gas are the three forms of fossil fuels mostly used worldwide. These non-renewable sources of energy are so called because they have been formed from the organic remains of prehistoric plants (plants which grew on earth millions of years ago) and animals and have rotted away over million of years and became solids, liquids and gasses. They will run out one day. Fossil fuels must be located, excavated and transported before they can be used. These carbon-based fuels are employed to feed power plants to produce electrical energy [1]. They must be burned to produce electricity. Burning them creates unwanted by-products such carbon dioxide. These unwanted by-products pollute the environment (air and water pollutions) and contributes to the global warming due to the release of huge amount of greenhouse gasses into the atmosphere. To minimize this major problem, there is a need to replace (at least partially) these fossil fuels with an environment friendly alternative. For a long time, it has been thought that the nuclear-based power plants would be the ideal solution for the increased demand for electrical energy, ever increasing oil price and environmental concern. It is true that nuclear energy has several benefits: absence of airborne pollutants, no greenhouse effect and reduction in dependence on oil. However, the accidents of Three Mile Island (1979), Tchernobyl (1986) and the recent tragedy of Fuckushima (2011) increased anti-nuclear

sentiment. This public awareness pushed several countries to rethink the use of this energy. Germany decided to close all of its reactors by 2022, while Italy and others countries halted expanding their nuclear power plants.

## 2 Renewable Energies

In the 1970s with the energy crisis, the interest in green power was primarily driven by the goal of replacing fossil fuels to reduce the dependence on oil and gas. Nowadays, with climate change, ozone layer depletion, global warming etc, the principle goal is the preservation of the environment by minimizing carbon-dioxide emissions in the atmosphere. There is a wide variety of renewable energies. These energies use resources that are naturally replenished on a human timescale and will exist infinitely. The list of these resources, ordered by the amount of contribution to the production of electricity, currently includes: hydro, wind, biomass, geothermal heat and sunlight. Electricity derived from these energies is considered “green” because of the negligible negative impacts on the environment.

### 2.1 Hydro source of Energy

The contribution from renewable energy sources for electricity production is small with the exception of hydro. Over the last 100 years, hydro has been the most mature renewable source of electricity around the world. **Figure-1.1** (left) depicts a huge energy stored in a dam which can be used to generate hydroelectric power. Today, hydro power contributes to about 21% of electricity capacity worldwide [2].

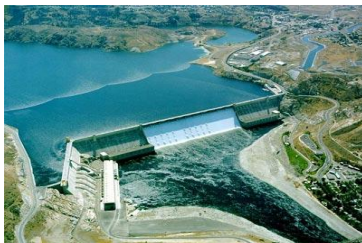


**Figure-1.1.** (left) A dam to energize a hydroelectric power station.  
(right) Airflows used to run wind turbines.

## 2.2 Wind Source of Energy

Wind is the next most popular source of green electricity and the fastest growing renewable energy world-wide. **Figure-1.1(right)** illustrates airflows used to run wind turbines. An average of wind speed of 14 miles/hour ( $\approx 20$  Km/hour) is needed to efficiently convert wind energy into electricity. Today, large new wind farms at excellent wind sites generate electricity at a cost in the range that is competitive with that of electricity from conventional power plants, while offshore areas experience average wind speeds larger than that of land.

## 2.3 Biomass Source of Energy

Wood remains the largest biomass energy source today. Grasses, agricultural crops, or other biological materials can be converted to heat, then steam, and then electricity. Biomass power is the third largest source of renewable electricity. **Figure-1.2** shows biological material derived from living, or recently living organisms used to feed a power plant to produce electricity.

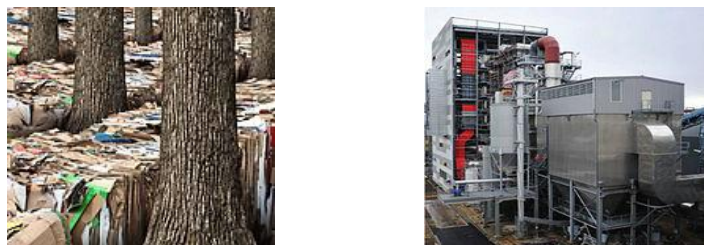


**Figure-1.2** Wood chip bio fuel a renewable alternative source of energy

## 2.4 Geothermal Source of Energy

Heat contained in the core of the earth can be exploited to produce electricity through steam. The geothermal source while this is an abundant source with today's technology only a small fraction can be converted commercially to electricity. Geothermal power plants are highly capital intensive because enough steam-supply wells have to be drilled up-front to provide the full plant capacity at startup.

## 2.5 Solar Energy

Among all renewable energy sources available, solar energy is believed to be the most promising source. It is free, secure, pollution-free, available all over the world, and will last forever [3, 4].

The sun creates its energy through a thermonuclear process that converts about 650,000,000 tons of hydrogen to helium every second [5]. The process creates heat and electromagnetic radiation. The heat remains in the sun and is instrumental in maintaining the thermonuclear reaction. The electromagnetic radiation (including visible light, infra-red light, and ultra-violet radiation) streams out into space in all directions. Only a very small fraction of the total radiation produced reaches the Earth [6]. One of many ways of generating electricity from solar energy is the use of solar panels which convert sunlight into direct electricity (DC) using the photovoltaic effect. Solar panels are formed out of interconnected photovoltaic cells that are arranged in series/parallel fashion.

A Photovoltaic Cell (PV) or solar cell is a semi-conductor device used to convert lights directly into electricity by the photovoltaic effect. The efficiency and the cost of the photovoltaic cells depend greatly on the material chosen. Present PV cells come into three major categories: Multi-crystalline, Single crystal, and Amorphous, **Figure-1.3**.

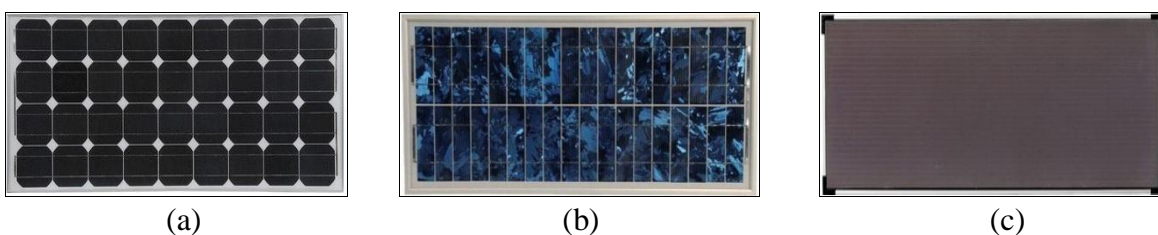


**Figure-1.3** (a) Multi-crystalline-based solar panel. (b) Single crystal-based solar panel. (c) Amorphous-based solar panel

There are several factors that affect the efficiency (percentage of sun's energy striking the PV cell that is converted into electricity) of the solar panel. The two major ones are: (1) the PV cell efficiency and, (2) the intensity of sun rays received on the surface of the solar panel.

Although there is a continuous improvement in the PV materials to enhance PV cell efficiency, current technology delivers PV cells with an efficiency level ranging from 10 to

20% (some laboratories reached efficiencies of more than 30% but not yet available commercially). Therefore, to lower the per KWh cost, we need to rely on the dimensions of the panels and/or the irradiation intensity. Increasing the surface area of the solar panels is not a viable solution. It increases investments cost and requires more ground surface. A more feasible and economical solution however, is to maximize power extraction from the panel by operating the cell arrays at their full potential. This can be achieved by continuously exposing the surface of the panel perpendicular to the sun's rays. This strategy can be accomplished by a sun tracker, a device onto which a solar panel is fitted to track the movement of the sun across the sky (mimicking sunflower).

### **3 Sun Tracker Types**

The efficiency of a photovoltaic panel depends on the incident angle of the sun rays with respect to the surface of the panel. For the solar panel to harvest maximum energy from the sun, a high-precision sun tracking system is necessary to track the sun in the sky from early morning until late in the afternoon. A sun tracking system is a mechatronic system. It consists of the mechanics, electric drives and information technology [7]. The mechanics consists mainly of a tracker onto which a solar panel is fitted to track the movement of the sun by maintaining the panel surface perpendicular to the sun incident radiations (mimicking sunflower). The mechanics provide the necessary torque to change the azimuth and elevation positions of the solar panel with respect to the sun, while the controller determines when and how much to tune the driving motors to minimize the misalignment of the solar panel surface with the sun's incident rays.

Sun trackers are classified according to the number and orientation of their axes. They are grouped into single- and dual-axis tracking devices. Single-axis trackers have one degree of freedom. They are used to vary the azimuth angle in order to follow the movement of the sun East-West during the day with fixed tilt angle. These types of trackers are more suitable in

tropical regions. Dual-axis trackers accommodate two degrees of freedom, azimuth and tilt. Their axles are typically normal to one another. They have the capability to tune the solar panel east-west and north-south and follow the sun's apparent motion anywhere in the sky.

**Figure 1.4** illustrates the structure of a dual-axis sun tracker. Angle  $\alpha$  is an azimuth angle of the solar panel and  $\beta$  is a tilt angle.

Motor 1 changes the azimuth angle along the east-west direction, whereas motor 2 changes the elevation angle along the north-south direction.

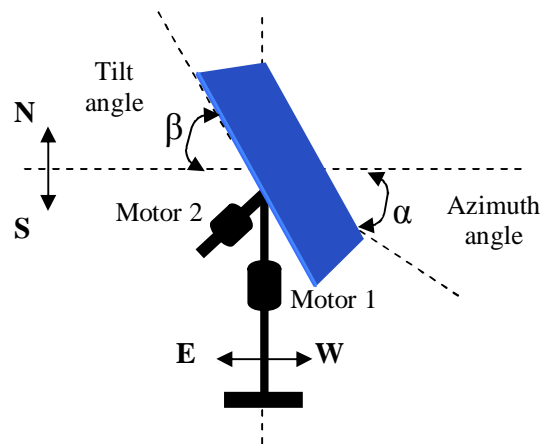


**Figure 1.4** Structure of a dual-axis sun tracker

#### 4 Sun Tracker Driving Modes

There are three methods of tracking: passive, chronological and active. Passive trackers use a low boiling point compressed fluid (often Freon) as a means of tilting the solar panel. When heated by the solar heat, it creates a gas pressure in the system, the fluid pressure increases causing the liquid to move inside the tracker from one side to another allowing gravity to rotate the tracker to follow the sun. These trackers do not use motors or control and hence do not consume any energy. They are also less precise and therefore, operate with low efficiency compared to active trackers. Passive trackers are however, unpractical in cold locations. Chronological trackers employ electronic logic to control the actuators to follow the sun based on mathematical formulae based on astronomical references with the data of a whole one-year sun trajectory to calculate the sun movement in the sky. This data is usually



the current time, day, month and year of a specific geographical location. These trackers are also known as open-loop trackers as they do not require any feedback for the controlled system. Active trackers also known as closed-loop dynamic trackers on the other hand employ motors and gear trains to direct the PV panel as commanded by the controller. They commonly use light detecting sensors to provide raw data as inputs to the controller to track in real-time the real position of the sun in the sky. They are more reliable than open loop trackers. The use of the feedback makes their system response less sensitive to external disturbances [8], [9].

## **5 Computing Platforms**

At the heart of most embedded control systems is usually a real-time digital controlling unit. Nowadays, designers are blessed by the variety of computing platforms they have at their disposal to address these controlling units. These latter can be implemented using one or a combination of design methodologies [10-11]. There are three major methodologies, namely:

- (i) Dedicated (fixed) digital logic or application-specific integrated circuits or ASICs,
- (ii) Software-programmed logic platforms, and
- (iii) Hardware reconfigurable logic platforms.

### **5.1 The ASIC Solution**

There is no doubt, of all solutions; dedicated controllers or ASICs provide highest performance as they are optimally tailored for particular use. They are great at speed and power consumption. Moreover, they have reduced size and cost at high volume. They exhibit high reliability of system operation. ASICs present some disadvantages. They are fixed function integrated circuits, that is, the design is frozen in silicon with no possibility to make any change.

## 5.2 Software-Programmed Logic

For years, digital designers largely relied on general-purpose microprocessors, microcontrollers, personal computers (PCs), digital signal processors (DSPs) and digital signal controllers (DSCs) for the design of digital embedded systems. Despite the large number of commercially available off-the-shelf products, designers of embedded systems are often challenged to find the exact processor and the appropriate peripherals that will fit their needs [12]. Often, designers must make compromises between performance, chip count, flexibility, cost and power consumption in their choices.

Although flexible and able to implement complex algorithms, processor-based solution presents some disadvantages. Off-the-shelf processors and peripheral devices have fixed hardware, leaving software as the unique alternative to the designer to develop/enhance his/her desired application. Moreover, the sequential nature of program execution with these processors leads to several orders of magnitude inferior to ASICs in terms of performance, silicon area usage and power consumption [10], [13].

## 5.3 Reconfigurable Logic or Programmable Hardware

In the above modalities, the hardware architecture is settled in the early stage of the design cycle making even minor changes affect dramatically the ASIC design, processor selection and printed-circuit board (PCB) design. An elegant and cost effective solution is obtained when using the reconfigurability of the FPGA. In such computing platform, the system hardware needs no longer to be frozen. The processor and peripheral devices as well as the target FPGA can all be changed during development time, or migrated to new more performant FPGA.

With today's high density FPGAs, the emerging and revolutionary SoPC design methodology provides a new paradigm in the design of embedded systems. This methodology

allows the integration of embedded processor(s) (hard-core and/or soft-core) with or without user defined hardware accelerator blocks tailored to fit the desired application. The heterogeneity of this approach allows the co-existence of the embedded microprocessor with the FPGA logic in the same chip, taking the benefit of both the microprocessor and the ASIC. Partitioning the controller into two main blocks makes the design process easier while achieving better performance by avoiding the processor to get bogged down. The embedded microprocessor will be used to implement non-timing critical functions, while timing critical are best implemented as hardware accelerators in the FPGA fabric. To cope and design efficient complex systems with this new paradigm, Altera for example provides sophisticated and powerful electronic design automation (EDA) tools; Quartus II and the SoPC builder.

#### **5.4 Implementation of Fuzzy Controllers**

Fuzzy systems implementation has been exploited since the mid-1980s and different architectures were devised. Naturally, the realization of these controllers will always be digital because its algorithm is primarily based on rule inference using the “IF-THEN” statements [14]. An efficient and effective implementation should satisfy two main requirements: flexibility and performance. There exist two main branches of fuzzy systems implementations: software and hardware implementations. A third branch can be a combination of the first two.

Early fuzzy systems were mostly implemented in software by means of general-purpose microprocessors, and microcontrollers. These implementations are flexible, require the least hardware resources and can be developed rapidly. However, the sequential nature of execution of these processors may not permit real-time processing.

Fuzzy systems hardware implementations can be realized as a dedicated hardware, as an ASICs or on a reconfigurable FPGAs. Hardware implementations use a certain level of parallelism and pipelining leading to a very high increase in processing speed. Nowadays,

with ceaseless increasing density of FPGAs and the SoPC approach, it is possible to take advantage of both the flexibility of software and the performance of hardware [15].

Several survey and review papers were published to highlight fuzzy systems implementations. In [16], the authors reviewed many interesting fuzzy hardware/software architectures from a categorical and historical point of view. Recently, in [17], Bosque et al surveyed fuzzy systems and neural networks with a particular focus on hardware taxonomy and highlighted the characteristics of the different applications covering the paradigms done over the last two decades.

## 6 Structure of the Sun Tracking System

Figure-1.5 depicts the hardware structure of the FPGA-based intelligent sun tracking system. The proposed architecture consists of several units linked together to form an integrated autonomous programmable system. These units are partitioned into two major modules:

(i) The off-chip or on board module, realized on breadboards, is implemented with off-the-shelf discrete components. It is composed of a panel equipped with a sun finder, used to determine the position of the sun in the sky, mounted on an azimuth-elevation dual-axis tracker, a signal conditioning circuit, a data acquisition unit built around an analog-to-digital converter (ADC), a bidirectional voltage level translator (3.3V-5V) and two unipolar 4-phases

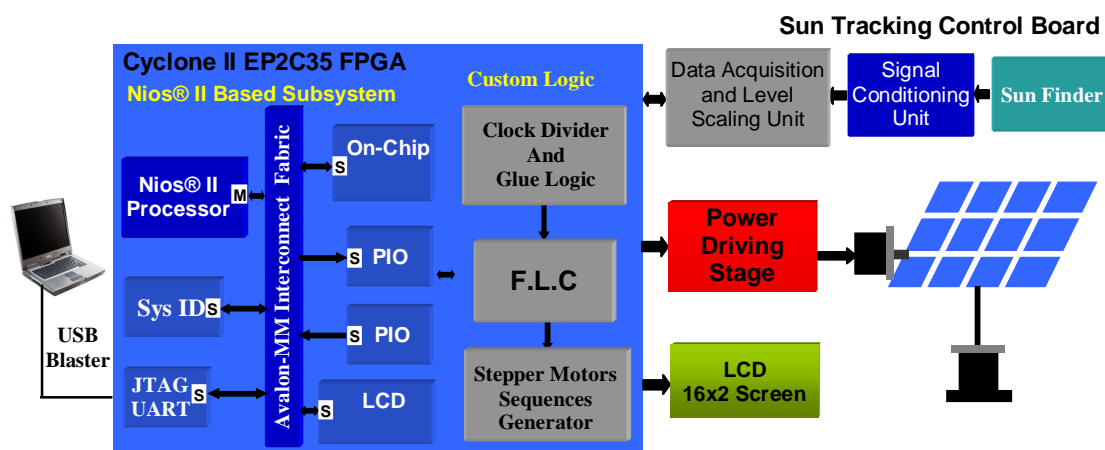


Figure-1.5 High-level representation of the FPGA-based intelligent dual-axis sun tracking system

1.8° per step bidirectional stepper motors with their power driving circuits.

(ii) The on-chip module which is the digital controller is implemented onto the FPGA chip of the low-cost DE2 board. The digital controller consists of two subsystems: a System-on-a-Programmable-Chip or SoPC based subsystem built around the Altera Nios® II embedded soft core processor and a custom non-SoPC subsystem. The SoPC Builder subsystem includes several functional blocks such as the ADC interface, the liquid crystal display or LCD controller, and an interface with the custom logic. It controls and gathers data from the data acquisition unit by scheduling and generating the necessary signals to the analog-to-digital converter, it performs the necessary data processing, monitoring and control of the external actuators. The non-SoPC Builder subsystem consists of several custom hardware components developed in VHDL that operates in conjunction with the processor-based system. The core system of which is the fuzzy-like PD-type FLC and the stepper motors sequence generator.

## 7 Objectives of the Thesis

This thesis addresses the design process of a FPGA-based fuzzy logic controller (FLC) applied to a sensors-driven dual-axis sun tracking system. The digital controller is implemented using the SoPC approach. This methodology combines a soft processor core the Nios® II, on-chip memory, intellectual property (IP) peripheral components and a user defined hardware accelerator components integrated into a single FPGA device, **Figure-1.6**.

The approach combines the features of software programming and reconfigurable hardware implementations into two inter-related modules: (i) a Nios® II embedded processor-based subsystem which constitutes the upper layer of the digital controller and (ii) a PD-like fuzzy logic module to steer the tracker actuators.

The first subsystem provides an ideal platform for microcontroller applications. Its mission is to keep track of the data gathered from the sun finder unit by scheduling and initiating the signals required by the data acquisition unit. It computes the angular errors and

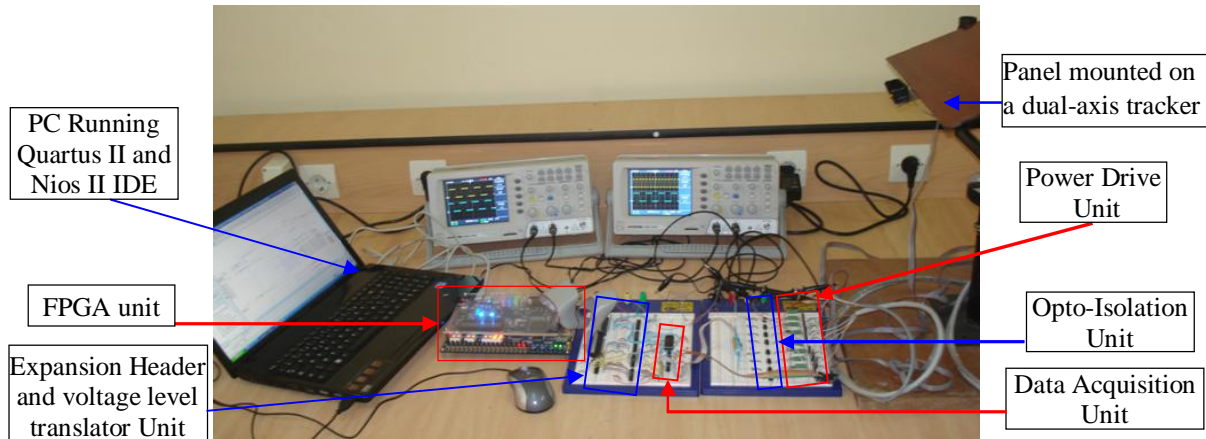


**Figure-1.6.** Pictorial representation of the FPGA-based intelligent Dual-axis sun tracking system

the rates of change of these errors and applies them as crisp inputs to the PD-like fuzzy logic module. In addition, the Nios® II subsystem controls the liquid crystal display (LCD) to display in real-time the system's status messages on a two-line LCD, and manipulates the general-purpose input-output peripherals. The control program that runs on the Nios® II processor is written in assembly language for highest performance and minimal code density.

The second module, the PD-like fuzzy logic module, which demands more computational power, is designed and implemented in the FPGA's massively parallel logic elements using a handcrafted VHDL code as a custom reconfigurable application-specific accelerator component to maximize parallel processing. The fuzzy logic module calculates the necessary energy by which the system modifies the process in such a way the control objective can be obtained.

The approach allows a processor to co-exist with custom logic in the FPGA fabric, provides the flexibility to combine reconfigurable hardware and software based controls to achieve a simple and better control of the sun tracker. This hardware/software solution runs on an Altera low-cost Cyclone II FPGA, the EP2C35, to control the motion of two stepper motors used as the mechanical drive system to keep the solar panel surface continuously facing the sun during the day.

## 8 Organization of the Thesis

This thesis is compiled into 7 chapters including this introduction and followed by references used in this work. Chapter 1 introduced the problematic. It also reviewed existing computing platforms used to implement digital controllers: processor-based and FPGA-based with or without the SoPC technology.

In chapter 2, a literature review that surveys relevant research works on sun tracking systems conducted in the last few decades is presented. Chapter 3 introduces fuzzy set theory and fuzzy logic control. Chapter 4 presents background material to highlight the possibilities and advantages using the FPGA. It also describes the most versatile and industry-standard soft-core processor, the Nios® II as well as the emerging and revolutionary SoPC technology.

Chapters 5 and 6 constitute the bulk of the thesis. The former describes in details the design and implementation of the fuzzy logic module. The latter begin by reviewing the merits of the SoPC approach over the off-the-shelf processor and peripheral devices as platforms for industrial applications. It lays out in detail the hardware and software design. This chapter also presents the simulation and implementation of the FPGA-based intelligent dual-axis sun tracking system. It reports the setup of the simulations and a prototyping real-time implementation of the system which can be seen as a proof-of-concept. Chapter 7 concludes the thesis with some discussions and remarks for future research.

Finally, the thesis terminates with an extensive list of references for additional information on the subject.

Part of the work reported in chapters 1, 5 and 6 has been published in [90].

---

---

**Chapter 2**

---

---

**Literature Review**

---

---

**1 Introduction**

Before diving into the practical of this thesis, a review of literature in the core area will be presented with the aim to provide the reader with a survey on active sun tracking systems using different types of computing platforms and control strategies, as well as developments in FPGA-based designs with or without model-based fuzzy logic control systems. Also, we report by whom, when and how.

Over the past four decades or so, a large number of contributions have been reported in seminars and literature showing the increasing interest in the design and implementation of sun tracking systems to increase their performances and efficiencies to harvest maximum power from the solar panels mounted on trackers. Several control strategies as well as different computing and control platforms have been used and tested to tackle this problem [7], [8], [18-66]. These strategies can be categorized into three main classes: open-loop, closed-loop and hybrid sun tracking control systems.

- (i) Open-loop control strategies rely on a fixed control algorithm [7], [8], [18-29].

These controllers use mathematical formulae with the data of a whole one-year sun trajectory to calculate the sun's movement in the sky and need not sense the sunlight to position the solar panel. This data is usually the current time, day, month and year of a specific geographical location. The algorithms do not use any



feedback from the controlled system to determine if it has achieved or not the desired goal.

- (ii) Closed-loop types of sun tracking systems are based on feedback principles. They usually use light sensors such as light dependent resistors (LDRs) to determine the position of the sun in the sky with respect to the surface of the solar panel [8], [30-37]. They are more reliable than open loop type controllers. The use of the feedback makes their system response less sensitive to external disturbances.
- (iii) Hybrid implementations, a strategy that combines both open- and closed-loop control are also reported in literature [31], [38].

There is a large variety of techniques used to implement closed-loop type controllers. These range from the On-Off control laws to more advanced techniques based on fuzzy logic control including the classical controllers: the Bang-Bang controller, proportional-integral (PI), proportional-derivative (PD) and proportional-integral-derivative (PID).

A myriad of physical implementations of sun tracking strategies are also reported in literature. Similar to other industrial applications, these implementations have gone through several stages of evolutions. They evolved from the early mechanical designs to the use of discrete analog and digital standard integrated circuits. The general-purpose microprocessor-, microcontroller- and DSP-based were the dominant platforms for the implementation and realization of control algorithms based on conventional PID and alike, Bang-Bang and fuzzy controllers. The use of the FPGA with or without the system-on-programmable-chip approach emerged during the last decade.

## 2 Open-Loop Tracking Strategies

An open-loop type controller computes its input into a system using only the current state and the algorithm of the system to determine if its input has achieved the desired goal. These

types of controllers based on mathematical algorithms/programs provide predefined trajectories for the tracking system. These trajectories can be accurately determined because the relative position of the sun can be precisely calculated at any time for any location on the earth [7], [18] [19].

It is in 1975, that McFee [20] presented the first automatic solar tracking system. The algorithm used to control the tracker computes the flux density distribution and the total received power in a solar power system. Since that time, numerous works using open-loop control have been carried out in the design and implementation of algorithms based on astronomical formulae. They were used to drive electromechanical actuators to steer single- and dual-axis sun tracking systems.

Semma et al [21] were among the first to use a microprocessor as a replacement of the hard-wired logic used in earlier sun trackers to control the motion of a two-axis sun tracking system. The controller was based on an active sun tracking approach and allows an array to track the sun within five arc-minutes. This resulted in significant improvements in reliability via parts screening and packaging and increased the functional capabilities of former basic tracking systems.

In [22], the authors derived a general formula arguing that it embraces all the possible one-axis tracking methods. To derive the formula, they used coordinate transformation technique. This consists in transforming the sun's position vector from earth-center frame to earth-surface frame and then to collector-center frame. In doing so, they could resolve it into solar azimuth and altitude angles relative to the solar collector making it simpler to the controller to determine by how much it should tune the solar collector to minimize the misalignment.

In 2004, Abdallah [23] designed and implemented four electromechanical open-loop solar tracking systems: two-axis, one-axis vertical, one-axis east-west, and one-axis north-south in

order to investigate the effects of the current, voltage and power characteristics of a flat-plate photovoltaic system compared to a fixed one with an inclination of  $32^\circ$  to the south. The movement of the tracker was controlled by an algorithm in which the pre-calculated position was programmed into a programmable logic controller (PLC). The author claimed that the tracking systems increased the electrical powers of the collector by 43.87, 37.53, 34.43 and 15.69% respectively for the two-axis, one vertical axis, one-axis east-west and one-axis north-south compared to that of the fixed one.

In paper [24], Grena describes an algorithm for obtaining highly precise values of the solar position. Taking the fractional Universal Time (UT), the date, and the difference between UT and Terrestrial Time (TT) (longitude, latitude, pressure and temperature) as inputs, the algorithm computed the angular position of the earth with respect to the sun in the ecliptic plane and then used this angle and the inclination angle of the earth's rotational axis to calculate the position of the sun.

In reference [25], the authors argued that the open-loop tracking strategies used to compute the direction of the solar vector should be both accurate and computationally straightforward to minimize the price of the tracking system. They developed an algorithm for predicting the solar vector given knowledge of the time and the location.

In 2004, Reda et al [26] presented a simple step-by-step procedure for implementing a solar position algorithm. In this algorithm, the solar zenith, azimuth and incident angles were derived using ecliptic longitude and latitude for mean Equinox of data along with other information. They reported that the solar zenith and azimuth angles could be calculated with uncertainties of  $\pm 0.0003^\circ$ .

In [27] an open-loop control algorithm was developed to control a dual-axis sun tracking system. The algorithm implemented into the LOGO-24 RC programmable logic controller (PLC) is based on the mathematical definition of surface position. This latter is defined by

two angles: the slope of the surface and the surface azimuth angle. The authors used two tracking motors, one for the joint rotating about the horizontal north-south axis to adjust the slope of the surface and the other motor to rotate the collector about the vertical axis to control the surface azimuth angle. A computer software has been developed to calculate the optimal positions of the tracking surface during the daylight hours which were divided into four identical time intervals. For each interval, the solar and motors speed are defined and programmed into the PLC. The authors concluded the gain is considerable with an increase in the daily collection of about  $41.34^\circ$  as compared to that of a fixed surface.

In 2010, Duarte et al [28] presented in an international conference on renewable energies the design of a microcontroller-base two-axis solar tracker using solar maps. They employed solar maps with the sun coordinates which depend on the time and geographical location.

Mousazadeh et al [29] and Lee et al [8] reviewed different types of sun-tracking systems. They focused on the potential energy gain obtained by the application of both open- and closed-loop algorithms. They surveyed some of the most significant proposals of both types and discussed their pros and cons. They compared the outcomes of tracking systems with fixed-position counterparts. They concluded that solar systems which track the changes in the sun's trajectory over the course of a day collect far greater amount of solar energy. They also reported that the most efficient and popular sun-tracking devices was found to be in the form of polar-axis and azimuth/elevation types.

### 3 Closed-Loop Tracking Strategies

Closed-loop types of sun tracking systems are based on feedback control principles [8]. They use the concept of the open-loop for their forward path and feedback loop(s) between the system's output and input. In a closed-loop sun tracking system, light and image sensors are in general used to discriminate the sun's position and the induced signals

proportional to the sun light intensity employed as inputs to the controller. These data are processed by the controller to automatically achieve and maintain the desired output condition.

Roth et al [30] described the design and construction of an electromechanical automatic sun-following system. They used a pyrheliometer to measure direct solar radiation. A four-quadrant photo detector to sense the position of the sun and two small DC motors to move the instrument platform are controlled by a Z80 microprocessor to keep the sun's image at the center of the four-quadrant photo detectors. The presented tracker can be adapted to work with solar cell panels or concentrators. The interesting feature of this system is under cloudy conditions, when the sun is not visible; a computing program calculates the position of the sun and takes control of the movement, until the detector can sense the sun again. The same authors described in [31] an improved version of their sun tracker. Although they kept the same mechanical base they brought some novelties. The DC motors were replaced by stepper motors, the four-quadrant sensor replaced by two sensors and the Z80 computing platform was replaced by a microcontroller connected to a PC. The two sensors were used, one for sun position information and the other to measure the sun light intensity. The tracker can operate in two modes. In the clocked mode of operation, the position of the sun is calculated based on the date and time information of its clock. Light position errors are measured during the day and stored for later analysis. These data will be used the next day to compute more accurate positions of the sun. In the active or sun mode of operation, the tracker uses the data of the sun monitor to control the pointing.

In [32] Kalogirou described the design and construction of a one-axis sun tracking system where the position and status of the sun are detected by three LDRs. One LDR is used to detect the focus state of the collector; another one is responsible of detecting any cloud cover, while the third is employed to discriminate daylight. The controller is constructed with

standard analog and digital integrated circuits. The actuator used in the tracker to point the collector toward the sun is a low-power DC motor with speed-reduction gearbox. The author reported that the deviation from the ideal posture is  $0.2^\circ$  and  $0.05^\circ$  with solar radiation of 100 and  $600 \text{ Wm}^{-2}$  respectively.

Recently, an image-based sun-tracking system was developed by Cheng. D. Lee et al [33]. The system consists of a self-design reflecting Cassegrain telescope, a webcam and an embedded image processing algorithm to point to the sun. The central coordinates of the sun images are calculated then sent to the solar tracker to follow the sun. Authors claimed that their tracking system achieved a tracking accuracy of  $0.04^\circ$ .

In [34] Sefa et al designed and implemented a PC-based one-axis sun tracking system for production of clean energy. The data from the two light sensors is collected by the microcontroller-based data acquisition unit and transmitted serially to the PC for processing and storage. Software developed in C language processes the collected data and instructs a DC motor to follow the sun during day time. In addition, current, voltage and solar position panel are displayed on the PC's screen.

In reference [35], A. Konar et al employed a microprocessor to automatically position an optimally tilted photovoltaic flat type solar panel for the collection of maximum solar irradiation. The azimuth angle of the optimally tilted panel is controlled using one infrared light detector. The technique used is similar to "perturb and observe" to determine maximum irradiation. The use of step-tracking scheme instead of continuous tracking keeps the motor idle for most of the time which results in power saving. The adjustment of the tilt angle is done on a monthly basis. They suggested the use of a two-dimensional tracker for an automatic tracking. We believe that the use of a second light detector would have not only simplified the design but saved energy and motor aging due to continuous rotation in both direction of the motor searching for optimal position of the solar collector.

Another microprocessor controlled automatic sun tracker is reported in [36]. Two light sensors arranged in east-west direction are used to discriminate the position of the sun with respect to the solar panel. A DC motor is gear coupled to rotate the panel along the east-west direction to keep the panel perpendicular to the sun vector. Attached to the collector are two switches used to limit the movement of the panel beyond its maximum angular positions in the east and west directions.

In [37] Saxena et al designed and fabricated a microprocessor-based controller for a dual-axis sun tracker to follow the sun in azimuth and altitude directions using two stepper motors. The system operates in both open- and closed-loop modes. In closed loop mode the sensor card provides signals to the controller. In open-loop mode, the tracker is brought to a pre-calculated position depending on the month and time of the day.

In general, open-loop control systems are cheaper because they do not require any means to gather feedback information such as light sensors. However, they present a major problem as they have no error correction capabilities. In addition, a given algorithm is valid for a specific location only. Closed-loop systems use sun finding position sensors. They are more reliable than open-loop systems. However, they may not have capabilities to track the sun on cloudy days. Hybrid control systems which consist of a combination of open- and closed-loop strategies are also reported in literature [31], [38]. In such systems, the closed loop tracking strategies are used to check and calibrate the astronomical control system.

#### **4 FPGA-Based Tracking Strategies**

A FPGA-based digital controller has many advantages compared to processor-based and other platform types based controllers. It supports high-speed and concurrent control algorithms, provides a higher degree of flexibility and a rapid low-cost manufacturing solution. In the last decade, with high density FPGA chips, SoPC-based systems using Nios®

II soft core processor are being extensively used to implement control algorithms. This reconfigurable computing approach is bringing a major revolution in the design of these digital controllers. It allows the co-existence of the microprocessor with the user defined hardware accelerators developed in HDL in a single chip instead of the mixed structure microprocessor/FPGA [7], [39-48]. This approach is being adopted for its flexibility in hardware and software, higher performance, reduced chip count and low cost.

In [39], Xinhong et al studied the applications of a FPGA development board to intelligent solar tracking. Utilizing the Nios II Embedded processor, the authors developed a solar tracking system. The two motors are controlled by a fuzzy logic module. The fuzzy controller uses five fuzzy rules which reduce significantly the computation complexity in the real-time control. The tracking systems can be operated into three modes: balance positioning, manual mode and automatic mode. For the balance positioning, they used four mercury switches. In the automatic mode, the fuzzy controller processes signals induced by four Cadmium sulphide Photoresistors which discriminate the position of the sun in the sky. These signals are digitized using four single-channel ADCs. The manual mode is used if the system has a fault or needs to be maintained. The results of the experiment yielded more energy than the array as a stationary unit. They reported that their system can achieve the maximum illumination and energy concentration and cut the cost of electricity by requiring fewer solar panels, therefore, it has significance for research and development.

In [40], the authors aimed to test whether FPGAs are able to achieve better position tracking performance than software-based real-time platforms. The comparison was conducted by embedding the same fuzzy logic controller (FLC) into a Virtex-II (XC2v1000) FPGA from Xilinx and into software-based real-time platform NI CompactRIO-9002 architectures with the same sampling time. They concluded that the FPGA based FLC



exhibits much better performances (up to 16 times in the steady-state error, up to 27 times in the overshoot and up to 19.5 times in the settling time) over the software-based FLC.

In publication [7], the authors dealt with an open-loop two-axis sun tracking for a PV system. The tilt- and azimuth-angle trajectories of the tracking system are determined using an optimization procedure based on a stochastic search algorithm called Differential evolution. In this procedure, the objective function is evaluated by giving the models of available solar radiation, tracking system consumption, and the efficiency of solar cells.

In [41], the authors describe the design of a stand-alone solar tracking system using a FPGA. The design is based on astronomical equations to determine the position.

The basic software of the stand-alone tracking system is made up of (i) an Off-line calculations of the sun path equations (developed in C), and (ii) a FPGA with suitable data to the driving mechanical system.

Sun path equation determines the value of altitude and azimuth angles at any time of the day. These values are stored as 8-bit words in a ROM. Two look-up tables were used, one for the altitude angle and the other for the azimuth. The FPGA is designed to control the address allocation for the look up tables stored in the ROMs for the sun tracking application. The FPGA code is written in VHDL in Xilinx FPGA.

In [42], Monmasson et al reviewed the state of the art of FPGA design methodologies with a focus on industrial control system applications. Their review is followed with a short survey on FPGA-based intelligent controllers for modern industrial systems. To illustrate the benefits of an FPGA implementation using the proposed design methodology, two case studies were presented. They consist of the direct torque control for induction motor drives and the control of a diesel-driven synchronous generator using fuzzy logic.

In recent years, high density FPGA chips can efficiently integrate a reduced instruction set computer (RISC) embedded soft-core processor, ready made intellectual property (IP)

peripherals and user defined hardware accelerator modules. A technology termed SoPC. This hardware/software co-design combines the software-program executed by the embedded processor to implement non-timing crucial repetitive control laws, while timing critical intensive-computational functions are best implemented as hardware accelerator modules in the FPGA logic. A large number of contributions using SoPC technology in different fields of electrical engineering and control are reported in literature [49-54].

## 5 Fuzzy Control Tracking Strategies

Fuzzy control is the application of fuzzy logic to real-world control problems [55]. The first fuzzy control application belongs to Mamdani & Assilian where the control of a small steam engine is considered [56]. Since that time and due to its ease of use and robustness, fuzzy control technology witnessed a wide range of applications in almost all areas. Applications of fuzzy control include mechatronic systems (as manufacturing, robotics, automotive, etc), nuclear industry, telecommunications, medical services etc. There are a lot of contributions and reviews that illustrate the use of fuzzy control in industrial applications [55-66].

A fuzzy logic computer-controlled sun tracking system is described in [57]. This closed-loop dual-axis tracking system is driven by two permanent magnet DC motors to provide necessary torque to the PV panel. A PC-based basic fuzzy-like P-type controller with 14 fuzzy rules was implemented. A data acquisition and a serial communication were implemented. Back to 1999, in our opinion, it would have been simpler and more performant to use either the parallel port or the Industry Standard Architecture (ISA) bus to interface the sun tracking hardware circuitry with the PC.

In implementing a fuzzy system on a field programmable gate array, McKenna et al [58], implemented a fuzzy control system in a FPGA to have a control surface as smooth as possible. They used a weighted average approach to minimize the dimension of the look-up table (LUT). The approach uses 3 or 4 most significant bits of each input to determine the

address for the LUT and to eliminate the rawness, the remaining bits are used to perform the weighted average. Simulations were carried on using Matlab to verify the functionality of the approach. The authors concluded that even with a large number of inputs, this approach helps solve the exponential growth problem and complexity of LUT. The overall controller was written in Verilog HDL and implemented in Xilinx 4000 series FPGA chip.

In [59], Kim presents the design and implementation of a fuzzy logic controller on a FPGA. The controller is partitioned in many temporally independent functional modules, and each implemented module forms a downloadable hardware object that can reconfigure the FPGA chip. The controller was developed using the fuzzy logic controller Automatic Implementation System (FADIS) tool. This latter performs various tasks in real-time such as automatic VHDL code generation, synthesis, placement & routing and downloading. This implementation method was effective in early 2000s when a single FPGA chip cannot fit the controller due to the limited size of its capacity.

Poorani et al [60] advocate an approach to implement a fuzzy logic controller for motion control using FPGA. This real-time implementation of the controller for four different types of terrains is developed in VHDL and achieved on a Xilinx Spartan 2E board.

Precup and Hellendoorn [65] presented a survey on recent developments on analysis and design of fuzzy control systems focused on industrial applications in the 2000. With a sample of 244 references, the authors concluded that this can be viewed as a guarantee that future successful applications will be constructed.

Also an interesting survey on analysis and design methods of model based fuzzy control systems is given in [66].

This collection of papers is an interesting overview of the active research in the field of programmed and reconfigurable hardware in embedded systems altogether with or without the use of fuzzy logic control as a control strategy.

---

---

**Chapter 3**

---

---

**Fuzzy Logic**

---

---

**1 Introduction**

The Oxford English Dictionary defines the word “fuzzy” as “blurred, confused, vague, imprecisely defined”. We should disregard this definition and view this word as a technical adjective. As reminded by Lotfi. A. Zadeh, fuzzy logic is not fuzzy. Instead, fuzzy logic is a precise logic for imprecision and approximate reasoning [67].

Fuzzy logic is viewed as a generalization of multi-valued logic compared to switching (Boolean) logic which is a two-valued logic. It deals with degrees of membership and degrees of truth. Unlike Boolean logic where variable can take at any instant of time a value that belongs to the set  $\{0, 1\}$ , a fuzzy variable can take a value in the continuum  $[0, 1]$  of logic values between 0 (completely false) and 1 (completely true).

In the literature, there are two kinds of justification for fuzzy systems theory: (i) the real-world is too complicated for precise descriptions to be obtained; therefore, fuzziness should be introduced to obtain reasonable, yet tractable models, (ii) human knowledge is increasingly important as we move into the information era [68-70].

The objective of this chapter is to give an insight into this theory which allows the formulation of the human knowledge in a systematic manner and puts it into engineering systems when combined with other information such as sensory measurements [69].

## 2 Fuzzy Sets

Classical set theory deals with distinct and precise boundaries of inclusion. In this theory, the membership of elements in a set is assessed in binary terms according to a bivalent condition; an element either belongs to or does not belong to the set.

Let  $\mathbf{X}$  denote the universe of discourse (or universal set), and  $x$  denotes the individual elements in  $\mathbf{X}$ . A classical (crisp) set  $\mathbf{A}$  is defined by a characteristic function  $\mu_{\mathbf{A}}(x)$  that assigns the values 1 or 0 to each element  $x$ , respectively, if  $x$  belongs or does not belong to  $\mathbf{A}$ .

Formally, a classical set  $A$  in  $X$  is expressed as:

$$A = \{(x, \mu_{\mathbf{A}}(x)) \mid x \in X; \quad \mu_{\mathbf{A}}(x): X \longrightarrow \{0, 1\}\} \quad (3.1)$$

Fuzzy set theory, however, deals with uncertainty and imprecision. In this theory, the concept of characteristic function is extended into a more generalized form known as membership function MF.

While the membership of elements in a crisp set is described by a bivalent condition, the membership of elements in a fuzzy set is described by a multivalent condition. That is, the MF can take any value between the unit interval  $[0, 1]$ .

Formally, a fuzzy set  $A$  in  $X$  is expressed as:

$$A = \{(x, \mu_{\mathbf{A}}(x)) \mid x \in X; \quad \mu_{\mathbf{A}}(x): X \longrightarrow [0, 1]\} \quad (3.2)$$

Note that curly brackets in [equation 3.1](#) are used to refer to binary value, while square brackets in [equations 3.2](#) are used to represent a unit interval.

[Figure 3.1](#) illustrates a MF for a classical set  $C$  and a MF for a fuzzy set  $F$ .

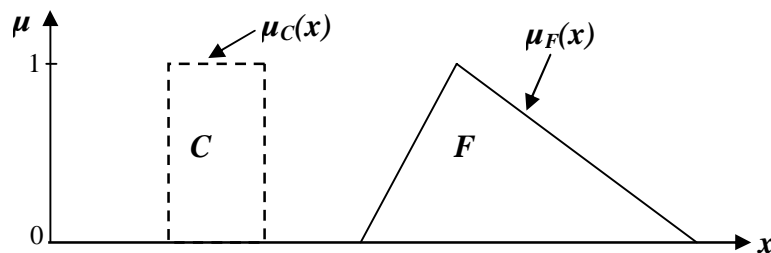


[Figure 3.1](#) Membership function for crisp and fuzzy sets.

## 2.1 Operations with Fuzzy Sets

This section deals with basic operations with fuzzy sets. In the classical set, its membership function assigns a value of either 1 or 0 to each individual in the universe of discourse, thereby discriminating between members and non-members of the crisp set under consideration [68].

Consider  $A$  and  $B$ , two non-empty fuzzy sets in the universe of discourse  $X$ . For a given element  $x \in X$ , the following function-theoretic operations are defined for  $A$  and  $B$  on  $X$ .

### i. Complement

The complement of set  $A$  denoted by  $\bar{A}$ , is defined as the collection of all elements in the universe of discourse that do not reside in the set  $A$ .

In set theoretic form, it is expressed as

$$\mu_{\bar{A}}(x) = 1 - \mu_A(x) \quad \text{for all } x \in X \quad (3.3)$$

### ii. Union

The union or t-conorm of  $A$  and  $B$  is a fuzzy set in  $X$ , denoted by  $A \cup B$  whose membership function is defined as

$$A \cup B = \{x \mid x \in A \vee x \in B\} \quad \text{for all } x \in X.$$

For the t-conorm operator, we have

$$\begin{aligned} \mu_{A \cup B}(x) &= \mu_A(x) \vee \mu_B(x) \\ &= \max \{ \mu_A(x), \mu_B(x) \} \quad \text{for all } x \in X. \end{aligned} \quad (3.4)$$

### iii. Intersection

The intersection or t-norm of  $A$  and  $B$  is a fuzzy set  $A \cap B$  in  $X$  with membership function defined as

$$A \cap B = \{x \mid x \in A \wedge x \in B\} \quad \text{for all } x \in X.$$

For the t-norm operator, we have

$$\begin{aligned}\mu_{A \cap B}(x) &= \mu_A(x) \wedge \mu_B(x) \\ &= \min \{ \mu_A(x), \mu_B(x) \} \text{ for all } x \in X.\end{aligned}\quad (3.5)$$

**Figure 3.2** illustrates graphically these three fundamental fuzzy operations.

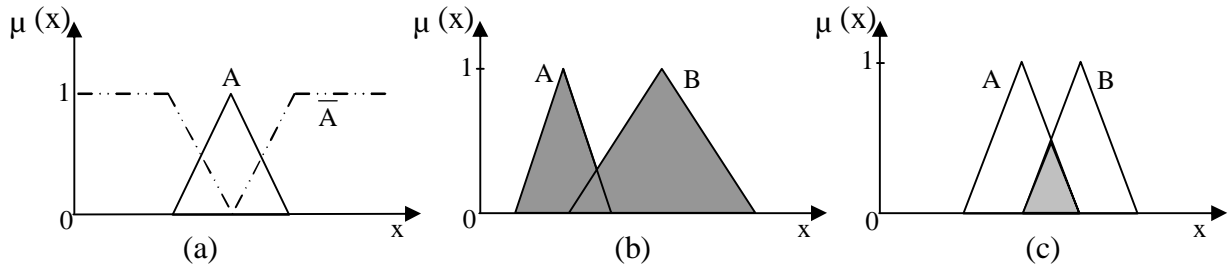


**Figure 3.2** Graphical representation of the a) Complement, b) Union, c) Intersection fuzzy operations

We used “max” and “min” for union and intersection respectively. To show that the union is equivalent to [equation 3.4](#), we note that  $\max[\mu_A(x), \mu_B(x)] \geq \mu_A(x)$  and  $\max[\mu_A(x), \mu_B(x)] \geq \mu_B(x)$ . If C is any fuzzy set that contains both A and B, then  $\mu_C(x) \geq \mu_A(x)$  and  $\mu_C(x) \geq \mu_B(x)$ . Therefore,  $\mu_C(x) \geq \max[\mu_A(x), \mu_B(x)] = \mu_{A \cup B}(x)$ . The intersection defined by [equation 3.5](#) can be justified in the same manner [69].

#### iv. DeMorgan’s Laws

DeMorgan’s laws stated for classical sets also apply for fuzzy sets. For the given sets A and B, we have

$$\begin{aligned}\overline{A \cap B} &= \bar{A} \cup \bar{B} \\ \overline{A \cup B} &= \bar{A} \cap \bar{B}\end{aligned}\quad (3.6)$$

#### v. Empty Set

A fuzzy set A is an empty set labelled  $\phi$ , if and only if  $\mu_A(x) = 0$  for each  $x \in X$ .

#### vi. Excluded Middle and Non-contradiction Laws

In classical set theory every object either belongs or does not belong to the universal set. The law of excluded middle,  $A \cup \bar{A} = X$  and the law of non-contradiction  $A \cap \bar{A} = \phi$  hold. In fuzzy set theory however, these two laws are not valid, **equation 3.7**.

$$\begin{aligned}
 A \cup \bar{A} &\neq X \\
 A \cap \bar{A} &\neq \phi
 \end{aligned}
 \tag{3.7}$$

Proof

Let  $A = 0.5$ , then we can easily demonstrate that

$$\begin{aligned}
 A \cup \bar{A} &= \max \{ \mu_A(x), \mu_{\bar{A}}(x) \} \\
 &= \max \{ 0.5, 1-0.5 \} \\
 &= 0.5 \neq 1
 \end{aligned}$$

$$\begin{aligned}
 \text{Similarly, } A \cap \bar{A} &= \min \{ \mu_A(x), \mu_{\bar{A}}(x) \} \\
 &= \min \{ 0.5, 1-0.5 \} \\
 &= 0.5 \neq 0
 \end{aligned}$$

Considering **equations 3.3 to 3.7**, we can conclude that operations on classical sets also hold for fuzzy sets except for the excluded middle and non-contradiction laws, [70].

**Figure 3.3** illustrates graphically these two laws.

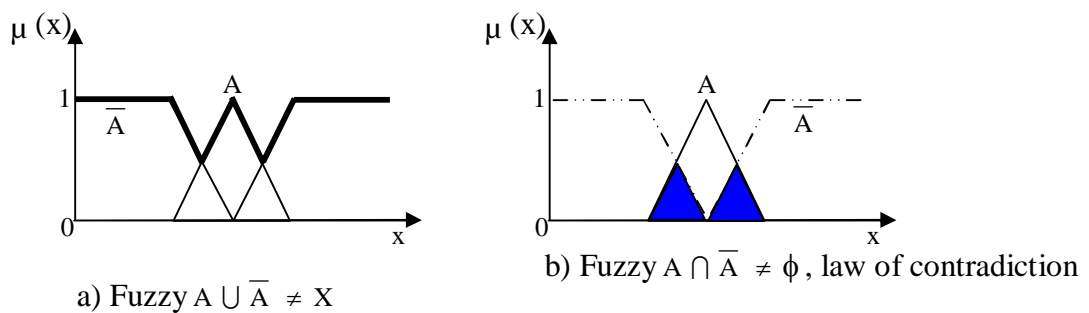


**Figure 3.3** Graphical representation of a) Fuzzy  $A \cup \bar{A} \neq X$  and b) Fuzzy  $A \cap \bar{A} \neq \phi$ .

## 2.2 Properties of Fuzzy Sets

The properties of classical sets, called crisp sets, also suit for the properties of fuzzy sets. Because the membership values of a crisp set are a subset of the interval  $[0, 1]$ , then, classical sets can be thought as a special case of fuzzy sets [70-71].



We will use set notations rather than membership functions in order to make easy comparison with classical sets.

Consider A, B, and C, three fuzzy sets in a non-empty universe of discourse X. the most common properties of fuzzy sets include:

#### **i. Commutativity**

The commutativity property of two fuzzy sets using logical operators AND and OR is given by

$$\begin{aligned} A \cup B &= B \cup A \\ A \cap B &= B \cap A \end{aligned} \quad (3.8)$$

#### **ii. Associativity**

The associativity property using logical operators AND and OR is given by

$$\begin{aligned} A \cup (B \cap C) &= (A \cup B) \cap C \\ A \cap (B \cup C) &= (A \cap B) \cup C \end{aligned} \quad (3.9)$$

#### **iii. Distributivity**

The distributivity property of three fuzzy sets using the AND and OR logical operators is given by

$$\begin{aligned} A \cup (B \cap C) &= (A \cup B) \cap (A \cup C) \\ A \cap (B \cup C) &= (A \cap B) \cup (A \cap C) \end{aligned} \quad (3.10)$$

#### **iv. Idempotency**

The idempotency property of a fuzzy set A with respect to logical operators AND and OR is given by

$$\begin{aligned} A \cup A &= A \\ A \cap A &= A \end{aligned} \quad (3.11)$$

#### **v. Identity**

The identity property of a fuzzy set  $A$  with respect to logical operators AND and OR and given the empty set  $\phi$  –having all degrees of membership equal to 0, and the universal set  $X$  having all degrees of membership equal to 1 is defined as:

$$\begin{aligned} A \cup \phi &= A & \text{and} & & A \cap X &= A \\ A \cap \phi &= \phi & \text{and} & & A \cup X &= X \end{aligned} \quad (3.12)$$

#### vi. Involution

The involution property which represents the double negation of a fuzzy set  $A$  is given by

$$\overline{\overline{A}} = A \quad (3.13)$$

### 3 Membership Function

A fuzzy membership function (MF) is a graphical representation of a fuzzy set. It defines how each point in the input space (universe of discourse) is mapped to a membership value (or degree of membership) between 0 and 1.

The MF noted  $\mu_A(x)$  describes the membership value of the element  $x$  of the universal set  $X$  in the fuzzy set  $A$ . **Figure-3.4** illustrates graphically fuzzy membership functions for speed. It plots three fuzzy MFs one for each fuzzy set across the universe of discourse.

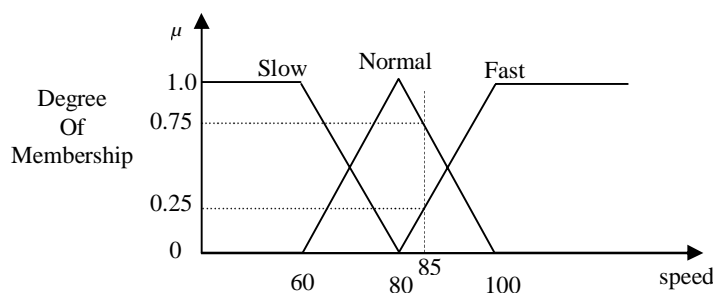


**Figure-3.4** Fuzzy membership functions for speed

At crisp speed 85, the degree of membership (slow) is 0.0. The degree of membership (normal) is 0.75 whereas for (fast) the degree of membership is 0.25.

Theoretically, membership functions can have any form of regular or irregular shapes as long as they are convenient to be described mathematically [72]. Reasonably, designers adopt

regular shaped of known parameterized membership functions such as piece-wise linear functions (triangular or trapezoidal) or nonlinear smooth functions such Gaussian, Sigmoidal and Bell-shaped membership functions.

### 3.1 Piecewise Linear Membership Functions

Piecewise linear functions are the simplest from of MFs. **Figure-3.5** illustrates a triangular and a trapezoidal asymmetric membership functions.

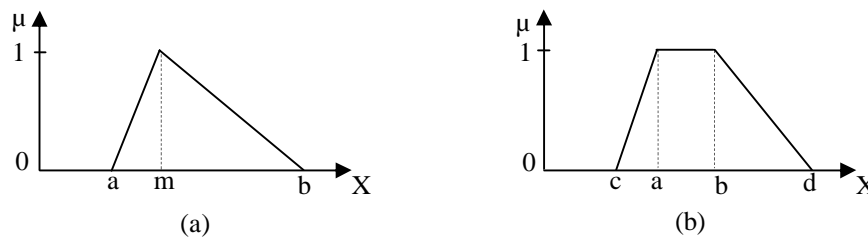


**Figure-3.5** Asymmetric triangular and trapezoidal membership functions

#### 3.1.1 Triangular Membership Function

A triangular MF is specified by three parameters: its peak (or center)  $m$ , left width  $a > 0$  and right width  $b > 0$ . It can be described through the equation:

$$\mu_A(x) = \begin{cases} 0 & x \leq a \\ \frac{x-a}{m-a} & a \leq x \leq m \\ \frac{b-x}{b-m} & m \leq x \leq b \\ 0 & x \geq b \end{cases} \quad (3.14)$$

It can also be expressed in a more compact form as:

$$\mu_A(x) = \max\left(\min\left(\frac{x-a}{m-a}, \frac{b-x}{b-m}\right), 0\right) \quad (3.15)$$

#### 3.1.2 Trapezoidal Membership Function

A trapezoidal MF is specified by its tolerance (core) interval  $[a, b]$ , the left width  $c$  and the right width  $d$ . It is defined by the following equation

$$\mu_A(x) = \begin{cases} \frac{x-c}{a-c} & c \leq x \leq a \\ 1 & a \leq x \leq b \\ \frac{d-x}{d-b} & b \leq x \leq d \\ 0 & \text{otherwise} \end{cases} \quad (3.16)$$

### 3.2 Features of the Membership Function

The feature of the membership function is defined by three properties. They are: core, support and boundary. **Figure-3.6** assists in the description of these three properties.

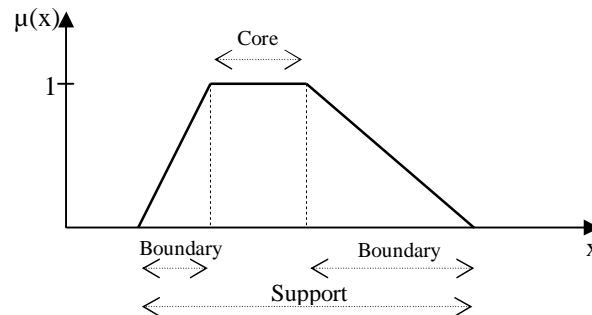


**Figure-3.6** Features of a membership function

#### 3.2.1 Core

The core of a membership function for a fuzzy set  $A$  is defined as the region of the universe of discourse that is characterized by complete full membership in the set  $A$ , that is:

$$\text{Core}(A) = \{x \mid \mu_A(x) = 1\} \quad \text{for all } x \in X \quad (3.17)$$

#### 3.2.2 Support

The support of a membership function for a fuzzy set  $A$  is the set of points on the universe of discourse where the membership grade in  $A$  is larger than 0, that is:

$$\text{Supp}(A) = \{x \mid \mu_A(x) > 0\} \quad \text{for all } x \in X \quad (3.18)$$

#### 3.2.3 Boundary

The boundaries of a membership function for some fuzzy set  $A$  are defined as that region of the universe of discourse containing elements that have a nonzero membership but non complete membership, that is:

$$\text{Bnd}(A) = \{x \mid 0 < \mu_A(x) < 1\} \quad \text{for all } x \in X \quad (3.19)$$

#### 3.2.4 Height

The height of a fuzzy set  $A$  is the peak value reached by the MF, also called supremum. Formally, the height is defined as:

$$\text{Hgt}(A) = \max \{ \mu_A(x) \} = \sup_{x \in X} \mu_A(x) \quad (3.20)$$

### 3.3 Structure of Membership Functions

To illustrate the structure of MFs, [figure-3.7](#) depicts a graphical representation of the linguistic variable Temperature (T) with five partitions.

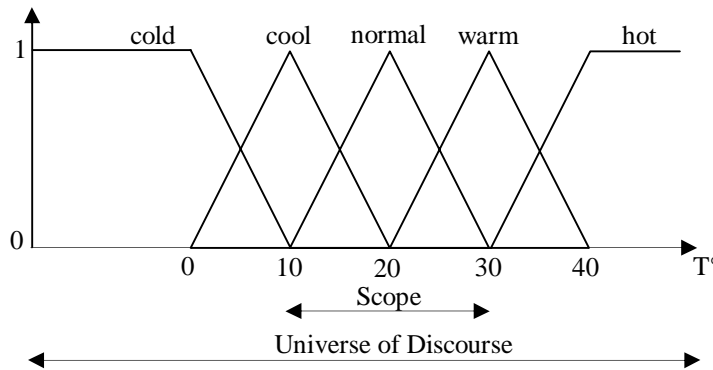


**Figure 3.7** Graphical representation of a fuzzy variable with 5 fuzzy sets

- The universe of discourse is the range of all possible values applicable to a system variable.
- The label indicates the name used to identify a MF in each region of behaviour.
- The scope or domain is the width of the MF. It is identified by a range of numerical values that correspond to a label. Also, it indicates the range of concepts over which a MF is mapped. These sub-divisions of the universe of discourse are usually uniform but in certain cases some MFs can accumulate in zones where a more accurate control (higher sensitivity) of the controller is desired and sparse elsewhere.

March [71] noted some interesting points which should be taken into account while defining the domain of MFs:

- Every point in the universe of discourse should belong to the domain of at least one MF.
- Two MFs cannot have the same point of maximal meaningfulness
- When two MFs overlap, the sum of membership grades for any point in the overlap should be  $\leq$  to 1.

- When two MFs overlap, the overlap should not cross the point of maximal meaningfulness of either MF.

Another characteristic to be considered is the subdivision of the universe of discourse. This is usually uniform, but in some applications the MFs can be denser in certain zones if higher sensitivity of the controller is desired.

### 3.4 Number and Degree of Overlapping of Membership Functions

The number of MFs for each controller input as well as the shape and the overlapping degree of the antecedents of the MFs has a strong influence on the characteristic of the fuzzy logic controller.

The larger the number of MFs, the finer the fuzzy partitions of the controller inputs (higher resolution) the better the approximation. However, more MFs means a larger number of linguistic rules in the rule-base component and hence more computation complexity. Moreover, this causes rapid firing of the fuzzy conclusions for changes in the inputs, resulting in large output changes, which may cause instability in the system. On the contrary, few MFs, result in a coarse fuzzy partitions of the input variables. With a reduced number of rules, the controller does not require an intensive computation, it may however, cause a slower response of the system and may even fail provide sufficient output control in time to recover for small input changes. To date, there is no systematic approach to have an optimal fuzzy partition of the fuzzy input/output, a rule of thumb is to have at least three and at most nine MFs for each controller input [73].

The overlapping degree of the antecedents of MFs greatly influences the form of the output of the fuzzy logic controller. Small overlapping degrees generate step characteristics, whereas higher overlaps between MFs promote higher robustness of the controller and generate smoother curves at the output.

### 3.5 Linguistic Variables and Linguistic Values

A sensor measures a variable and provides a numerical and precise value to the user. Human perception however, evaluates a variable in linguistic terms i.e, in words. In order to incorporate human perception into engineering systems in a systematic manner, input and output variables of fuzzy logic based control systems are represented by variables that take words as values [72]. Just as a variable that takes on a numerical value, for example 123.4, is called an algebraic variable, a variable that can take words or sentences in natural or artificial languages as its values is called a linguistic variable. These words or sentences, which form a term set, are characterized by fuzzy sets defined in the universe of discourse in which the variable is defined. A fuzzy partition, then, determines how many fuzzy sets should exist in the term set, a number that determines the granularity of the linguistic variable. For example, if cold, warm, hot, etc are values of temperature, then temperature is a linguistic variable and these words are linguistic terms, values or labels.

In control systems, the linguistic variables are usually the error and the rate of change of error where a term set is associated to each linguistic variable. The term set is usually represented by the linguistic values or labels {NL, NM, NS, AZ, PS, PM, PL} where NL means “Negative Large”, NM “Negative Medium”, NS “Negative Small”, AZ “Approximate Zero”, PS “Positive Small”, etc.

The linguistic variables and the linguistic values provide a mean for the expert to express his/her ideas about the decision-making process.

#### 4 Fuzzy IF THEN Rules

Knowledge is the main source of intelligence [72]. In fuzzy control, knowledge is expressed by a fuzzy rule-base model where each fuzzy linguistic rule is represented by a fuzzy IF-THEN statement. The fuzzy conditional statement is symbolically expressed as:

$$\text{IF } \langle \text{fuzzy proposition} \rangle \text{ THEN } \langle \text{fuzzy proposition} \rangle$$

where, a fuzzy proposition can have a value within the interval [0, 1].

The fuzzy proposition can be either an atomic or a compound proposition. An atomic proposition is a single statement such as “IF *Speed is Slow* THEN... “. Whereas a compound proposition is made up of two or more atomic propositions connected by fuzzy union (OR) or intersection (AND) operators such as “IF *e is Large AND Δe is small* THEN...”.

The IF-THEN linguistic rule consists of two parts: the “antecedent” (or premise) is the block between the IF and THEN constructs whereas the “consequent” (or conclusion) is the block following the THEN construct.

For example, the Mamdani-type fuzzy IF-THEN rule with multiple conjunctive antecedents has the following form:

$$\text{IF } x_1 \text{ is } A_1 \text{ AND } x_2 \text{ is } A_2 \text{ AND } \dots \text{ AND } x_N \text{ is } A_N \text{ THEN } y \text{ is } B \quad (3.21)$$

where  $x_i$ ,  $i = 1, 2, \dots, N$  and  $y$  are the input and output linguistic variables of the fuzzy system respectively. The  $A_i$ 's and  $B$  are the linguistic values of the linguistic variables  $x_i$ 's and  $y$  in the universes of discourse  $X_i$ 's and  $Y$  respectively.

If standard mathematical notation for IF-THEN and AND is used, the above rule can be reformulated as follows:

$$A_1(x_1) \wedge A_2(x_2) \wedge \dots \wedge A_N(x_N) \Rightarrow B(y) \quad (3.22)$$

$$\text{or} \quad \mu_{A_1}(x_1) \wedge \mu_{A_2}(x_2) \wedge \dots \wedge \mu_{A_N}(x_N) \Rightarrow \mu_B(y) \quad (3.23)$$

where

$$\mu_{A_1}(x_1) \wedge \mu_{A_2}(x_2) \wedge \dots \wedge \mu_{A_N}(x_N) = \min \{ \mu_{A_1}(x_1), \mu_{A_2}(x_2), \dots, \mu_{A_N}(x_N) \} \quad (3.24)$$

## 5 Properties of Fuzzy Rules

The fuzzy rule-base included into the knowledge base of a fuzzy control system consists of a set of fuzzy rule list. For the fuzzy system to exhibit excellent performances the set of fuzzy rules should cover all the possible situations that the system may face. Moreover, there should not be any conflict among the fuzzy rules, while satisfying continuity. In other words,



the fuzzy rule list should fulfil the following three characteristics: completeness, consistency, and continuity.

In order to define the above characteristics, it is desirable to consider a two-input one-output fuzzy control system. The input linguistic variables  $x_1$  and  $x_2$  are partitioned into  $N$  and  $M$  subspaces respectively, and represented by  $A_1, A_2, \dots, A_N$  and  $B_1, B_2, \dots, B_M$  on the universe of discourse  $X$ . **Table 3.1** shows the fuzzy rule list in the matrix form. The size of the rule matrix depends on the number of system's inputs and the number of fuzzy subspaces representing these inputs. In general, the size of the matrix is the product of the fuzzy subspaces of the system's inputs.

$y$		$x_2$					
		$B_1$	$B_2$	$B_2$	$B_2$	...	$B_M$
$x_1$	$A_1$	$R_{1,1}$	$R_{1,2}$	$R_{1,3}$	$R_{1,4}$	...	$R_{1,M}$
	$A_2$	$R_{2,1}$	$R_{2,2}$	$R_{2,3}$	$R_{2,4}$	...	$R_{2,M}$
	$A_3$	$R_{3,1}$	$R_{3,2}$	$R_{3,3}$	$R_{3,4}$	...	$R_{3,M}$
	$A_4$	$R_{4,1}$	$R_{4,2}$	$R_{4,3}$	$R_{4,4}$	...	$R_{4,M}$
	$\vdots$					...	
	$A_N$	$R_{N,1}$	$R_{N,2}$	$R_{N,3}$	$R_{N,4}$	...	$R_{N,M}$

**Table 3.1** The  $N \times M$  set of fuzzy if-then rules in matrix form

### 5.1 Completeness

A set of fuzzy IF THEN rules  $\{R_i, i = 1, 2, \dots, (N \times M)\}$  is complete, if for any  $x \in X$  it produces an appropriate output value for any possible combination of input values.

Formally, completeness can be expressed as

$$\forall (x_1, x_2): \text{hgt}(\Psi(x_1, x_2)) > 0$$

where  $\Psi$  denotes the output function of crisp inputs  $x_1$  and  $x_2$ .

### 5.2 Consistency

A set of fuzzy IF THEN rules is consistent if it does not include any contradictory rule. That is, two fuzzy rules with the same antecedent (IF part of rule) have mutually-exclusive rule consequents (THEN part of rule), as for example

$R_i$ : IF  $R_{PQ}$  THEN  $C$

$R_j$ : IF  $R_{PQ}$  THEN  $C$

### 5.3 Continuity

To define continuity we need the notion of fuzzy rule neighbourhood or adjacency. The neighbor rules of rule  $R_{ij}$  are  $R_{(i-1),j}$ ;  $R_{i,(j-1)}$ ;  $R_{i,(j+1)}$ ;  $R_{(i+1),j}$ .

A set of fuzzy IF THEN rules satisfies continuity if there is no such a pair of neighboring rules whose consequent fuzzy sets have empty intersection (are disjoint). The continuity of fuzzy rules provides the continuity of controller output which is a desirable feature in control applications.

When designing fuzzy logic control systems, completeness, consistency and continuity in rule-base must be ensured otherwise, the system may encounter severe problems like instability and/or oscillations behaviour [69], [73].

## 6 Fuzzy Logic Controller

Fuzzy control is based on fuzzy logic. It provides a formal methodology for representing, manipulating and implementing a human's heuristic knowledge, rather than traditional logical systems, about how to control a system. The fuzzy logic controller which is an approximate reasoning-based controller is a static nonlinear mapping between its inputs and outputs [72]. Similar to a conventional controller, from outside, both the input and output values of the FLC are crisp values. The input values consist of measured values from the controlled plant or some control errors computed from the measured values.

**Figure 3.8** Shows the structure of a generic Mamdani-type fuzzy control system with  $n$  inputs  $x_i \in X_i$  where  $i = 1, 2, \dots, n$  and  $m$  outputs  $y_i \in Y_i$  where  $i = 1, 2, \dots, m$  where the crisp sets  $X_i$  and  $Y_i$  are universes of discourse for  $x_i$  and  $y_i$  respectively.

The fuzzy system is composed of four principle modules: a fuzzification interface, a fuzzy knowledge-base, a fuzzy inference mechanism and a defuzzification interface. The processes

performed by these modules are executed sequentially. That is, before being processed by the inference engine, the real-world (crisp) data inputs must first be fuzzified. Next, the defuzzifier takes as inputs the fuzzy conclusions from the inference engine and provides a result which will serve as an input to the object of control.

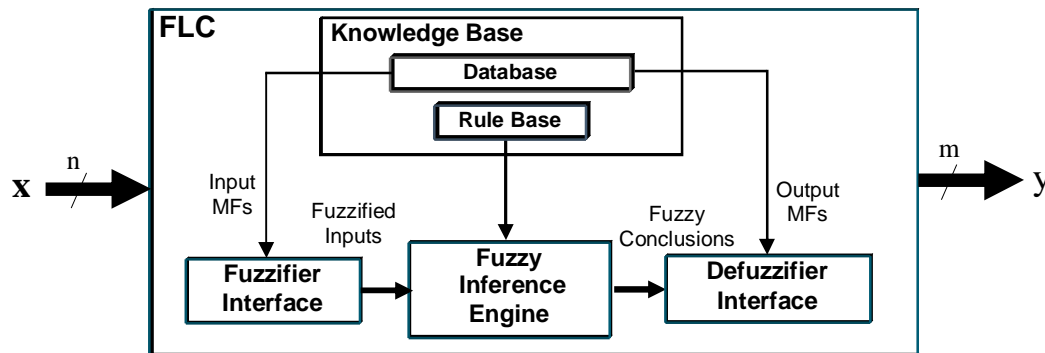


**Figure-3.8.** Structure of a generic Mamdani type fuzzy logic controller.

### 6.1 Fuzzification Interface

The first step in the fuzzy inference process is fuzzification. This mathematical encoding procedure is performed by the fuzzification interface module. This module transforms the crisp inputs applied to the fuzzy logic controller into fuzzy sets. Each crisp input will have its proper set of MFs within the universe of discourse set, a set that holds all relevant values that the crisp input can possess. The universe of discourse is partitioned into a number of fuzzy sets where a MF is associated with each set. In general, the fuzzification interface module performs the following functions:

- i- Reads the real-world values of the input state variables,
- ii- Performs a scale mapping that transfers the range of values of input variables into the corresponding universe of discourse.
- iii- Takes as inputs these scaled data and convert them into suitable linguistic format by means of MFs used to quantify linguistic terms.

### 6.2 Fuzzy Knowledge-Base

The fuzzy knowledge base encapsulates the human expert knowledge. This critical module for the performance of the fuzzy logic controller has two sections: a database and a rule base.

The database provides the necessary definitions for the fuzzification module, the rule base component and the defuzzification interface module. It contains the MFs of the input and output linguistic variables and the fuzzy sets used in the fuzzy rules. In addition, the database includes fuzzy set definitions as well as other data (normalization/denormalization scaling factors, processing periods, etc) which are required during the inference process.

The rule base of the controller is actually a list of fuzzy conditional IF-THEN statements that quantify the actions a human expert would take to achieve a good control.

### **6.3 Fuzzy Inference Mechanism**

The fuzzy inference engine is the kernel of the FLC. This crucial module emulates the human expert's decision-making about how to best achieve a desired control strategy of the plant. It employs the linguistic rules provided by the rule-base component included in the knowledge base module and the relevant fuzzified state variable inputs of the controlled system to infer the fuzzy control actions for the controlled object. The combination of this engine and the knowledge base constitutes the process of fuzzy reasoning system of a FLC.

The management of the fuzzy linguistic rules and the relevant fuzzified state variable inputs to obtain the fuzzy control actions is one of the most important concerns in fuzzy control systems. It is the inference mechanism. This latter consists of two sub-functions: (1) fuzzy implication, and (2) aggregation of fuzzy conclusions.

#### **6.3.1 Fuzzy Implication**

Irrelevant of what the form and number of fuzzy rules we may have in the rule-base, the main concern is how to interpret the meaning of each rule. That is, the process to determine

the influence produced by the antecedent part of the fuzzy rule on the conclusion part of the rule. This procedure is known as the fuzzy implication.

There are many possible ways to define these implications. Two of the most commonly used in control applications are: (1) the  $\min(\cdot)$ , (known as Mamdani's fuzzy implication) which truncates the consequent's membership function and, (2) the algebraic-product (known as the Larsen's fuzzy implication) which scales it.

In order to illustrate these two fuzzy implication types, we consider a fuzzy system with two inputs  $x1$  and  $x2$  and a single output  $y$  is described by a set of linguistic IF-THEN rules in the Mamdani's form

$$R^i: \quad \text{IF } x1 \text{ is } A_1^i \text{ AND } x2 \text{ is } A_2^i \text{ THEN } y \text{ is } B^i \quad \text{for } i= 1, 2, \dots, n \quad (3.25)$$

where  $A_1^i$  and  $A_2^i$  are the fuzzy sets representing the  $i$ -th antecedent membership function pairs and the  $B^i$  is the fuzzy set representing the  $i$ -th conclusion.

For the  $i$ -th rule, the fuzzy implication function is given by

$$\mu_{R^i}(x1, x2; y) = \Gamma^i(\mu_{A_1^i}(x1), \mu_{A_2^i}(x2)) \quad \text{for } i= 1, 2, \dots, n \quad (3.26)$$

where  $\Gamma^i$  is an implication function.

i- The Mamdani's implication is defined by the  $\min(\cdot)$  operator as:

$$\mu_{B^i}(y) = \min(\mu_{A_1^i}(x1), \mu_{A_2^i}(x2)) \quad \text{for } i= 1, 2, \dots, n \quad (3.27)$$

ii- The Larsen's implication is defined by the product operator as:

$$\mu_{B^i}(y) = \mu_{A_1^i}(x1) * \mu_{A_2^i}(x2) \quad \text{for } i= 1, 2, \dots, n \quad (3.28)$$

### 6.3.2 Aggregation of Fuzzy Conclusions

Aggregation is the process of combining into a single fuzzy set the results of the fuzzy rules obtained during the fuzzy implication phase. In fuzzy control, the individual rule-based inference engine is usually used to compute the contribution of each activated (fired) rule. The individual rules can be aggregated into a variety of ways. The most commonly used

aggregation operators are the maximum, the sum and the probabilistic sum. Out of these three operators, the best-known in literature and most frequently applied is the maximum. When combined with the  $\min(\cdot)$  or product fuzzy implication operators, yields the well known Max-Min also known as the Mamdani's inference method or the Max-Prod or the Larsen's inference method.

In the Max-Min inference, the membership functions of the fuzzy sets of the consequents are limited to the degree of truth and in turn combined into a single fuzzy set by forming a maximum, [equation 3.29](#).

$$\mu_{B_{aggr}}(y) = \max_i [\min [\mu_{A_1^i}(x1), \mu_{A_2^i}(x2)]] \quad \text{for } i= 1, 2, \dots, n \quad (3.29)$$

In the Max-Prod however, the membership functions of the fuzzy sets of the consequents are multiplied with the degree of truth of the condition and then combined, [equation 3.30](#).

$$\mu_{B_{aggr}}(y) = \max_i [\mu_{A_1^i}(x1) * \mu_{A_2^i}(x2)] \quad \text{for } i= 1, 2, \dots, n \quad (3.30)$$

[Equations 3.27, 3.28, 3.29](#) and [3.30](#) are graphically represented in [Figure-3.29](#). In this figure each fuzzy rule antecedent and inference are shown in a separate line. The aggregation

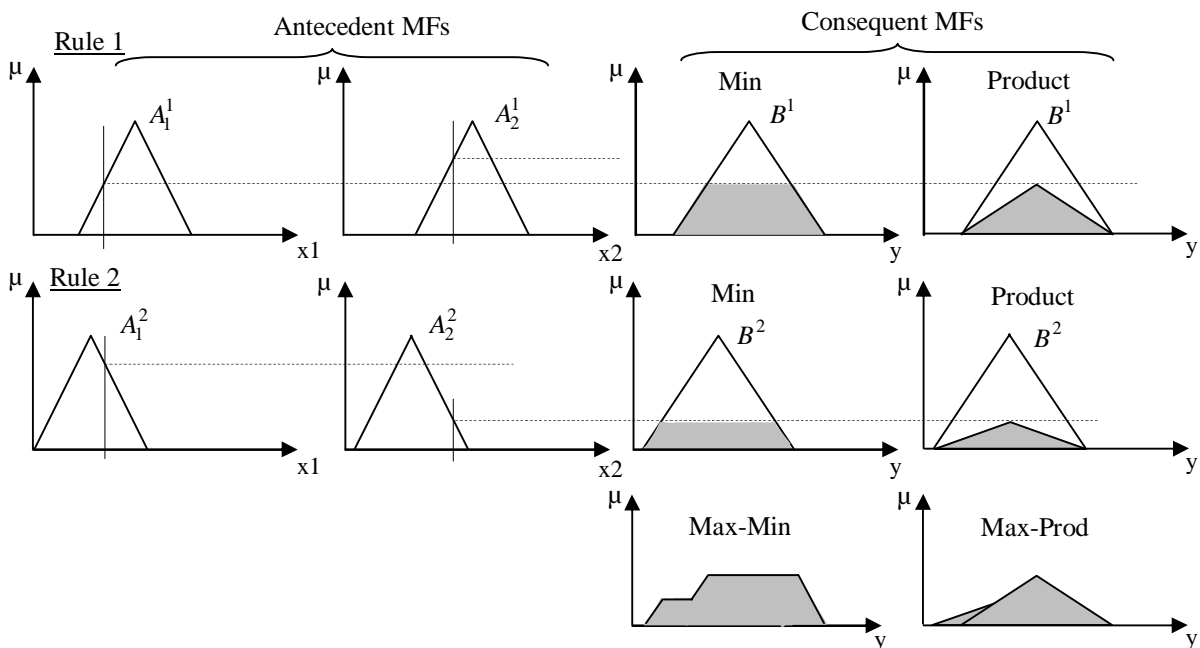


**Figure-3.9.** Graphical representations of the Max-Min and Max-Prod inference methods of two rules of a two inputs system two with crisp inputs.

of the consequents fuzzy sets are also shown vertically for both Max-Min and Max-Prod operators. The symbols  $A_1^1$  and  $A_2^1$  refer to the first and second fuzzy antecedent of the first fuzzy rule, while the symbol  $B^1$  refers to the fuzzy consequent of the first rule. Similarly, the symbols  $A_1^2$  and  $A_2^2$  refer to the first and second antecedent of the second rule, and the symbol  $B^2$  refers to the fuzzy consequent of rule 2.

In the  $\min(\cdot)$  fuzzy implication, the inferred output of each rule is a fuzzy set chosen from the minimum firing strength, whereas the Max-Min inference is the fuzzy union of the resulting fuzzy conclusions, column 3. Graphically, the union of these two membership functions is the outer envelop of the two shapes.

In the product fuzzy implication, the inferred output of each rule is a fuzzy set scaled down by its firing strength via algebraic product, whereas the Max-Prod inference is also the fuzzy union of the resulting fuzzy conclusions of the fuzzy implications, column 4.

#### 6.4 Defuzzification Interface

Defuzzification is the final step in the fuzzy logic program. Although it is a part of the fuzzy controller, the sole reason of this module is to provide an interface between the fuzzy set domain and the real world crisp domain.

This mathematical decoding procedure is a mapping of fuzzy set actions, defined over an output universe of discourse, implied by the fuzzy inference engine, into a space of non-fuzzy actions. In this context, the resulting crisp value should provide the best representation of the information inferred by the inference module.

Assume we have the result in **Figure-3.10** at the end of the fuzzy inference procedure.

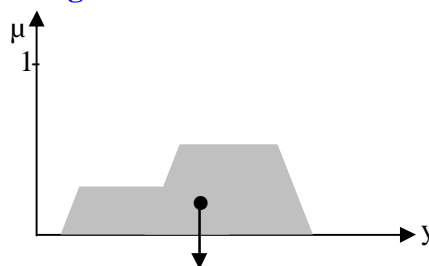


**Figure-3.10** Example of defuzzification for two-rule fuzzy inference

In this figure, the shaded area represents the fuzzy action result. The purpose of the defuzzification module is to obtain a crisp value (represented by a dot in the figure) from the fuzzy result.

There exist different defuzzification techniques proposed in the literature for defuzzifying a fuzzy set described by a membership function. These techniques can be classified into two principle groups based on their technical and structural characteristics [74]. They are: maxima methods and distribution methods. Some of the most common defuzzifying techniques from both classes will be described and graphically represented in the following sections.

### **6.4.1 Maxima Methods**

The maxima methods have the common property that they select an element from the core of a fuzzy set as defuzzification value. The strength of maxima methods is their simplicity and speed of execution because they require passing through values of the core only.

The process consists in choosing the fuzzy set with the highest membership. The remaining fuzzy sets are ignored and hence their information is lost. These defuzzifying methods are not well suited in fuzzy logic controllers because they cannot guarantee the continuity of the controller [72]. Maxima techniques can be classified as the first, the last or the median maxima. These give rise to the following defuzzification techniques:

- i- First of maxima (FOM)
- ii- Last of maxima (LOM)
- iii- Middle of maxima (MOM)

#### **6.4.1.1 First Of Maxima (FOM)**

The FOM, also called the left most maximum, method uses the union of the fuzzy sets and takes the smallest value of the domain with the maximum membership degree, which is expressed as:



$$y^* = \inf \{ y \in Y \mid \mu_B(y) = \text{hgt}(B) \} = \min \text{core}(B) \quad (3.31)$$

where  $\text{hgt}(B)$  is the highest membership of  $B$ .

#### 6.4.1.2 Last Of Maxima (LOM)

Similarly, the LOM, also called the right most maximum, method uses the union of the fuzzy sets and takes the greatest value of the domain with the maximum membership degree, which is expressed as:

$$y^* = \sup \{ y \in Y \mid \mu_B(y) = \text{hgt}(B) \} = \max \text{core}(B) \quad (3.32)$$

where *inf* denotes infimum (greatest lower bound) and the *sup* denotes supremum (least upper bound).

#### 6.4.1.5 Middle Of Maxima (MOM)

The middle of maxima is taken as the average of the above two values. The MOM is expressed as

$$\text{MOM}(B) = \frac{\min \text{core}(B) + \max \text{core}(B)}{2} \quad (3.33)$$

These three defuzzifying methods are illustrated in **Figure-3.11**.

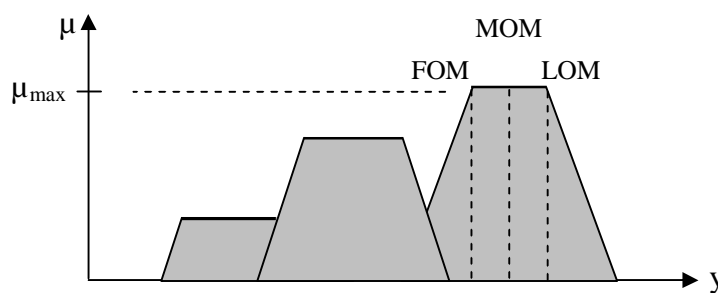


**Figure-3.11.** First, Middle and Last of Maxima defuzzification methods

#### 6.4.2 Distribution Methods

The main characteristic of this group of methods is that the output fuzzy set  $MF$  is treated as a distribution for which the average value is evaluated. Among the many methods using this structural concept, we can list:

- i- Max-membership method
- ii- Weighted average method
- iii- Mean-max
- iv- Center of Gravity COG
- v- Center of Gravity for Singleton (COGS)

#### 6.4.2.1 Max-Membership Defuzzifying Method

The Max-membership method is also known as the height method. The crisp value is obtained by considering the peak value of the fuzzy output function. This method is described by the following expression:

$$\mu_B(y^*) \geq \mu_B(y) \text{ for all } y \in Y \quad (3.34)$$

where  $y^*$  is the defuzzified value as illustrated in [Figure-3.12](#).

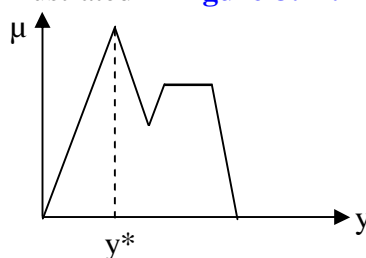


[Figure-3.12](#). Max-membership defuzzification method

#### 6.4.2.2 Weighted Average Method

This method is restricted to symmetrical output membership functions only. It is described by the expression:

$$y^* = \frac{\sum \mu_B(y_c) \cdot y_c}{\sum \mu_B(y_c)} \quad (3.35)$$

where  $\Sigma$  denotes the algebraic sum and  $y_c$  is the centroid of each symmetrical membership function. [Figure-3.13](#) Illustrates this defuzzification method.

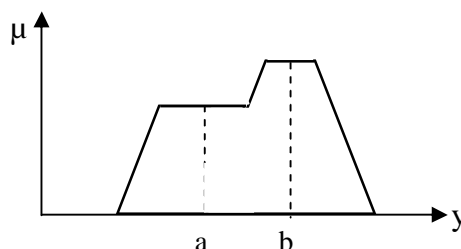


[Figure-3.13](#) Weighted average defuzzification method

### 6.4.2.3 Center of Gravity (COG)

This is the most prevalent and physically appealing of all the defuzzification methods [70]. This method uses the same technique employed to calculate the center of gravity of mass. The defuzzified value is determined as the abscissa of the centroid of the single geometric shape representing the fuzzy output action of the fuzzy system. The centroid divides the area under the membership function into two areas of equal size, **Figure-3.10**.

The center of gravity defuzzified method in the discrete form is defined as:

$$y_{\text{COG}} = \frac{\sum_{i=1}^M \mu_B(y_i) \cdot y_i}{\sum_{i=1}^M \mu_B(y_i)} \quad \text{for } i = 1, 2, \dots, M \quad (3.36)$$

where  $y_{\text{COG}}$  is the centroid of the area which is the defuzzified value of the combined overlapped conclusion fuzzy sets of fired rules,  $M$  is the number of rules,  $y_i$  is the centroid of the area under the membership function  $\mu_B$  and  $\mu_B(y_i)$  is the membership value of  $y_i$ .

Although less convenient for hardware implementation because it requires a large number of multipliers as well as the fact of passing through the whole universe of discourse of the output variable, nevertheless, its continuity and the smoothness of changes of defuzzified values makes it a convenient choice in fuzzy controllers.

### 6.4.2.4 Center of Gravity for Singleton (COGS)

Center of gravity for singleton or COGS defuzzification method is the most widely applied in industry [75]. It has similar smoothness properties of the COG method but it is simple and has relatively good computational complexity.

A rule of a singleton fuzzy system has the following form:

$$R^i: \quad \text{IF } x_1 = A_1^i \text{ AND } x_2 = A_2^i \text{ AND } \dots \text{ AND } x_M = A_M^i \text{ THEN } y = s_i \quad (3.37)$$

where  $s_i$  is a real value called the singleton of rule  $i$ . It determines the position of the output membership function of each rule which is a singleton.

The computation of the control signal value simplifies to a weighted sum since the output MFs do not overlap.

The crisp output value is calculated using the expression of [equation \(3.38\)](#). Singletons  $s_i$  are weighted by fuzzy output membership  $\mu_i$  for  $M$  such outputs, normalized to a degree of truth of 1.

$$y_{\text{COGS}} = \frac{\sum_{i=1}^M \mu_i(s_i) \bullet s_i}{\sum_{i=1}^M \mu_i(s_i)} \quad \text{for } i = 1, 2, \dots, M \quad (3.38)$$

where  $y_{\text{COGS}}$  denotes the result of defuzzification,  $M$  denotes the number of singletons,  $s_i$  is the position of the output singleton  $i$  on the output variable universe of discourse and  $\mu_i(s_i)$  denotes the degree of truth of rule  $i$  according to the fuzzy implication.

# FPGA Technology

---

## 1 Introduction

FPGAs are at the leading edge of each new technology node. They are one of the largest growing segments of the semiconductor industry. An FPGA is a semiconductor device. At the highest level, it is a highly configurable silicon chip. This digital integrated circuit (IC) is designed to be electrically configured by the customer after manufacturing to become almost any customized digital system.

FPGAs belong to a large family of field programmable devices (FPDs). The three main categories of FPDs are: simple programmable logic devices (SPLDs), complex PLDs (CPLDs), and FPGAs. FPDs have grown from being used as simple “glue logic” to provide programmable connectivity (such as address decoding, bus extender, etc) between major components to today’s FPGAs where complete multi-processing system designs can be implemented on a single chip.

The purpose of this chapter is to give an insight to the reader of the challenges to implementing digital controllers with FPGAs. It describes a new paradigm which consists of integrating the microprocessor and the FPGA architecture into a single device. In section two, we relate a brief historical perspective of programmable logic. Section three deals with the architecture of FPGAs. The last section is dedicated to the emerging technology the SoPC along with one of the most versatile and industry-standard processor from Altera’s FPGA design, the Nios® II soft core processor.

## 2 History and Evolution of Programmable Logic devices

The origins of the contemporary FPGA are tied to the development of the first silicon chip invented in the early 1960s by Jack Kilby and Robert Noyce. This showed that it is possible to integrate components on a single block of semiconductor material, hence the name integrated circuit or IC [76].

The process of designing digital hardware has changed dramatically over the past five decades. In the 1960s-1970s and prior the invention of programmable logic, designer of digital logic systems used standard logic devices, the popular Texas Instruments 74xx series of Small Scale Integration and Medium Scale Integration (SSI and MSI) Transistor Transistor Logic (TTL) and the CMOS 4000 series to load printed circuit boards (PCBs). It was the era of hard-wired logic, where the principal concern was to create a design with as few chips as possible in order to reduce cost and minimize board area. Moreover, it necessitated the manufacture of a large number of device types requiring shelves full of data books just to describe them. It also required the designer to design with current device inventory in mind.

Starting from the mid-1970 however, a series of PROM-based ICs were introduced with the idea to have programmable hardware. This concept provided a new way of implementing logic functions. Although the first programmable hardware was the *programmable read only memory* (PROM), it is in 1975 that Ron Cline from Signetics introduced the first truly programmable logic device (PLD), the *programmable logic array* or PLA. The PLA is a two-programmable planes device. These two planes provided any combination of “AND” and “OR” gates as well as sharing of AND terms across multiple ORs. This architecture was very flexible but at that time (10  $\mu\text{m}$  technology) made the device relatively slow and hard to configure because of the limited software tools [77]. To overcome the weaknesses of both the PLA and the PROM, Monolithic Memories Inc (MMI) developed the *programmable array logic* or PAL. This device has a programmable AND array feeding a fixed OR array.

Registered and non-registered PALs were available. The combinational PALs were used to implement Boolean logic functions and could replace a handful of 74xx ICs while registered PALs allowed the implementation of finite state machines. The PAL was a success compared to the PLA and PROM. In literature, PROMs, PLAs and PALs are commonly called simple programmable logic devices or SPLDs.

The advancement in semiconductor technology and the idea of extending the SPLD further produced a device with higher capacity, the *complex PLD* or CPLD. The general architecture of a generic CPLD is depicted in [Figure-4.1](#). It includes an array of blocks called logic array blocks (LABs), a *programmable interconnect array* or PIA and general-purpose input-output pins. The PIA is capable of connecting any LAB input or output to any other LAB. Also, the inputs and outputs of the chip connect directly to the PIA and to LABs.

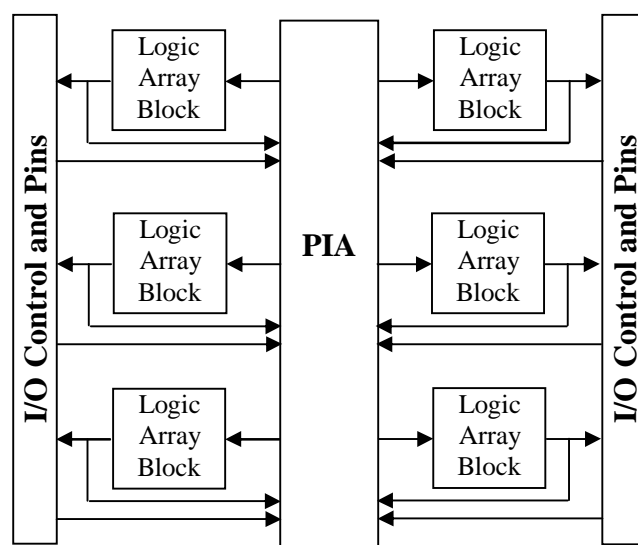


**Figure-4.1** Generic structure of a CPLD

CPLDs brought a new dimension to programmable logic because of the large amount of logic that could fit in a single chip. In theory, we could keep adding logic array blocks to a CPLD to continue the increase of the available logic. However, the extra routing required in the programmable interconnect array for routing between all these logic blocks increases

exponentially until the amount of routing fabric overtakes the amount of the actual logic.

At the end of 1984, instead of surrounding the PIA with logic blocks, Xilinx co-founder Ross Freeman and Bernard Vondershmitt came up with a new arrangement. They reorganized the logic blocks named *configurable logic blocks* (CLBs) as a two-dimensional array of CLBs. These blocks can be interconnected via horizontal and vertical routing channels, similar to the streets in a large city. The first commercially viable FPGA in is born. It is the XC2064. It contains 64 CLBs and surrounded by 58 general-purpose input-output blocks or IOBs. The first FPGA has the equivalent of 2000-ASIC-gate (i.e., 2-input NAND).

### 3 Architecture of FPGAs

**Figure-4.2** depicts the architecture of the early FPGA which is a regular array of programmable logic blocks and programmable interconnect matrix. It comprises programmable logic units that Xilinx calls a configurable logic blocks (CLBs) and what Altera refers to as logic array blocks (LABs) that can be used to realize different digital functions. These logic units are surrounded by a configurable ring of general-purpose I/O pins named input-output elements IOEs by Altera and input-output blocks, IOBs by Xilinx. The FPGA also includes programmable interconnect to allow different blocks to be connected together. In the remaining of this chapter, we will deal with Altera FPGAs and notations.

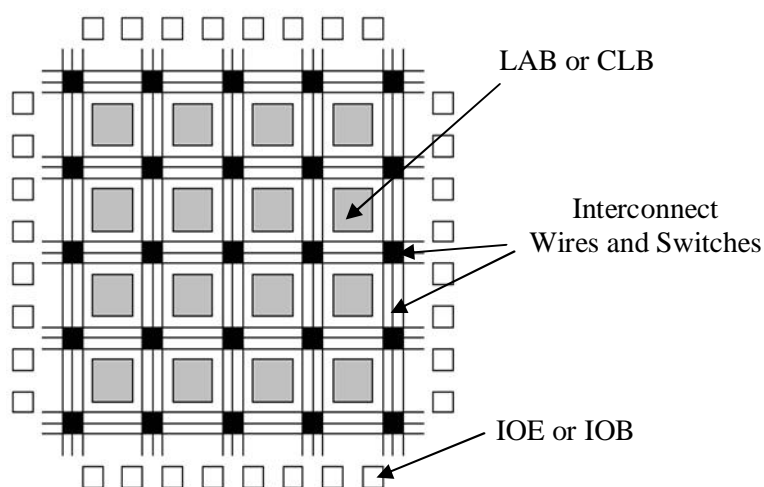


**Figure-4.2** Generic structure of an early FPGA



### 3.1 Logic Element

The core block in the Altera low cost cyclone device family of FPGAs is the logic element (LE). LEs are compact and provide advanced features with efficient logic usage [78]. Figure-3.3 illustrates a typical block diagram of a LE structure. The LE features a 4-input look-up table (LUT), the carry chain connection and a programmable register (or flip flop). The LUT is a function generator that can implement any function of four variables of a combinational logic in an FPGA. It is internally implemented as a set of 2:1 multiplexers functioning as a  $2^4:1$  multiplexer. Multiplexer inputs are programmable, while select lines are the inputs of the implemented functions. The sequential part of the LE comes from the programmable register, which can be configured as a D, T, or JK flip-flop. The carry chain logic is required to link the LE to other LEs. It also supports both register packing and feedback.

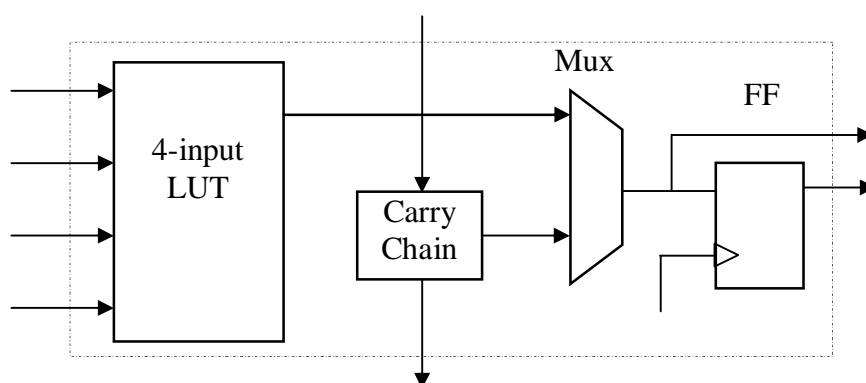


**Figure-4.3** Block diagram of the Altera logic element

### 3.2 Logic Array Block

Moving one level higher in the hierarchy, we have the logic array block or LAB. The LAB consists of 10 to 16 LEs, LAB control signals, LE carry chain, register chain and local interconnect. Figure-3.4 depicts block diagram of a Cyclone II LAB.

The local interconnect transfers signals between LEs in the same LAB. Register chain connections transfer the output of one LE's register to the adjacent LE's register within a LAB [78]. The LAB local interconnect is driven by column and row interconnects and

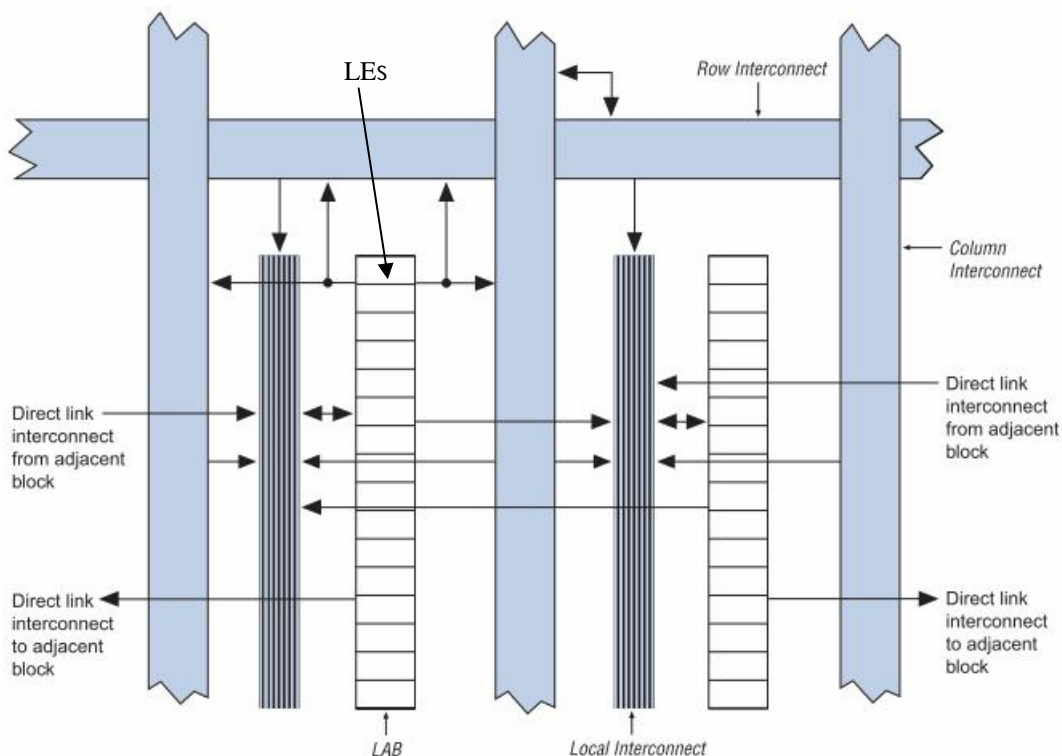


**Figure-4.4** Block diagram of a Cyclone II LAB [78]

LE outputs within the same LAB.

### 3.3 Adaptive Logic Module

In the high performance FPGAs such as the Stratix family, Altera extended the concept of the LE to lead to the so-called *adaptive logic module* or ALM. The ALM provides advanced features with efficient logic usage and is completely backward-compatible. Each LAB in the Stratix-III and above is composed of 10 such ALMs that can be configured to implement logic functions, arithmetic functions, and register functions.

**Figure-4.5** illustrates the high-level block diagram of the Altera Stratix-V ALM [79]. Each ALM contains an 8-input LUT which can be fractured into several possible configurations including two completely independent 4-input LUTs, or a 3-input and 5-input LUTs or a 6-input and 6-input LUTs where 4 of them are common to both LUTs. The ALM also includes two dedicated embedded full adders for fast arithmetic/carry chain and four dedicated registers (flip-flops) for the implementation of sequential functions.

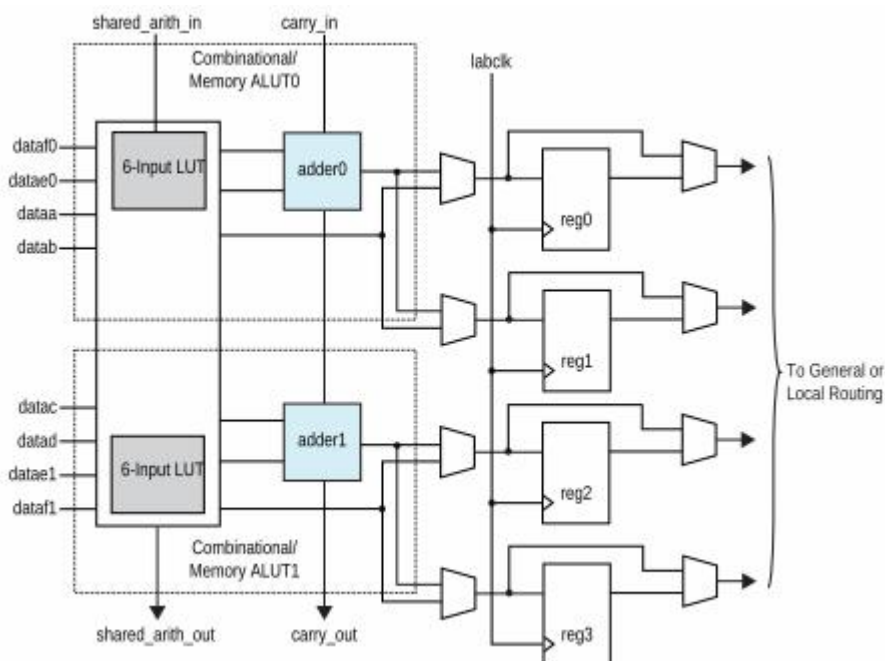


**Figure-4.5** High-level block diagram of the Altera Stratix-V ALM [79]

### 3.4 Integrated Functional Blocks

Early FPGAs were a homogenous sea of logic elements, I/Os and interconnects. Modern FPGA devices are heterogeneous. Only 40% of the area of an FPGA is a logic fabric, the rest of the chip contains an unprecedented level resources: configurable embedded SRAM, high-speed transceivers, high-speed I/Os, embedded multiplier blocks and even embedded hard core processors.

#### 3.4.1 Embedded RAM Blocks

A lot of applications require the use of memory. Today's FPGAs include relatively large chunks of embedded RAM. These devices might contain anywhere between tens to hundreds of these RAM blocks. **Figure-4.6** shows an M4K RAM block of used in the Cyclone family of FPGAs. Each M4K block can implement various types of memory, including true dual-port, simple dual-port, and single-port RAM, ROM, and first-in first-out (FIFO) buffers. The R4, C4, and direct link interconnect from adjacent LABs drive the M4K block local interconnect. The M4K blocks can communicate with LABs on either the left or right side

through these row resources or with LAB columns on either the right or left with the column resources. Up to 16 direct links input connections to the M4K block are possible from the left adjacent LAB and another 16 possible from the right adjacent LAB.

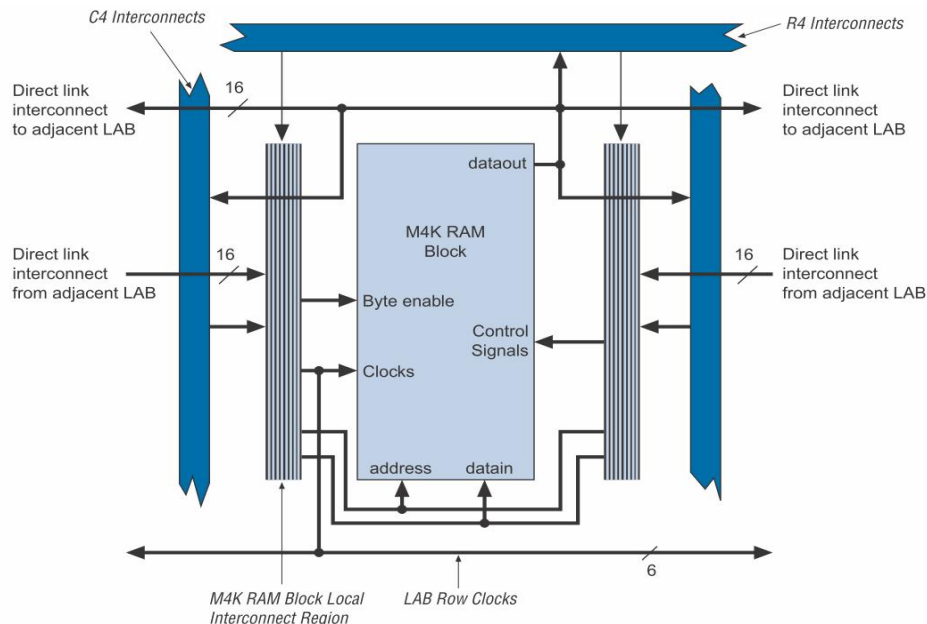


**Figure-4.6** An M4K RAM embedded memory block in a Cyclone FPGA [78]

### 3.4.2 Embedded Multiplier Blocks

Multiplication operations are required by a lot of applications. Time execution of these operations is inherently long if implemented by connecting a large number of programmable logic blocks together using schematic capture or HDL. For this reason modern FPGA devices incorporate special hardwired multiplier blocks optimized for multiplier-intensive digital signal processing (DSP) functions, such as finite impulse response (FIR) filters, fast Fourier transform (FFT) functions, and discrete cosine transform (DCT) functions. These blocks are often located close to embedded RAM blocks. **Figure-4.7** depicts the architecture of an embedded multiplier block contained in the Cyclone family of FPGAs.

The embedded multiplier consists of the multiplier block, the input and output registers and input and output interfaces. Control signals are provided to control the representation of the operands. The latter can be either signed or unsigned operands. The embedded multiplier

block can be used as an 18-bit or 9-bit multiplier. In 18-bit multiplier, it supports a single 18 x 18 multiplier, in 9-bit configuration, it can support two 9 x 9 independent multipliers.

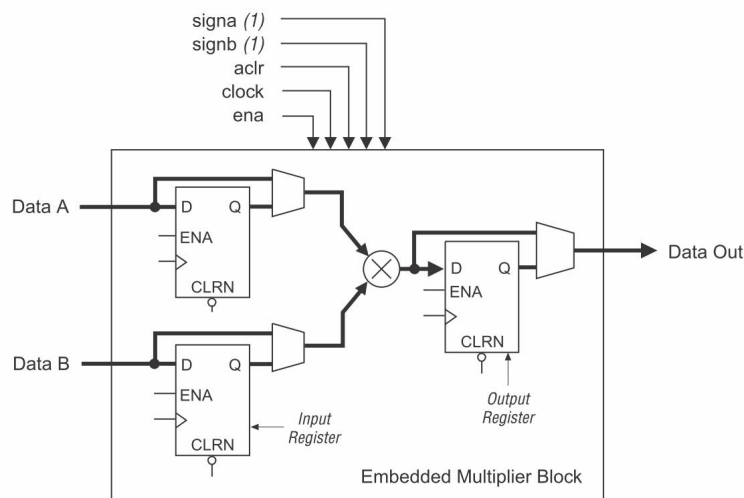


Figure-4.7 Architecture of an embedded multiplier block in a Cyclone FPGA [78]

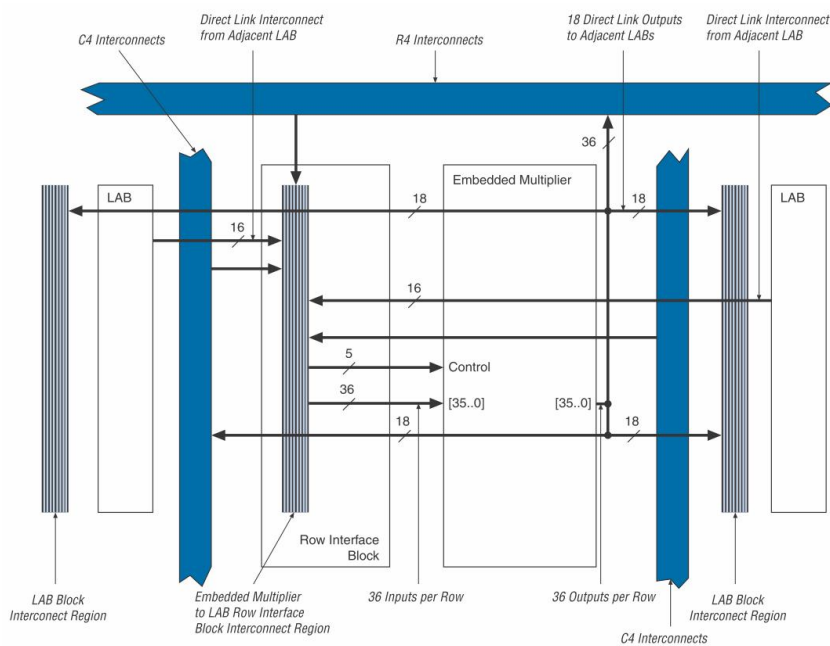


Figure-4.8 Architecture of an embedded multiplier block in a Cyclone FPGA [78]

Figure-4.8 shows the embedded multiplier routing interface. The R4, C4, and direct link interconnect from adjacent LABs drive the embedded multiplier row interface interconnects. The embedded multipliers can communicate with LABs on either the left or right side through these row resources or with LAB columns on either the right or left with the column

resources.

### 3.4.3 Gigabit Transceivers

Today's high-end FPGAs include special hard-wired gigabit transceiver blocks. They operate at incredibly high speeds allowing them to transmit and receive billions of bits of data per second.

### 3.4.4 Embedded Processor Cores

The majority of designs make use of microprocessors in one way or another. Until recently, these appeared as discrete standard off-the-shelf devices on the circuit board. Starting mid-2000, a new semiconductor process allowed major vendors of FPGAs to offer high-end FPGA devices with embedded hard processors along side with the FPGA fabric. Altera Corp offers mid-range Arria V SoC and low-cost Cyclone V SoC FPGA devices with integrated dual-core ARM® (Advanced RISC (Reduced Instruction Set Computer) Machine) Cortex™-A9 MPCore™ processor operating at 1.05 GHz and 925 MHz respectively. These SoCs FPGA integrate an ARM-based hard processor system (HPS) consisting of processor, peripheral, and memory interface with the FPGA fabric using a high-bandwidth interconnect backbone. The high-end and highest bandwidth FPGA devices (100 Gbps), the Stratix 10, includes a 64-bit quad-core ARM Cortex™-A53 processor in its 14 nm FPGA fabric [80]. Xilinx [81] also has integrated hard core processors in its FPGA devices. The high-end Virtex-4 (and above) and the mid-range Kintex family of FPGA include one or two IBM PowerPC 405 or 440 32/64-bit processor cores, whereas the Zynq-7000 (lastest of Xilinx) all programmable SoC integrates a dual-core ARM® Cortex™-A9 processor.

Today, it makes sense to move all of the tasks used to be performed by the external microprocessor into the internal core [82]. This provides a number of advantages the least of which are reduced cost, and reduced circuit board while improving performance and maximizing reliability.

## 4 FPGA Programming Technologies

Three technologies are nowadays available for implementing reconfigurable FPGAs. These are defined based on the way the routing between logic elements is configured. They are: SRAM-, Flash- and Antifuse-based FPGAs.

### 4.1 SRAM-Based FPGA

The dominant type of FPGA devices is SRAM-based. This type is at the forefront of FPGA technology, all large FPGAs use this technology. Static memory cells are distributed throughout the FPGA fabric to provide configurability. These memory cells (an array of latches) is used to program interconnect and look up table (LUT) function levels. Their major advantage is that new design ideas can be quickly implemented and tested. The main downside is their volatility. Whenever the device is powered-off, the array of latches is cleared losing the configuration of the design (bit-stream information) mapped into the FPGA chip. Therefore, a back up battery is required when power is removed from the system, or the programming information must be stored in a non-volatile media so that the FPGA can be configured at power-on. In general, an electrically erasable programmable read only memory (EEPROM) or flash memory device is used for this purpose.

### 4.2 Antifuse-Based FPGA

Antifuse programming technology is one-time programmable (OTP), that is, it cannot be used for prototyping. Moreover, unlike SRAM-based FPGAs which are configured on site, antifuse-based FPGAs are configured off-line using a special device programmer. Antifuse are non volatile. This feature is of particular interest in some applications such as military and aerospace because of high radiation tolerance. This type of FPGA is only fabricated by Microsemi (previously Actel).

### 4.3 Flash-Based FPGA

Flash-based FPGAs use non-volatile memory cells to provide configurability. Their main

advantage is they do not require an external non-volatile memory to hold the configuration information of the design. The major downside of this technology is the relatively smaller density of integration, that is, flash cells are much larger than SRAM cells. They are also used in military and aerospace because of high radiation tolerance.

## **5 Applications of FPGAs**

Nowadays, FPGA devices are everywhere. They are widely used in both research and industry. They provide market solutions and are key elements in a broad range of application areas. In military applications FPGAs are found in radar and sonar as well as in secure communications. Modern high definition video camera and displays integrate FPGA in their circuitry. FPGA devices are widely used in industry. We can find them in motor/motion control, smart energy, machine vision, medical imaging and industrial Ethernet.

Another area of application of FPGA devices is application-specific integrated circuit (ASIC) and application specific standard product (ASSP) prototyping. Because the FPGA platforms provide a faster, smoother path to delivering an end working product, they are used in the verification of both register transfer level (RTL) and initial software development of ASIC and ASSP devices. This standard practice not only provides the opportunity to have a hardware platform early in the design cycle, it also decreases development time and reduces the risk of silicon failure.

## **6 The Nios® II and SoPC Builder**

### **6.1 The Nios® II Processor**

The Netware Input-Output Subsystem, Nios® II, is the Altera's flagship intellectual property (IP) second generation soft-core processor. It is a 32-bit embedded processor designed and optimized for the use in FPGA designs targeting Altera's mainstream FPGA families [83-84].

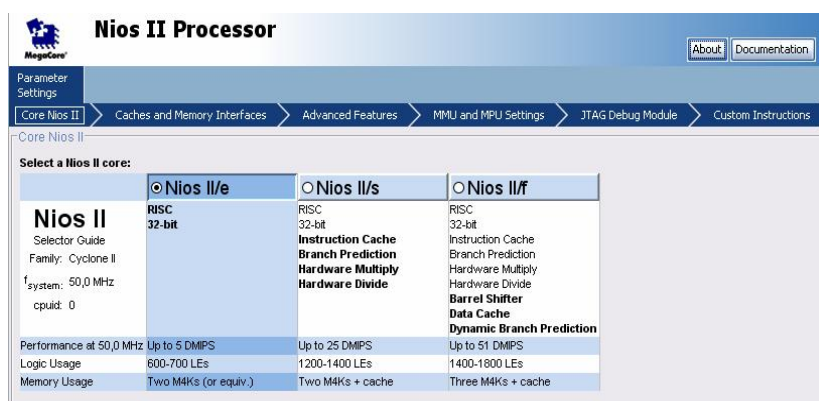


It is a general-purpose pipelined scalar Reduced Instruction Set Computer (RISC) and features Harvard memory architecture (separate instruction and data buses). This load-store processor core features a full 32-bit data path, instruction word, and address space with integer only arithmetic logic unit.

The processor has 32 general-purpose registers with a MIPS-ISA-like (Microprocessor without Interlocking Pipe Stages – Instruction Set Architecture) instruction format. The arithmetic and logic operations are performed on operands in the general purpose registers. Nios® II processor uses a memory-mapped scheme for accessing memory and peripherals, where each component is assigned a unique set of memory addresses in which byte addresses in a 32-bit word are assigned in little-endian style. The architecture of the processor has 32 internal hardware interrupts and can support external interrupt controller interface for more interrupt sources.

The Nios® II is a soft-core processor. It is a hardware description language (VHDL or Verilog) model of a specific microprocessor customized as an intellectual property (IP) core. It can be instantiated and synthesized for an Altera’s FPGA target using the Quartus II software development suite tools. Unlike a “hard” core processor which is implemented in dedicated silicon of the FPGA; a soft-core processor is targeted onto the FPGA’s fabric logic elements.

The Nios ® II processor comes in three variants cores to trade FPGA area and power



The screenshot shows the 'Nios II Processor' configuration window. It has a navigation bar with tabs: 'Core Nios II', 'Caches and Memory Interfaces', 'Advanced Features', 'MMU and MPU Settings', 'JTAG Debug Module', and 'Custom Instructions'. The 'Core Nios II' tab is active, showing a table to 'Select a Nios II core:'. The table compares three variants: Nios II/e (selected), Nios II/s, and Nios II/f. Each variant lists its RISC architecture (32-bit), performance (DMPS), logic usage (LEs), memory usage (M4Ks), and supported features like Instruction Cache, Branch Prediction, Hardware Multiply, Hardware Divide, Barrel Shifter, Data Cache, and Dynamic Branch Prediction.

	<input checked="" type="radio"/> Nios II/e	<input type="radio"/> Nios II/s	<input type="radio"/> Nios II/f
<b>Nios II</b>	RISC 32-bit	RISC 32-bit	RISC 32-bit
Selector Guide			
Family: Cyclone II			
f <sub>system</sub> : 50.0 MHz			
cpuId: 0			
Performance at 50.0 MHz	Up to 5 DMPS	Up to 25 DMPS	Up to 51 DMPS
Logic Usage	600-700 LEs	1200-1400 LEs	1400-1800 LEs
Memory Usage	Two M4Ks (or equiv.)	Two M4Ks + cache	Three M4Ks + cache
	Instruction Cache Branch Prediction Hardware Multiply Hardware Divide	Instruction Cache Branch Prediction Hardware Multiply Hardware Divide	Instruction Cache Branch Prediction Hardware Multiply Hardware Divide Barrel Shifter Data Cache Dynamic Branch Prediction

Figure-4.9 The 3 flavors of the Nios® II soft core processor [79].

consumption for speed of execution. These flavors are: fast, standard and economy, **Figure-4.9**. Each core version modifies the number of pipeline stages, cache memories for data and instructions, number of cycles per instruction, addressable memory space, and hardware or software implementation of multiplication and division operations and so on.

- i- The fast version (Nios® II/f) is designed for performance-critical applications at the expense of core size. It includes separate optional instruction and data caches, where caches are implemented in the FPGA memory blocks. It employs a 6-stage pipeline to achieve maximum DMIPS/MHz. This high performance variant provides optional hardware multiply, divide, and shift options to improve arithmetic performance. It executes one instruction per cycle. When the memory management unit (MMU) is present, the processor can access up to 4 GBytes of memory.

To give the processor a fast access to the on-chip memory, the Nios® II fast core architecture provides optional tightly-coupled memory interface arrangements (memory connected directly to the processor) for both instructions and data. When the tightly-coupled memory is present, its access bypasses cache memory.

- ii- The standard core version (Nios® II/s) is optimized for medium-performance and cost-sensitive applications. It employs a 5-stage pipeline. Unlike the fast version, the standard has an instruction cache, but no data cache.
- iii- The economy variant (Nios® II/e) is designed with the smallest possible logic utilization of FPGA. It is not pipelined (one stage) and contains no cache. It has a limited feature set, and many settings are not available when this version is selected, **Figure-4.9**. The economy variant executes at most one instruction per six clock cycles. The major advantage of this core is it is licence free while the /f and /s versions require a \$500/year licence.

---

While the performance and size are different, the three flavours share the same native instruction set.

## 6.2 The SoPC Builder

The SoPC Builder is a system integration tool included as part of the Altera's Quartus II software development tool environment. It is a powerful tool to construct microprocessor-based systems on an FPGA. It streamlines the process of integrating blocks of intellectual properties (IPs) and accelerates development of system-on-a-programmable-chip designs compared to traditional, manual integration methods. The SoPC platform also allows the integration of custom I/O peripherals and hardware accelerators into a system. The designer is responsible for the development of hardware as well as the software.

The tool consists of two major parts: a graphical user interface or GUI and a system generator program [85]. [Figure-4.10](#) depicts a screenshot of a SoPC builder system. The menu on the left side is the library of available IP cores from which the designer picks up the desired components required by the design. This library includes: the Nios® II soft core processor, microcontroller peripherals such as interval timer and general-purpose I/O interface. The SoPC Builder library contains serial communication components such as the universal asynchronous receiver transmitter (UART) and the serial peripheral interface (SPI). It also provides a variety of controllers to interface with off-chip devices such as SDRAM controller and flash memory interface.

The central part, the contents page, is where the system is built. The construction of the system is accomplished by means of a drag-and-drop style. The GUI is used to select and customize system components from a rich set of pre-made SoPC Builder components. The required components are dragged and parameterized in the contents page. The connections panel column shows a graphical representation of how the components are interconnected.

Use	Connections	Module Name	Description	Clock	Base	End	IRQ
<input checked="" type="checkbox"/>		On_Chip_RAM	On-Chip Memory (RAM or ROM)				
<input checked="" type="checkbox"/>		s1	Avalon Memory Mapped Slave	clk_0	0x00008000	0x0000ffff	
<input checked="" type="checkbox"/>		Nios_2_CPU	Nios II Processor				
<input checked="" type="checkbox"/>		instruction_master	Clock Input	clk_0			
<input checked="" type="checkbox"/>		data_master	Avalon Memory Mapped Master				
<input checked="" type="checkbox"/>		d_irq	Interrupt Receiver				IRQ 0
<input checked="" type="checkbox"/>		ftag_debug_module	Avalon Memory Mapped Slave		0x00010800	0x00010fff	IRQ 31
<input checked="" type="checkbox"/>		custom_instruction_master	Custom Instruction Master				
<input checked="" type="checkbox"/>		JTAG_UART	JTAG UART				
<input checked="" type="checkbox"/>		avalon_ftag_slave	Avalon Memory Mapped Slave	clk_0	0x00011098	0x0001109f	
<input checked="" type="checkbox"/>		irq	Interrupt Sender				
<input checked="" type="checkbox"/>		SysID	System ID Peripheral	clk_0	0x00011090	0x00011097	
<input checked="" type="checkbox"/>		Ch_Select	PIO (Parallel I/O)	clk_0	0x00011000	0x0001100f	
<input checked="" type="checkbox"/>		EOC	PIO (Parallel I/O)	clk_0	0x00011030	0x0001103f	
<input checked="" type="checkbox"/>		ALE_ST	PIO (Parallel I/O)	clk_0	0x00011040	0x0001104f	
<input checked="" type="checkbox"/>		Error_EW	PIO (Parallel I/O)	clk_0	0x00011050	0x0001105f	
<input checked="" type="checkbox"/>		cError_EW	PIO (Parallel I/O)	clk_0	0x00011060	0x0001106f	
<input checked="" type="checkbox"/>		cError_NS	PIO (Parallel I/O)	clk_0	0x00011080	0x0001108f	
<input checked="" type="checkbox"/>		cError_NS	PIO (Parallel I/O)				
<input checked="" type="checkbox"/>		s1	Avalon Memory Mapped Slave	clk_0	0x00011070	0x0001107f	
<input checked="" type="checkbox"/>		clk_0	Clock Source				

Figure-4.10 Screenshot of a SoPC Builder system

Finally, the beginning and end of the memory addresses of the various components used in the design are shown under Base and End columns on the right side of the SoPC Builder GUI window. The addresses of all the slave components can be assigned either manually or automatically generated by the SoPC builder generator.

The system interconnect fabric or SIF for memory-mapped interfaces is a high-bandwidth interconnect structure for connecting components that use the Avalon<sup>®</sup> Memory-Mapped (Avalon-MM) interface. The system interconnect fabric consumes less logic, provides greater flexibility, and higher throughput than a typical shared system bus. Figure-4.11 shows a simplified diagram of the system interconnect fabric in an example memory-mapped system with multiple masters. The SIF logic provides the following functions: Address Decoding, Datapath Multiplexing, Wait State Insertion, Pipelined Read Transfers, Dynamic Bus Sizing, Arbitration for Multi-master Systems, Arbiter Details, Interrupts and Reset Distribution [85].

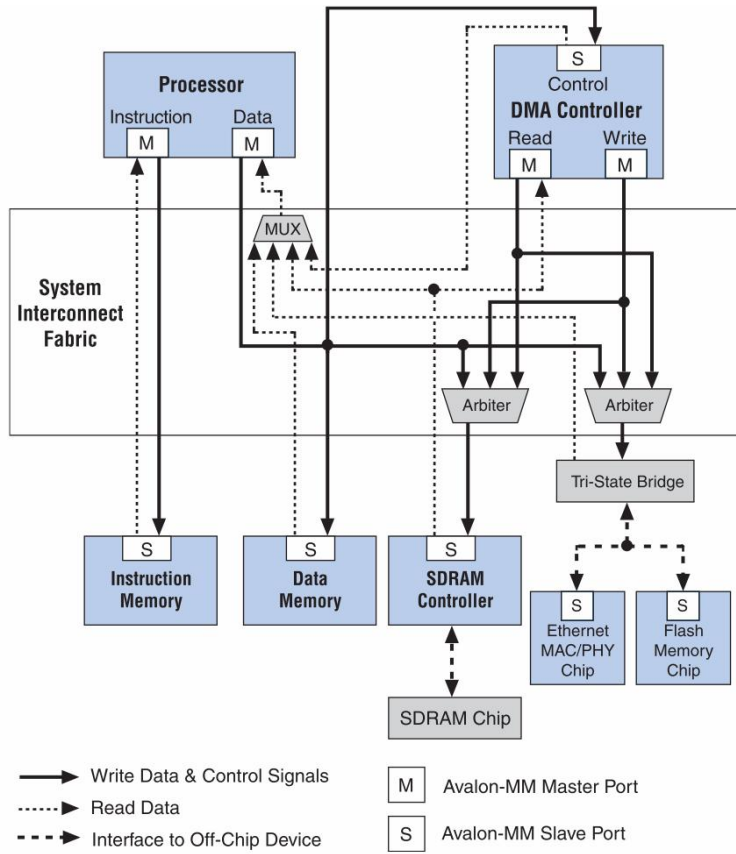


Figure-4.11 System interconnect fabric with multiple mastering components [85]

---

## Design of the Fuzzy Logic Module

---

### 1 Introduction

Sun is permanently changing its position in the sky. Everyday, it moves from east to west between sunrise and sunset; the azimuth movement. It also, moves from north to south throughout the course of the year; the elevation movement. Because the energy extracted from the PV panel is at its maximum when the surface of the solar panel is perpendicular to the sun's rays, then an ideal tracking system should maintain a solar panel accurately pointing towards the sun, compensating for both changes in the azimuth and elevation angles of the sun with respect to the panel throughout the day. It is desirable to develop a control system based on fuzzy logic methodology to fulfill these requirements.

Fuzzy control is based on fuzzy logic which is close in spirit to human thinking and natural language [86]. It provides a convenient way to build the control strategy by requiring only qualitative knowledge for the behavior of the control system. In recent years, fuzzy control is used to enhance control engineering solutions. It brought high promising alternatives to conventional controllers by providing higher degree of robustness (immunity to external disturbance) and by achieving better performances (short rise-time, small overshoot) over linear controllers [87]. Fuzzy controllers revolutionized the field of control engineering by their ability to perform process control by the utilization of human knowledge, thus enabling solutions to control problems for which mathematical models may not exist, or may be too difficult or computationally too expensive to construct [88].

2 Structure of the Fuzzy Logic Module

The high-level fuzzy logic module consists of two independent fuzzy-like PD-type controllers; one to steer the azimuth angle and one to steer the tilt (elevation) angle of the dual-axis sun tracker. The module controls the two stepper motors used as mechanical actuators to position the solar panel’s surface perpendicular to the sun intensity vector to harness maximum energy from the sun. **Figure-5.1** shows the high-level structure of the dual-axis sun tracking fuzzy logic module.

The reason behind the use of the fuzzy-like PD-type controller is driven by the fact this controller has a simple control structure compared to the proportional-integral-derivative (PID) type gives better sensitivity and increases the overall stability of the closed loop system. Also, the fuzzy-like PD-type controller reliably predicts large overshoots and adds damping to the overall closed loop system making it an excellent solution in position control [89].

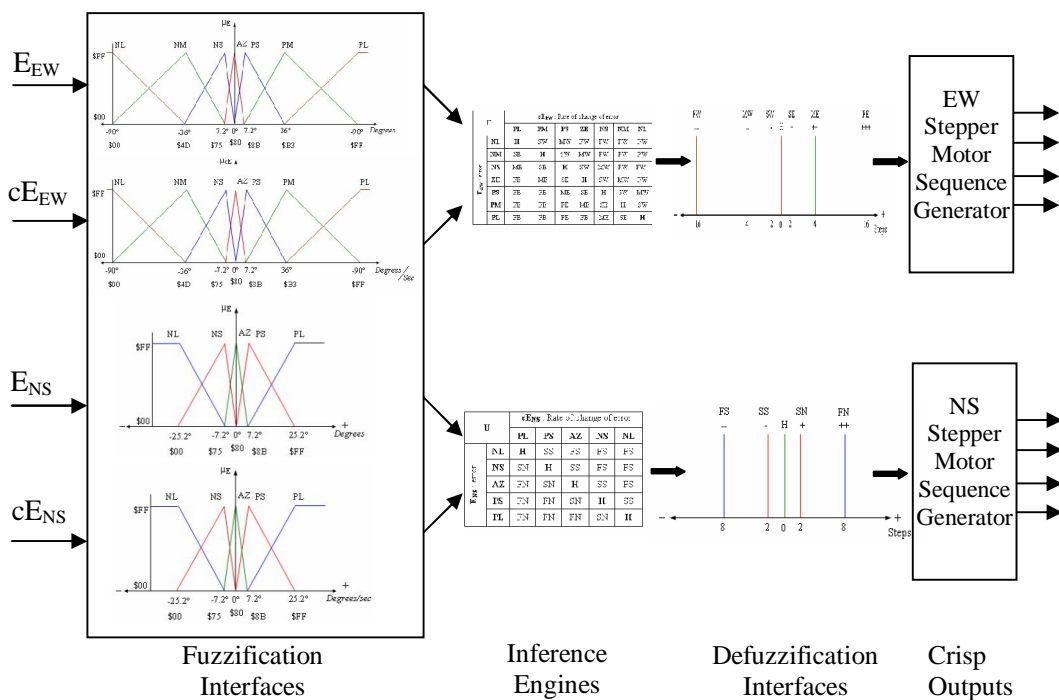


**Figure 5.1** Operational block diagram of the intelligent dual-axis sun tracking fuzzy logic module

3 Fuzzy Logic Controller Design Flow

Most works in fuzzy control use the error and the rate of change of error as input variables

regardless of the complexity of controlled plants [72].

Figure-5.2 depicts the sun tracking fuzzy logic module with errors and rate of change of errors generator. The crisp data discriminating the position of the sun in the sky with respect to the panel's surface are measured by the data acquisition unit via the ADC interface. The state variables inputs are the angular error  $E_{EW}$  ( $E_{NS}$ ) defined as the voltage differences between the signals corresponding to irradiances received on each pair of sensors and its rate of error change  $cE_{EW}$  ( $cE_{NS}$ ). The commonly used approach to obtain these quantities is the use of differential amplifiers and differentiators. In this work these quantities are computed in software using the digital error and rate of change of error generator which is implemented onto the FPGA resources. This approach does not make use of any extra analog components. It is thereby, more accurate, reliable and cost effective. The evaluation of the angular errors and their rates of change are given by Equations 5.1 through 5.4, [90].

$$E_{EW}(k) = V\_LDR_E(k) - V\_LDR_W(k) \tag{5.1}$$

$$E_{NS}(k) = V\_LDR_N(k) - V\_LDR_S(k) \tag{5.2}$$

$$cE_{EW}(k) = \Delta(E_{EW}(k)) = E_{EW}(k) - E_{EW}(k-1) \tag{5.3}$$

$$cE_{NS}(k) = \Delta(E_{NS}(k)) = E_{NS}(k) - E_{NS}(k-1) \tag{5.4}$$

where  $V\_LDR_i(k)$  is the digital equivalent value of the sunlight irradiance received on  $LDR_i$  and  $E_i(k)$  and  $E_i(k-1)$  are respectively the present and previously measured errors at a one second (1-sec) sampling time.

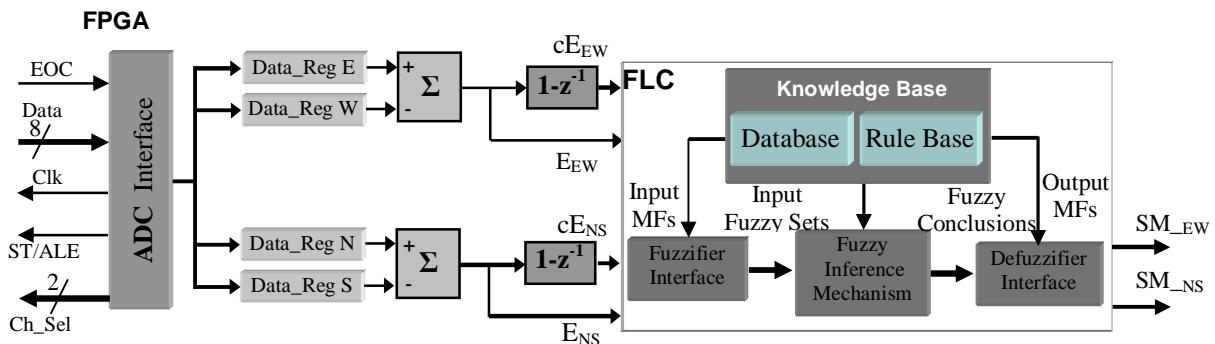


Figure-5.2 Sun tracking fuzzy logic module with errors and rate of change of errors generator



The fuzzy logic controller design flow consists of the following steps:

- Identify the input state variables and the ranges spanned by each variable.
- Identify the output variables and the ranges spanned by each one.
- Choose appropriate scaling factor for the input variables in order to normalize the variables to the  $[0, 1]$  or  $[-1, 1]$  interval.
- The shapes of membership functions have to be fixed.
- The number of membership functions and their locations on the universe of discourse has to be determined for every input state variable.
- Assign a linguistic label to each membership function
- Create the degree of fuzzy membership function for each variable
- Construct the rule base
- Use fuzzy approximate reasoning to infer the output contributed from each rule.
- Aggregate the fuzzy outputs recommended by each rule.
- Apply defuzzification to form a crisp output
- Choose appropriate post-processing to suite the crisp output of defuzzification module into actual inputs for the process.

#### 4 The Azimuth Fuzzy Logic Controller

The state variable inputs of the azimuth fuzzy-like PD-type controller are the angular error  $E_{EW}$  and its rate of change of error  $cE_{EW}$ . The universe of discourse for the azimuth angular error is defined as the maximum deviation from the optimal position of the solar panel with respect to sun rays. **Figure-5.3** illustrates the sun vector hitting a solar panel. The incident angle  $\alpha$  is zero when sun rays are normal to the solar panel's surface. This angle can range from  $-90^\circ$  at sunrise to  $+90^\circ$  at sunset.

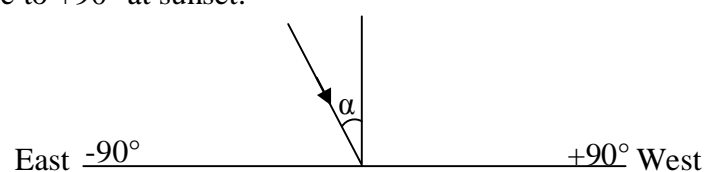


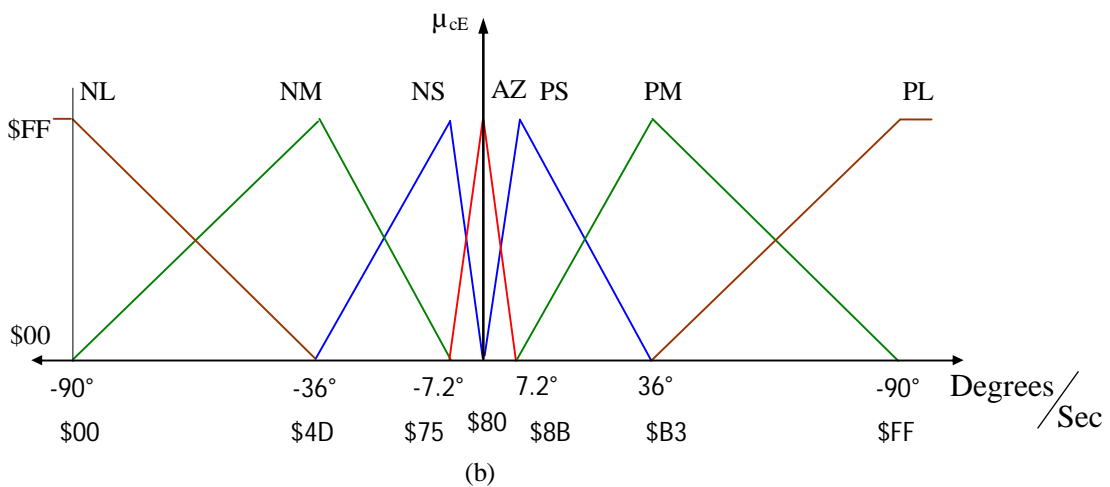
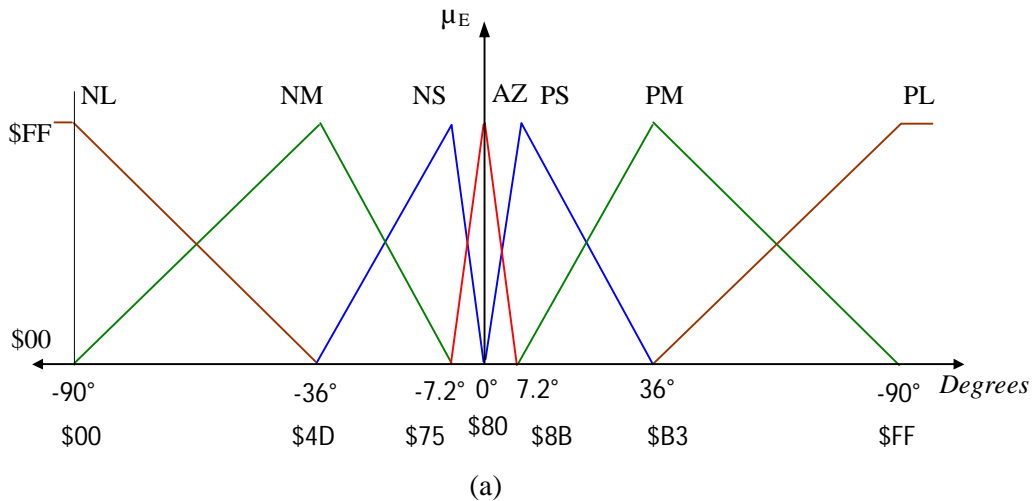
**Figure-5.3** Incident angle of sunrays with solar panel surface

4.1 Input/Output Membership Functions

The azimuth error,  $E_{EW}$  and the rate-of-change of azimuth error,  $cE_{EW}$  are fuzzily partitioned in seven fuzzy sets with triangle-like membership functions distributed in the interval  $E_{EW} \in [-90^\circ, +90^\circ]$  and  $cE_{EW} \in [-90^\circ/\text{sec}, +90^\circ/\text{sec}]$  respectively.

We used seven discrete levels to provide an adequate resolution for the azimuth angle due to its sensitivity. The size, shape and labels of the membership functions representing the two input variables are illustrated in **Figure-5.4** (a) and (b).

The input variables are quantified into fuzzy sets defined by linguistic labels: Negative large (NL), Negative Medium (NM), Negative Small (NS), Approximate Zero (AZ), Positive Small (PS), Positive Medium (PM) and Positive Large (PL).



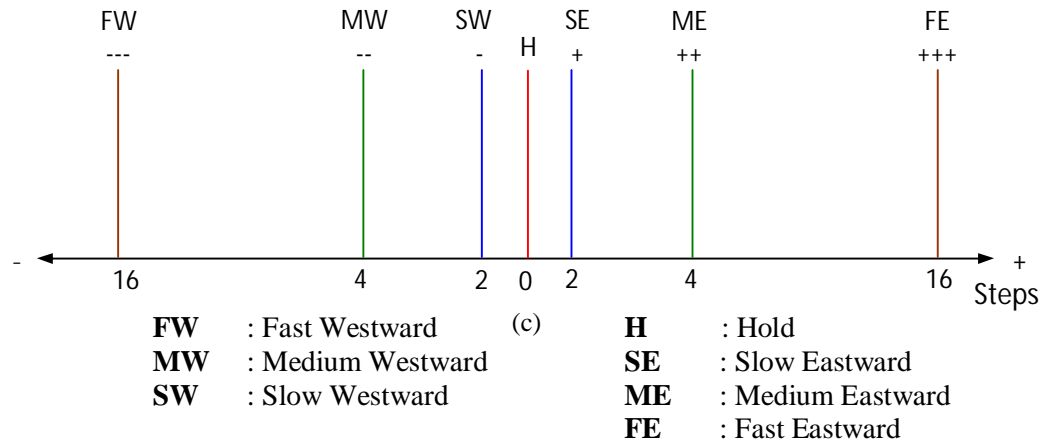


**Figure-5.4** (a) MFs of the angular error  $E_{EW}$  in degrees. (b) MFs of  $cE_{EW}$  in degrees/sec  
(c) Singleton membership functions of the output variable ‘U’ in number of steps.

The membership functions representing the input values degree of truth for each set are triangular functions with sufficient overlap provided for neighbor fuzzy sets. At any point of the universe of discourse, only two fuzzy sets will have non-zero degree of membership.

This overlapping permits a smooth mapping of the system and reduces the computation complexity. We used asymmetrical MFs with coarse resolution for large errors and fine resolution in the vicinity of the origin (desired posture of the solar panel) [86]. Since most of the action rules operate at the center of the universe of discourse, the scope of the “AZ” membership function is made narrow. This headband of the controller is set to  $\pm 3.6^\circ$  which is a multiple of the stepper motor’s step angle. All the MFs are however, symmetrical for positive and negative values of the state variables.

The values of the x-axis of the membership functions of the error and rate of change of error state variable inputs are quantized by a biased (a bias of \$80) 8-bit words (\$00-\$FF). The bias hexadecimal 80 (\$80) is for the zero. Values less than \$80 are for negative deviations and values greater than \$80 are for positive deviations. The y-axis representing the grade or degree of membership (DoM) is scaled as an 8-bit unsigned value \$00 to \$FF [90].

The control output signal of the fuzzy-like PD-type controller is the number of steps applied to the azimuth stepper motor phases computed by the fuzzy inference engine. It is characterized by seven singleton membership functions over the interval [-16, +16] with the

support values equal to 1. The seven singletons defined by the seven linguistic terms: FW fast westward, MW medium westward, SW slow westward, H hold, SE slow eastward, ME medium eastward, and FE fast eastward as depicted in **Figure-5.4 (c)** [90].

**4.2 Construction of Rule Base**

The derivation of the control rules is heuristic and relies on the qualitative knowledge for the behaviour of the process to control.

The fuzzy rules are derived in such a way that the deviation (azimuth angular error) from the desired posture can be minimized to achieve the control objective [86].

The general equation of the proportional-derivative (PD)-type controller is given by

$$u(k) = k_p e(k) + k_d \Delta e(k) \tag{5.5}$$

where  $k_p$  and  $k_d$  are the proportional and differential gain coefficients,  $e$  is the error,  $\Delta e$  is the change of error.

The fuzzy-like PD-type FLC consists of rules of the form

$$R^i: \quad \text{IF } E_{EW} \text{ is } A_1^i \text{ AND } cE_{EW} \text{ is } A_2^i \text{ THEN } u \text{ is } B^i \quad \text{for } i= 1, \dots, 7 \tag{5.6}$$

$u$		$cE_{EW}$ : Rate of change of error						
		PL	PM	PS	AZ	NS	NM	NL
$E_{EW}$ : error	NL	H <sup>1</sup>	SW	MW	FW	FW	FW	FW <sup>7</sup>
	NM	SE	H	SW	MW	FW	FW	FW
	NS	ME	SE	H	SW	MW	FW	FW
	AZ	FE	ME	SE	H	SW	MW	FW
	PS	FE	FE	ME	SE	H	SW	MW
	PM	FE	FE	FE	ME	SE	H	SW
	PL	FE <sup>42</sup>	FE	FE	FE	ME	SE	H <sup>49</sup>

**Table-5.1** The 7x7 fuzzy rule-base matrix used in the fuzzy-like PD-type FLC for the vertical pivot shaft (east-West)

where  $A_1^i$  and  $A_2^i$  are the linguistic values representing the  $i$ -th antecedent pairs and the  $B^i$  is the fuzzy set representing the  $i$ -th conclusion.

Since both state variable inputs have seven MFs, then the total number of non-conflicting fuzzy if-then rules is  $7 \times 7 = 49$ .

**Table-5.1** summarizes these rules for the azimuth angle fuzzy-like PD type FLC in a matrix form. The control rules are best visualized as a 2-dimensional matrix structure where the most left column and the top row contain the fuzzy sets of the two antecedents  $E_{EW}$  and  $cE_{EW}$  respectively. The fuzzy sets of the output control action are shown in the body of the matrix.

The matrix can be partitioned into several subgroups. The central part of which for example describes the situation where the azimuth angular error and its rate of change are both either small or null, i.e., the misalignment is very small. Therefore, the control action to correct this error should be null (H) or small in magnitude ((+) or (-)). In the situation where the panel surface is too far from the desire posture (negative large or positive large), then, if the rate of change of error is of the same sign, fast control action is provided ((+++ or ---)) to position the panel. The latter situations are illustrated by the upper right and lower left corners. Referring to the rule base matrix, the physical meanings of some rules are described below.

**Rule 7:** IF  $E_{EW}$  is NL AND  $cE_{EW}$  is NL THEN  $u$  is FW

The statement “angular error is negative large” represents the situation where  $LDR_W$  receives significantly more sunlight than  $LDR_E$ , and “change in error ( $cE_{EW}$ ) is negative large” can represent the situation where the tracker is moving eastward. Therefore, to track the sun, the controller must apply a large control action “fast westward” to move the tracker westward.

**Rule 25:** IF  $E_{EW}$  is AZ AND  $cE_{EW}$  is AZ THEN  $u$  is H

This rule describes the situation the deviation is within the fuzzy AZ zone, and in the presence

of a rate of change of error within the same zone, then, the controller holds current situation, meaning that the sun is tracked.

**Rule 32:** IF  $E_{EW}$  is PS AND  $cE_{EW}$  is AZ THEN  $u$  is SE

The statement “if azimuth error is positive small AND change in error is nearly zero” represents the situation where the solar panel is slightly misaligned eastward and since the change in error is nearly zero, then the controller should move the panel slightly eastward, “slow eastward”.

**Rule 49:** IF  $E_{EW}$  is PL AND  $cE_{EW}$  is NL THEN  $u$  is H

This rule quantifies the situation where the panel is misaligned with the eastern LDR receiving more sunlight than the western one. And because, the rate of change of the error is large and of opposite sign, then, it is not necessary to apply any action, the tracker will end up tracking the sun (self-correcting situation).

The matrix presents noticeable features. It has a skew symmetric property, that is, the eastward linguistic values (SE, ME and FE) of the control action are placed below the diagonal whereas the westward linguistic values (SW, MW and FW) are above the diagonal with a hold control action placed along the diagonal (H). Another feature of this matrix is that, in either direction, the number of steps to be applied for the actuators increases with increasing distance from the diagonal.

The parameters characterizing the azimuth FLC are as follows:

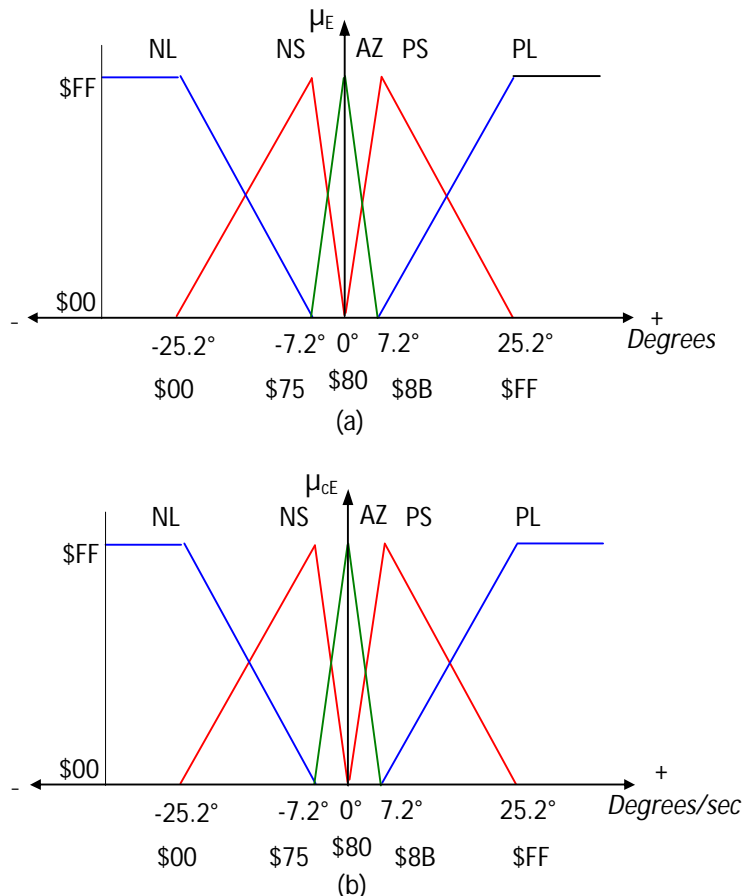
- |                            |                                |
|----------------------------|--------------------------------|
| 1. Number of inputs:       | 2                              |
| 2. Antecedent MFs          | seven triangular per fuzzy set |
| 3. Output                  | 1                              |
| 4. Consequent MFs          | seven singletons               |
| 5. Maximum number of rules | 49                             |
| 6. Inference method        | max-min                        |
| 7. Defuzzification         | COGS                           |

5 The Elevation Fuzzy Logic Controller

The second FLC adjusts the tilt angle of the tracker. It runs in parallel with the azimuth angle controller. The inputs to this fuzzy controller are the elevation deviation or  $E_{NS}$  and the rate of change of error  $cE_{NS}$ . The output is the control action that drives the second stepper motor.

The declination angle is the angle made by the line joining the centers of the sun and the earth with its projection on the equatorial plane and it varies from  $-23.45^\circ$  to  $+23.45^\circ$ . Because the change is on seasonal basis only, we provided a smaller number of quantization level by partitioning the  $[-23.45^\circ, +23.45^\circ]$  universe of discourse using five triangle shaped MFs. The linguistic terms used are: NL, NS, AZ, PS and PL. The driving force has five singleton MFs: FN, SN, H, SS, and FS.

Figure-5.5 depicts the graphical representation of the MFs of the elevation error and its rate of change.



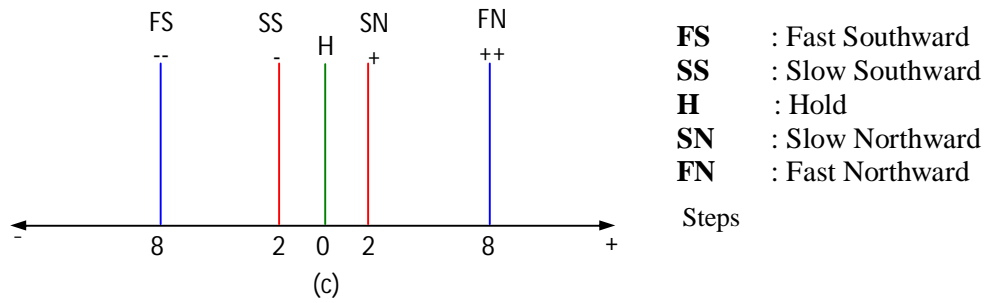


**Figure-5.5** (a) MFs of the angular error  $E_{NS}$  in degrees. (b) MFs of  $cE_{NS}$  in degrees/sec  
(c) Singleton membership functions of the output variable ‘U’ in number of steps.

**Table-5.2** summarizes these rules for the elevation angle fuzzy-like PD type FLC in a matrix form. The control rules are best visualized as a 2-dimensional matrix structure where the most left column and the top row indicate the fuzzy sets of the two antecedents  $E_{NS}$  and  $cE_{NS}$  respectively. The fuzzy sets of the output control action are shown in the body of the matrix.

$\tilde{U}_{NS}$		$cE_{NS}$ : Rate of change of error				
		PL	PS	AZ	NS	NL
$E_{NS}$ : error	NL	<b>H</b> <sup>1</sup>	SS	FS	FS	FS
	NS	SN	<b>H</b>	SS	FS	FS
	AZ	FN	SN	<b>H</b>	SS	FS
	PS	FN	FN	SN	<b>H</b>	SS
	PL	FN	FN	FN	SN	<b>H</b> <sup>25</sup>

**Table-5.2** The 5x5 fuzzy rule-base matrix used in the fuzzy-like PD-type FLC for the horizontal pivot shaft (North-South)

Similar to the rule base matrix of the azimuth fuzzy controller, the rule base of the elevation fuzzy controller also exhibits a skew symmetric property, that is, the northward linguistic values (SN and FN) of the control action are placed below the diagonal whereas the southward linguistic values (SS and FS) are above the diagonal with a hold control action placed along the diagonal (H). Another feature of this matrix is that, in either direction, the number of steps to be applied for the actuators increases with increasing distance from the diagonal.



---

**Chapter 6**

---

**Hardware/Software Codesign Implementation**

---

**1 Introduction**

This chapter describes the proof-of-concept implementation of the FPGA-based fuzzy logic controlled dual-axis sun tracking system on an Altera low-cost Cyclone II device. It details how to use the Quartus II software development suite tools and the Altera Monitor Program (AMP) software tool to design and build the application. The implementation integrates the SoPC Builder system with the Nios®-II soft core processor and a non-SoPC custom hardware accelerator developed in VHDL all into a single chip. Melding these two technologies creates a new level of customization in embedded system design. This heterogeneous approach provides a variety of benefits including. With its higher level of integration, this approach reduces overall system cost and reduces board size. In addition, it increases the flexibility of both the software and hardware designs.

**Figure-6.1(a)** illustrates a classical microprocessor-based system. It consists of a board with a number of discrete off-the-shelf components including a processor (central processing unit or CPU), a plentiful I/O peripherals (to support different I/O standards), a read-write memory (RAM), a flash memory, some dedicated logic hardware accelerators and an FPGA or some sort of PLD to glue together all these components.

The circuit board required for such a system should be quite large to contain all these chips. This increases the design cost and complexity while reducing speed and reliability. With the availability of multi million-gate FPGA devices, complex intellectual property (IP)

cores and soft core processors such as the Altera Nios® II, it is possible to contain a CPU, I/Os, the dedicated custom hardware accelerator and the RAM all in a single FPGA chip, **Figure-6.1(b)**. The only component that we cannot put into the FPGA is the flash memory.

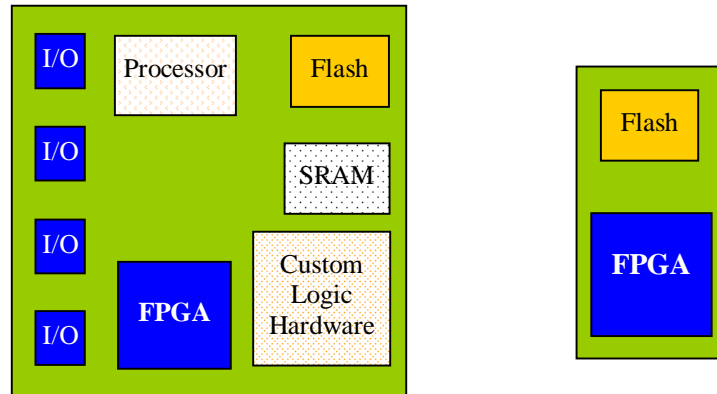


**Figure 6.1** Typical microprocessor-based system, (left) traditional method, (right) SoPC approach.

Integrating these devices on the same piece of silicon reduces cost and saves board space, while it increases reliability and enhances anonymity and secrecy. Also, because the signals between different components now reside on the same die, communication between them consumes substantially less power. In addition, this integrated solution results in a substantially higher bandwidth and lower latency compared to the former one.

## 2 FPGA Hardware Design Flow (SoPC Approach)

Designing and implementing embedded systems at system level targeting a programmable logic platform such as the FPGA is impossible without sophisticated computer aided design (CAD) tools. To cope with these complexities, Altera provides a Quartus II software development tool which includes a SoPC Builder system integration tool to allow designers to synthesize, simulate, program and debug their designs and build embedded systems on Altera's FPGA [91]. The remaining of this section, discusses the complete hardware/software design flow for creating a SoPC Builder system with a custom logic hardware accelerator (relevant details will be presented in forthcoming sections). **Figure-6.2** illustrates the FPGA hardware development design flow when using the SoPC approach.

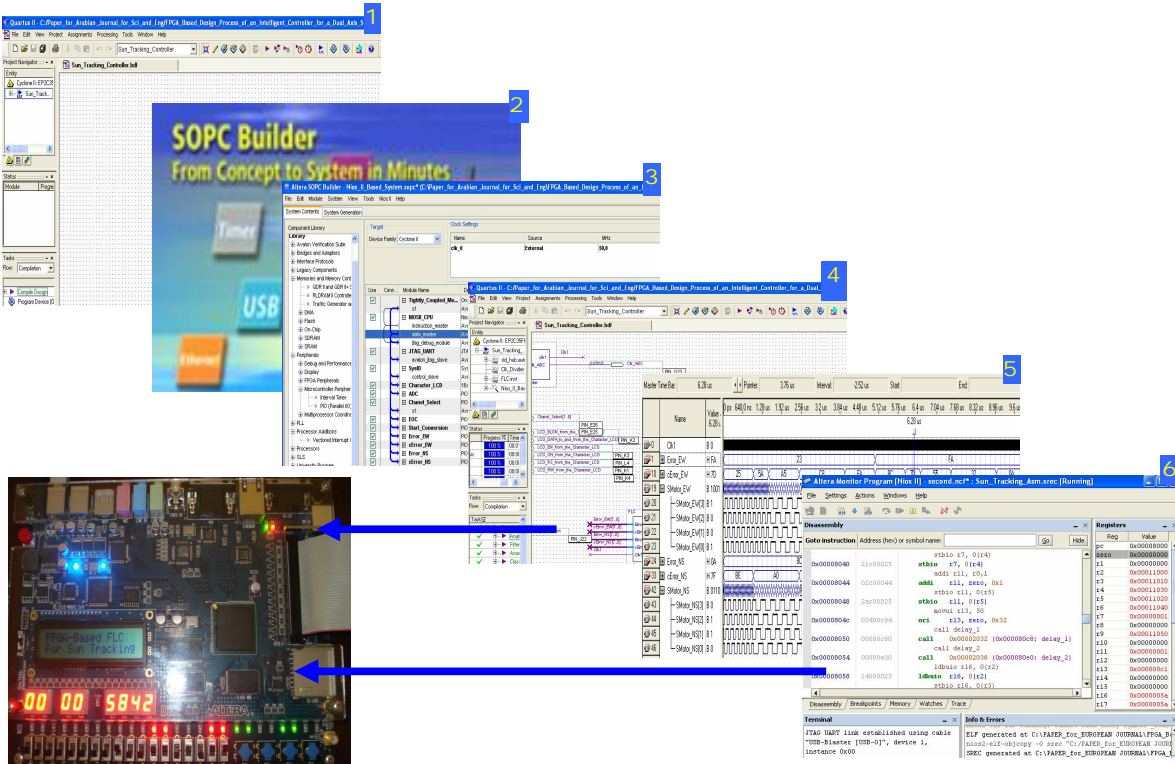


**Figure-6.2.** FPGA-Based Hardware/Software Design Flow using SoPC Approach

The design flow for any Altera FPGA-based system using SoPC approach starts by creating an FPGA project in Quartus II (window 1) [92], [93]. From within Quartus II project, we launch the SoPC Builder (window 2), a tool to build the desired embedded subsystem in the SoPC Builder with a Nios® II processor to program in the FPGA. The SoPC Builder fits in the design phase with which we can build an embedded system without having to develop any RTL coding. Instead, we use it in a drag-and-drop style Graphical User Interface (GUI) to add and parameterize the Nios® II soft core processor, memory and any other IP blocks required by the application (window 3).

Next, the Nios® II-based hardware system is generated by the SoPC Builder. The SoPC Builder produces an HDL code file of the design. It also always generates a Block Symbol File for the top level system in case we plan to use the schematic capture design approach. In this design flow, the generated Block Symbol File is integrated as a module in the Quartus II project as indicated in window-4. We may add some custom logic hardware developed in

HDL or using schematic capture as non-SoPC Builder logic and interconnect it with the Nios® II-based system. Next, we use Quartus II software to assign FPGA pin locations for the input/output signals. A successful compilation of the project produces a programmable file, the SRAM Object File (.sof), a file that determines the state of every programmable logic element inside the FPGA. When the .sof file is downloaded using the Quartus II programmer software, the FPGA on the development board is configured with the SoPC system hardware (both the Nios® II-based subsystem and the custom core components). At this stage, it is possible to perform a functional simulation (window-5).

The last step in the design flow is the development of the software program that we can download and run on the Nios® II processor. In this work, Altera Monitor Program utility is used to create in assembly language the firmware, compile, download and run the application software program on the Nios® II (window 6).

### 3 Implementation of the Intelligent Sun Tracking Controller

**Figure-6.3** depicts the conceptual top-level fuzzy control based dual-axis sun tracking digital controller block diagram implemented in the Cyclone II FPGA using the System-on-a-Programmable-Chip methodology. To reduce the complexity of the design process, the structure of the hardware is partitioned into two subsystems: (i) an on-chip hardware module implemented on the FPGA of the DE2 board. It encompasses the SoPC Builder system and the non-SoPC modules. The SoPC Builder module includes the Nios® II based system with all required peripherals and memory block. The non-SoPC system consists of custom clock divider, a hardware accelerator the fuzzy logic module and the sequence generator all developed in handcrafted VHDL and implemented on the FPGA fabric. (ii) An off-chip hardware module implemented on a protoboard using discrete off-the-shelf analog and digital components. It includes the sensing and data acquisition unit, the bidirectional voltage level translator and the motor driving unit to energize the actuators.

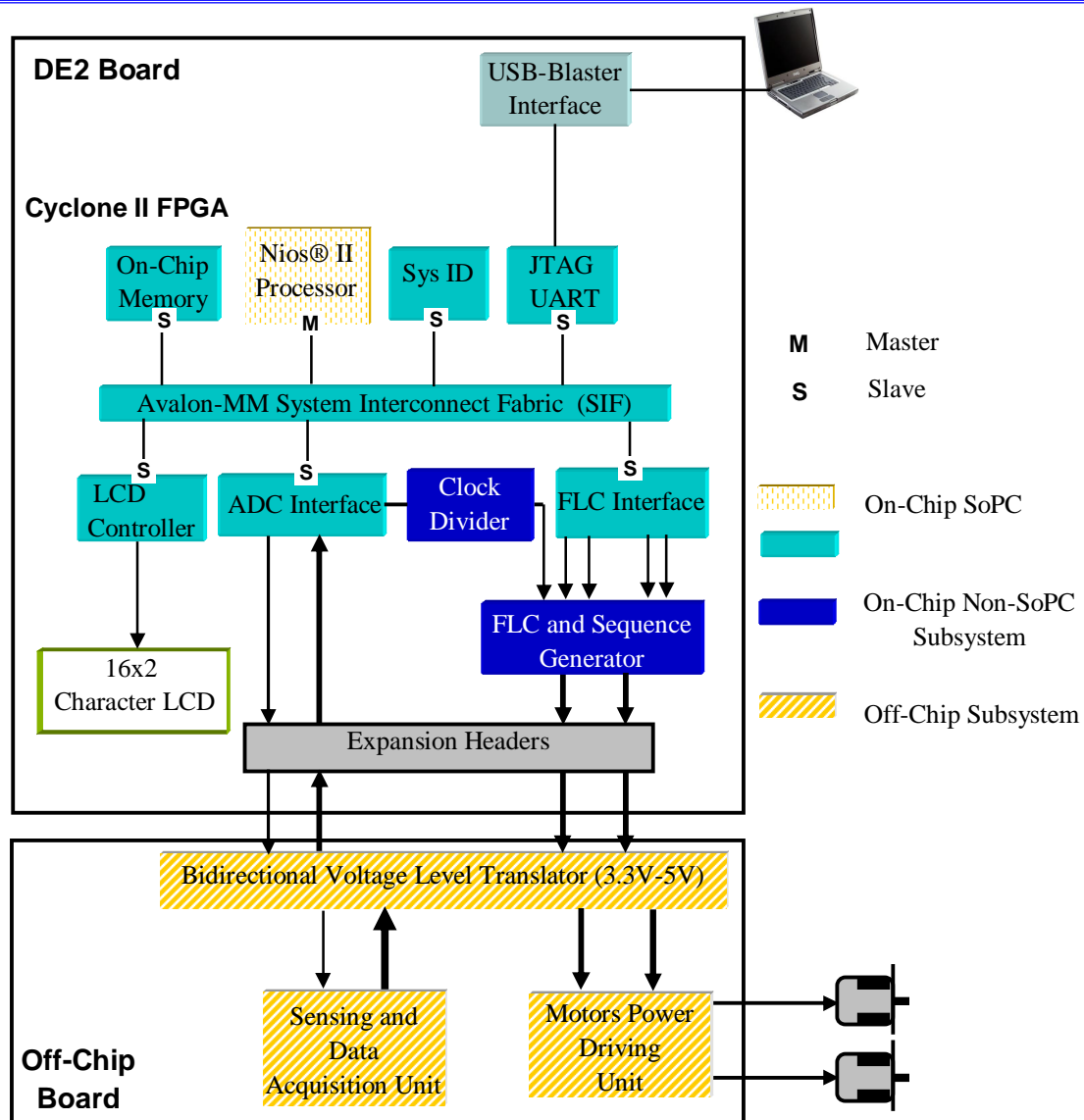


**Figure-6.3** The overall fuzzy control based dual-axis sun tracking system block diagram implemented in the Cyclone II FPGA.

### 3.1 Off-Chip Hardware Module

**Figur-6.4** illustrates the off-chip hardware functional block diagram. This diagram is made up of a set of pipelined units. These units are implemented onto the protoboard using commercial off-the-shelf discrete analog and digital components.

#### 3.1.1 Sun Finder Unit

The main idea behind the design of a sensor-driven active sun tracking system is the use of a sun finder to locate the sun in the sky to position the solar panel normal to the sun's incident

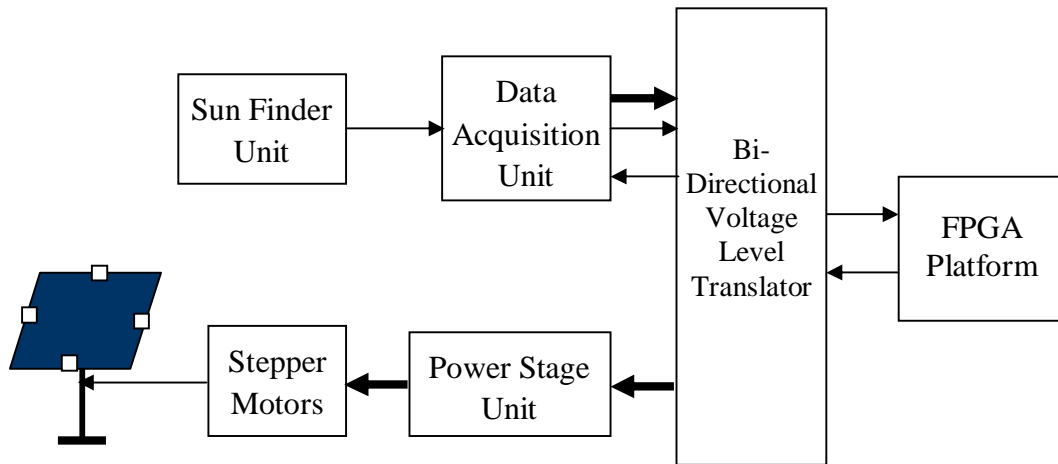


**Figure-6.4** The Off-Chip hardware functional block diagram

rays. This unit is composed of four similar Light Dependent Resistors (LDRs) as photo sensors mounted fixed on a four sided solar panel frame. Samples of the sun light intensity falling on the surface of the panel are captured by these sensors to determine the instantaneous position of the panel's surface with respect to the sun's light vector.

We used the MKY-76C59 LDR which has a light resistance of 10-20 K $\Omega$  and a dark resistance of 2 M $\Omega$ . The LDRs, installed in positions to gather accurate signals, are divided into two pairs. A pair positioned along the horizontal axis (LDR<sub>E</sub> and LDR<sub>W</sub>) to control the angle of azimuth and the second positioned along the vertical axis (LDR<sub>N</sub> and LDR<sub>S</sub>) to control the angle of elevation. This electronic system is used to notify the deviations (angular errors) from the desired posture of the solar panel to the control system.

The sensors are arranged in such a way that when the sun is shining normal to the solar panel, they all absorb the same amount of light and hence produce the same current. As the sun moves, one or more LDRs will be partially shaded and will not generate the same amount of current. The differential signals of a pair of LDRs are given by [Equations 6.1](#) and [6.2](#),

$$E_{EW} = V_{LDR_E} - V_{LDR_W} \quad (6.1)$$

$$E_{NS} = V_{LDR_N} - V_{LDR_S} \quad (6.2)$$

where the voltages  $E_{EW}$  and  $E_{NS}$  represent the angular errors of the azimuth and elevation angles respectively and  $V_{LDR_i}$  a voltage proportional to the intensity of light received by  $LDR_i$ . These errors are employed by the tracking controller to adjust the solar panel in order to minimize these angular errors.

For example, when  $E_{EW}$  is positive, it means that the eastern  $LDR_E$  is receiving more sunlight than the western  $LDR_W$ . Therefore, the actuator driving the vertical pivot shaft should rotate the solar panel eastward. Similarly, when  $E_{NS}$  is negative the horizontal axis driving actuator should rotate the panel southward. When the two errors are null the sun is perfectly tracked.

### 3.1.2 Data Acquisition Unit

The sensing and data acquisition unit is the key requirement for the sun tracking system. It provides the raw data to the processing unit. The real-time azimuth and elevation data are read in via the analog-to-digital converter (ADC). These data are the sunlight intensity degrees falling on the solar panel and sensed by the four LDRs.

A signal transformation circuit made up of a voltage divider and an operational amplifier used as a unit gain buffer (to avoid loading effect) converts the “induced” resistance value of the LDR into a voltage in the range 0 to 5 volts. This linear relationship between the intensity of light and voltage values is suitable for the ADC. The LDR outputs are first digitized by the converter before they are transferred through an input port to the Nios® II based system. **Figure-6.5** illustrates the circuit diagram of the sensing and data acquisition unit interfaced to the Nios® II system via the ADC interface.

The ADC chip used in the system to digitize the detectors’ analog inputs is the National ADC0808 a commercial low-cost converter. It is an 8-bit resolution successive-approximation converter. The ADC0808 device has eight input channels allowing it to monitor up to eight-

analog input signals. This eight-channel converter has a built-in 8-to-1 analog multiplexer where any one channel can be selected using three select input lines.

In the ADC0808,  $V_{\text{ref}(+)}$  and  $V_{\text{ref}(-)}$  are the reference voltage inputs. The values of these voltages dictate the dynamic range of the analog input voltage and determine the step size given by:

$$\text{Step size} = [V_{\text{ref}(+)} - V_{\text{ref}(-)}] / 2^n$$

where  $n$  is the number of bits. If  $V_{\text{ref}(+)}$  is connected to +5 V and  $V_{\text{ref}(-)}$  is grounded, then the step size is  $5 \text{ V} / 256 = 19.53 \text{ mV}$ .

The ADC0808 is not self-clocked, a clock signal must be provided from an external source to the clock input pin. The frequency of this latter determines the conversion time. When clocked with a 1 MHz, the analog to digital conversion is performed in less than 100 $\mu\text{sec}$ . During the conversion time, the value of the analog signal is kept constant by the built-in sample and hold circuit [94],[95].

The four analog signals representing the “induced” voltages which are proportional to

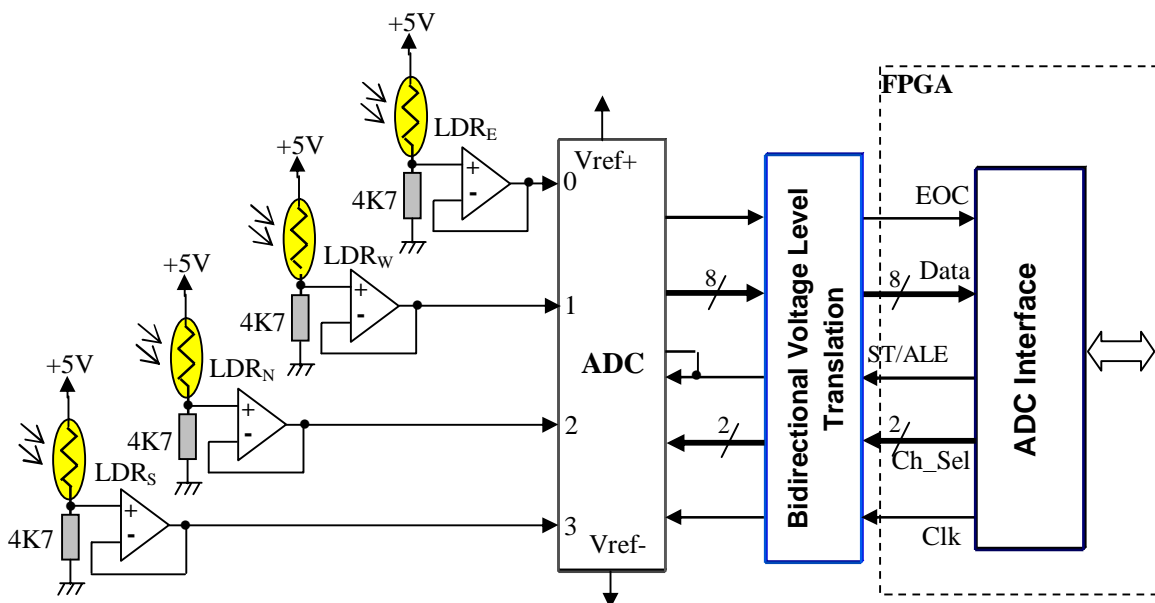


**Figure-6.5** Circuit diagram of the sensing and data acquisition unit



the light intensity falling on the four LDRs are sequentially captured and converted by a single parallel multiple channels ADC. The processor begins by selecting the desired channel of the ADC to which is associated one of the four light sensors. The address of this channel is latched on the rising edge of the ALE\_ST pulse, while the conversion begins on the falling edge of the pulse. The processor keeps polling for the end-of-conversion. Once the conversion is completed, (signaled by a change in the EOC signal), the data byte is read from the ADC's output register and saves it into one of the Nios® II registers.

The Nios® II-based system asserts the address of the next input channel and starts the conversion. This process is repeated to digitize the four data. **Figure-6.6** shows the flowchart

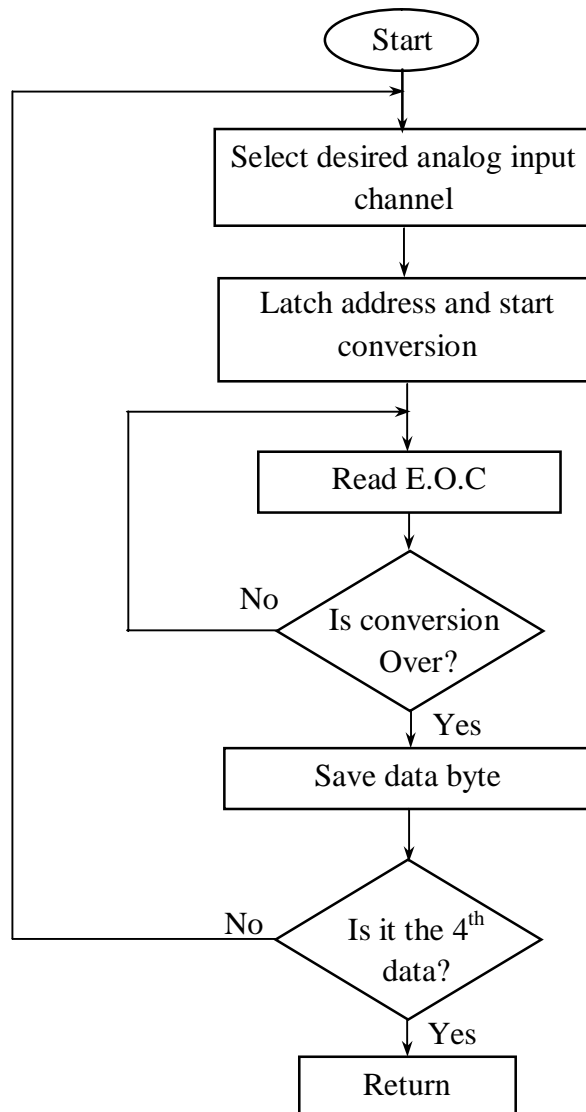


**Figure-6.6.** Flow chart for the data acquisition subroutine

of the data acquisition subroutine implemented and executed by the Nios® II-based system.

The use of a single multi-channel ADC to scan the several analog signals is a better alternative to using a dedicated single-channel ADC per channel which would lead to higher cost, bigger board size and more power consumption.

### 3.1.3 Bidirectional Voltage Level Translation Unit

Because the FPGA I/O pins are supplied with 3.3V and the voltage range used by the off-chip discrete components is 0-5V, a bidirectional 3.3V-5V voltage level translation unit is inserted between the DE2's expansion header and the data acquisition and power drive units. This unit is implemented using TTL low-power Schottkey and low-voltage TTL compatible logic families.

### 3.1.4 Motors Driving Unit

The 332-082 unipolar 4-phase, bidirectional stepper motors are employed as the main actuators to tune the sun tracker horizontal and vertical axels. Because tracking requires a high degree of accuracy, stepper motors are the most suitable for this application. Moreover, stepper motors are preferred over other type of motors because they have several advantages: no brushes, low cost, and high torque at a low speed. They also possess the holding torque, a characteristic that allows the stepper motor to hold its current position when it is not tuned, thus, eliminating the need to incorporate braking devices.

The stepper motor requires that its stator windings be energized in a programmed sequence to cause it to spin in a given direction and with a required speed. [Figure-6.7\(a\)](#) depicts the motors driver power stage unit used to energize the two stepper motors. This unit uses an array of eight BDX53 Darlington transistors (four transistors per stepper motor). The BDX53 is a silicon Epitaxial-Base NPN power transistor in a monolithic Darlington configuration mounted in Jedec TO-220 plastic package used to amplify the current level to accommodate the motor requirements.

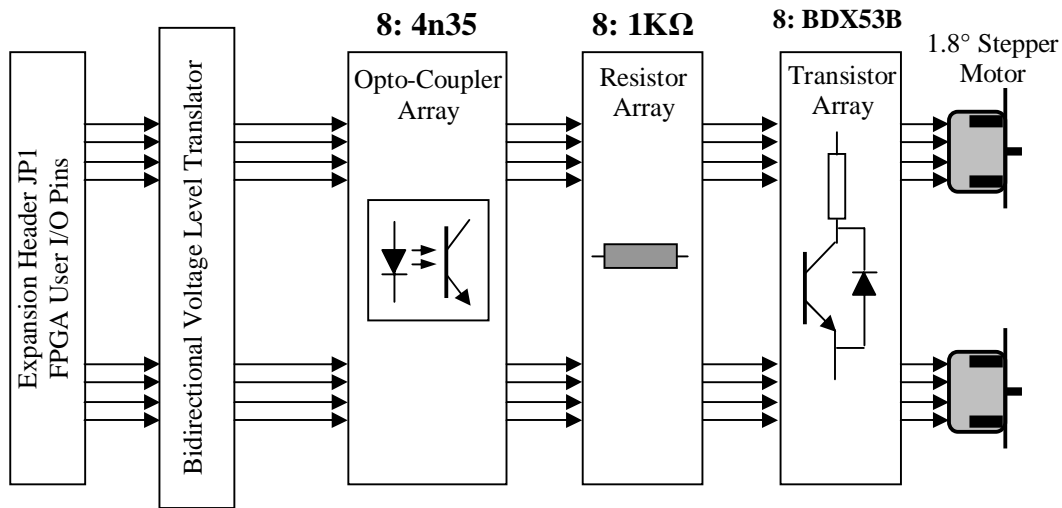


**Figure-6.7(a)** The motor driver power stage unit to energize the two actuators

This transistor is provided with a snubbing diode for inductive surge. It features a Collector-Emitter Sustaining Voltage of 100V and a Collector Current of 8A which large enough to drive our stepper motors. .

In order to avoid any direct “ohmic” connections between the low power digital circuit operating from 5V direct current and the power circuit with higher currents, an array of eight *4n35* optocouplers is used as a bridge between the FPGA user I/O terminals and the power stage circuit. This type of optocoupler uses a Gallium-Arsenide- Light Emitting Diode (LED) as an optical transmitter and a phototransistor as an optical receiver. The use of a beam of light to transmit data across a transparent barrier achieves an excellent isolation.

**Figure-6.7(b)** shows one branch of the power driving circuit. The input to the driver is one of the sequencer’s outputs. A ‘1’ on this output means that the corresponding stepper motor’s winding should be energized. This ‘1’ will drive the opto-coupler’s LED ON driving the coupled transistor into saturation. The resulting emitter current builds enough voltage across the 100Ω to saturate the switching power transistor providing a ground level to one terminal of the winding, whereas the other terminal is permanently connected to the positive supply.

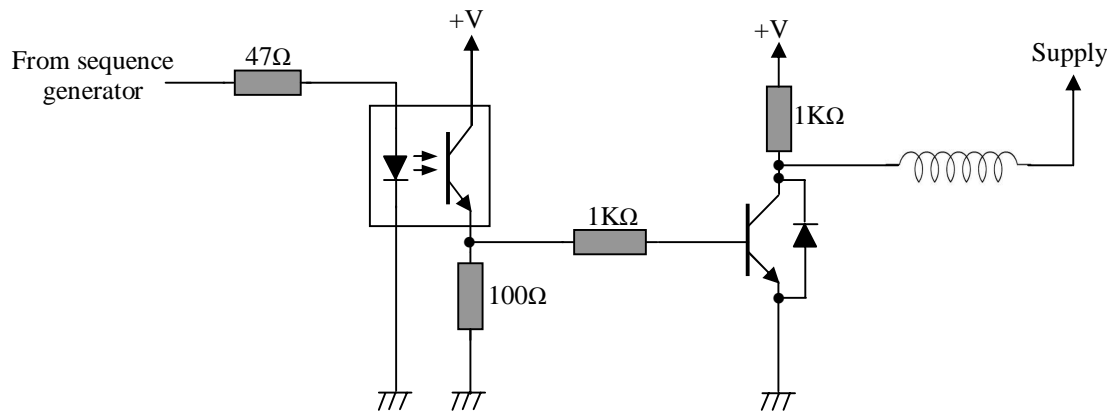


**Figure-6.7 (b).** One branch (out of 8) of the driver power stage unit

### 3.2 On-Chip Hardware Module

The On-chip module is the bulk of the hardware system. This module consists of two main parts: a SoPC Builder subsystem and a non-SoPC Builder subsystem. The former is built around the Nios® II embedded soft processor, the latter is developed in handcrafted VHDL as hardware accelerators. The overall module is implemented and ran on the Altera Cyclone II EP2C35 low-cost FPGA clocked at 50 MHz and features a 33,216 LEs, 35 hardware multipliers, 4 phase-locked loops (PLLs) and up to 475 user I/O pins. **Figure-6.8.** illustrates the overall on-chip hardware module.

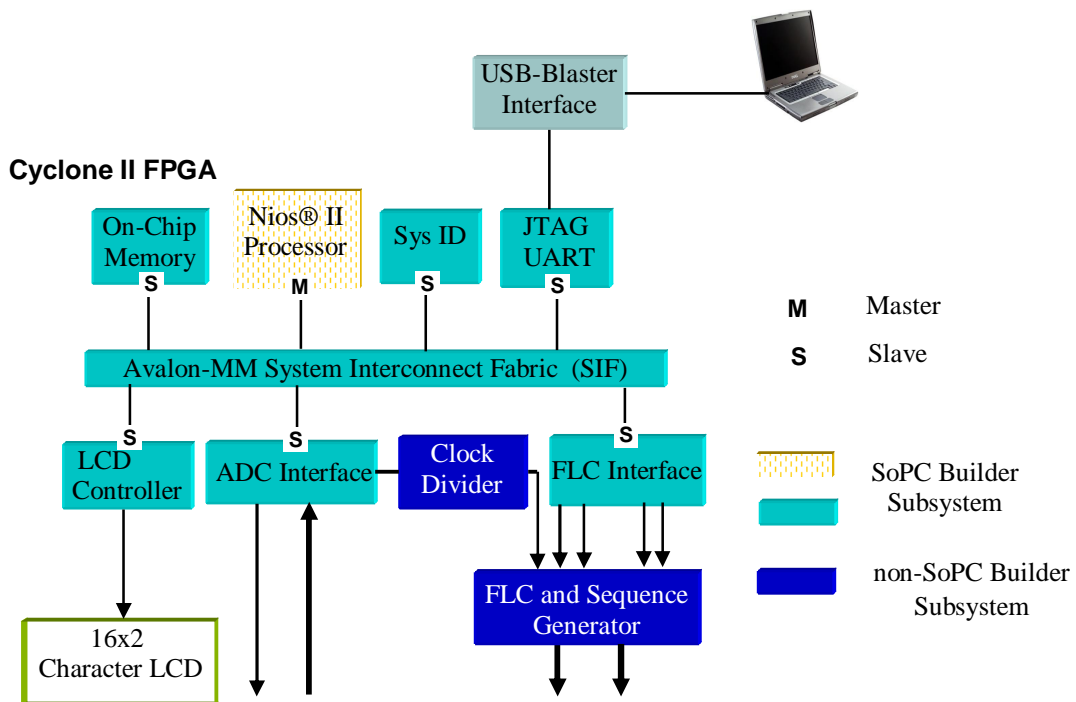


**Figure-6.8** The On-Chip hardware module

#### 3.2.1 On-Chip non-SoPC Builder Subsystem

This subsystem operates concurrently with the SoPC Builder subsystem to enhance performance and reduces system complexity. It is made up of several units, all of which are developed in VHDL.

##### 3.2.1.1 The clock divider module

The clock divider module developed in VHDL, takes as input the 50 MHz master clock of the DE2 board. It generates two clock signals: a 1 MHz clock signal suitable to trigger the ADC and a 12 Hz, clock signal to trigger the stepper motors drive sequencers. **Figure-6.9** illustrates the VHDL code to produce the required clock signals out of the DE2 board master clock.

```

library ieee;
use ieee.std_logic_1164.all;
use ieee.std_logic_unsigned.all;

entity Clk_Divider is
port(clk: in std_logic;
clk1, clk_ADC: out std_logic);
end Clk_Divider;

architecture behavioral of Clk_Divider is
signal state1: std_logic_vector(5 downto 0);
signal state2: std_logic_vector(26 downto 0);
begin
    ADC: process(clk)
begin
    if clk'event and clk = '1' then
        if state1 = 49 then state1 <= "000000";
        else state1 <= state1 + 1;
        end if;
    end if;
end process ADC;
    SM: process(clk)
begin
    if clk'event and clk = '1' then
        state2 <= state2 + 1;
    end if;
end process SM;
    clk_ADC <= state1(5);
    clk1 <= state2(22);
end behavioral;

```

**Figure 6.9** VHDL code of the clock divider custom hardware module

### 3.2.1.2 Implementation of the Fuzzy Logic Module

The fuzzy logic controller module described in chapter 5 is a custom hardware accelerator developed in VHDL is interfaced to the Nios® II based system. Custom components designed for intensive computation tasks are generally implemented in the FPGA fabric. The designer can integrate these components “inside” or “outside” the SoPC Builder system. When integrated “inside” the SoPC Builder system, it communicates with the other modules and the processor through the Avalon Memory-Mapped interface. On the other hand, the custom

component can exist within the FPGA alongside the Nios® II based system, that is, “outside” the SoPC Builder system. In this case, it can interact with the processor and other components through parallel input-output interface adapters. The latter approach has the advantage of having both custom cores and the Nios® processor execute concurrently, enhancing system response. The purpose of having a processor co-exist with conventional digital logic components is to provide flexibility of combining software and hardware based control in one chip. **Figure-6.10** depicts the synthesized schematic view of the fuzzy logic module in the Quartus II register transfer level (RTL) Viewer tool.

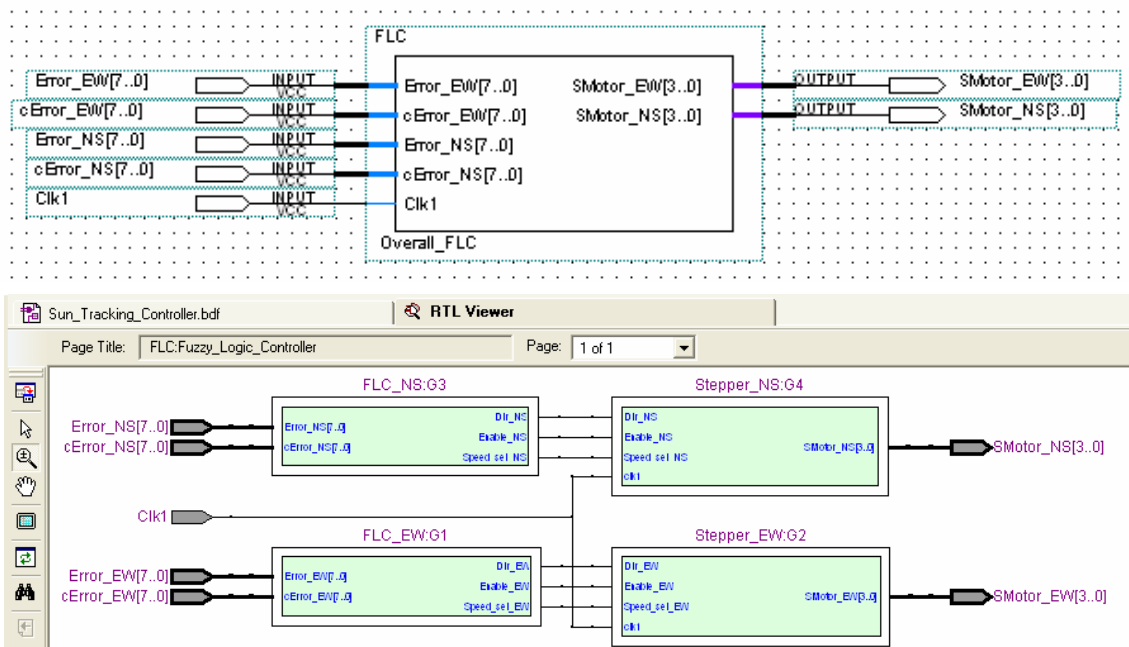


**Figure 6.10** A detailed view of the fuzzy logic module in Quartus II and the RTL Viewer

### 3.2.1.3 Stepper Motor Sequence Generator

The stepper motor requires that its stator windings be energized in a programmed sequence to generate a rotating magnetic field inside the motor, and the rotor will obediently follow it. For the motor to develop higher torque, it is desirable to apply a full-step sequence to its windings which involves powering two windings at one time. **Figure-6.11** shows a unipolar stepper motor windings and the full-step drive sequence.



**Figure 6.11** Unipolar stepper motor windings and full-step sequence.

**Figure-6.12** depicts the VHDL finite state machine implementation of the full-step driving sequence.

```

246  Speed_Select:  process(speed_sel_EW)
247  begin
248  case speed_sel_EW is
249  when "00" => clk1 <= clk_S;      -- Slow Speed
250  when "01" => clk1 <= clk_M;      -- Medium Speed
251  when others => clk1 <= clk_F;    -- Fast Speed
252  end case;
253  end process Speed_select;
254
255  stepping: process(Clk1)
256  begin
257  if Clk1'event and Clk1 = '1' then
258  if Dir_EW = '1' then  -- Eastward Steps
259  case state is
260  when s0 => state <= s1;
261  when s1 => state <= s2;
262  when s2 => state <= s3;
263  when s3 => state <= s0;
264  end case;
265  else
266  case state is  -- Westward Steps
267  when s0 => state <= s3;
268  when s1 => state <= s0;
269  when s2 => state <= s1;
270  when s3 => state <= s2;
271  end case;
272  end if;
273  end if;
274  end process stepping;
275  with state select
276  SMotor_EW <= "0011" when s0,
277  "0110" when s1,
278  "1100" when s2,

```

**Figure 6.12** VHDL code for a stepper motor full-step sequence generator.



### 3.2.2 On-Chip SoPC Builder Subsystem

The architecture of the SoPC Builder subsystem built around a Nios® II soft processor resembles that of a typical microprocessor-based system with the difference that it presents a set of peripherals tailored specifically for the application as well as the integration of special hardware accelerators that interact with the rest of the system. Traditionally, in a typical microprocessor-based system, the data is transferred using a shared bus, a collection of wires conveying address data and control signals to connect the processor with the remaining components of the system. Because the information (data and control) use the same bus, it becomes a bottleneck as the amount of information transfer increases. This degradation is accentuated when the I/O peripherals are mapped as memory-mapped I/Os, since these I/Os share the same bus with memory modules [96].

In the SoPC builder system, the components are interconnected by means of an interconnection network, the Avalon system interconnect fabric or SIF. This is the backbone of any SoPC Builder system. The Avalon SIF, generated by the SoPC Builder provides the necessary addresses and data paths to make memory-mapped connections between master and slave devices.

At the heart of the SoPC architecture sits a 32-bit processor which communicates with the other components through the Avalon SIF interface. It is the brain of the system and has several roles. It manages the data acquisition unit and calculates the crisp data input for the fuzzy logic controller module. It initializes and drives the LCD controller to display in real-time on the two-line LCD the sun tracking system's status. It communicates with the host computer via the USB Blaster interface, [Figure-6.8](#).

The use of a microprocessor always calls for memory where the instructions and data are stored. The embedded memory blocks in the FPGA are used to provide an on-chip RAM for the processor. The Cyclone II EP2C35 FPGA includes 105, M4K RAM Blocks leading to

483,840 total RAM bits. The Joint Test Action Group Universal Asynchronous Receiver/Transmitter (JTAG-UART) interface is used to provide a Universal Serial Bus (USB) link between the FPGA platform and the host computer. This circuitry and the associated software are called the USB-Blaster [92].

We also added a system ID peripheral. This component provides the SoPC Builder system with a unique identifier and therefore, safeguards it against any accidental downloading software compiled for a different Nios® II system. To drive the 16x2 character liquid crystal display (LCD) peripheral, we used a SoPC Builder LCD controller component.

The ADC interface module includes several parallel input-output peripherals tailored to accommodate different signals of the off-chip data acquisition unit. This later unit constructed around a low-cost multiple-channel analog-to-digital converter is used to sample the current position of the sun in the sky via four light dependent resistors (LDRs). The dark blue blocks: the clock divider and the FLC and the stepper motor sequence generator are the custom hardware logic blocks.

### 3.2.3 Building the Embedded System in the SoPC Builder

The SoPC Builder, part of the Quartus II software, is a powerful hardware generation tool. It streamlines the process of integrating blocks of IPs and accelerates development of system-on-a-programmable-chip designs compared to traditional, manual integration methods. The tool was introduced by Altera to design systems at block level. It consists of two major parts: a graphical user interface or GUI and a system generator program [93].

**Figure-6.13** shows a screenshot of the sun tracking controller optimized in an FPGA. The GUI consists of several parts. The window on the left side is the library of available pre-made IP cores (including the flagship Nios® II soft core processor) from which the designer picks up the desired components required by the application.

Component Library

Project

Library

- Avalon Verification Suite
- Bridges and Adapters
- Interface Protocols
- Legacy Components
- Memories and Memory Control
  - GDR II and GDR II+ SR
  - RLDRAM II Controller
  - Traffic Generator and
- DMA
- Flash
- On-Chip
- SDRAM
- SRAM
- Peripherals
  - Debug and Performance
  - Display
  - FPGA Peripherals
  - Microcontroller Peripheral
    - Interval Timer
    - PIO (Parallel I/O)
  - Multiprocessor Coordination
- PLL
- Processor Additions
- Processors
  - Nios II Processor
- SLS
- University Program

Target

Device Family: Cyclone II

Clock Settings

Name	Source	MHz
clk_0	External	50,0

Use	Connections	Module Name	Description	Clock	Base	End	IRQ
<input checked="" type="checkbox"/>		On_Chip_RAM	On-Chip Memory (RAM or ROM)	clk_0	0x00008000	0x0000ffff	
<input checked="" type="checkbox"/>		Nios_2_CPU	Nios II Processor	clk_0			
		clk	Clock Input	clk_0			
		instruction_master	Avalon Memory Mapped Master				
		data_master	Avalon Memory Mapped Master				
		d_irq	Interrupt Receiver				IRQ 0
		jtag_debug_module	Avalon Memory Mapped Slave		0x00010800	0x00010fff	IRQ 31
		custom_instruction_master	Custom Instruction Master				
<input checked="" type="checkbox"/>		JTAG_UART	JTAG UART	clk_0			
		clk	Clock Input	clk_0			
		avalon_jtag_slave	Avalon Memory Mapped Slave		0x00011098	0x0001109f	
		irq	Interrupt Sender				
<input checked="" type="checkbox"/>		SysID	System ID Peripheral	clk_0	0x00011090	0x00011097	
<input checked="" type="checkbox"/>		Character_LCD	16x2 Character Display	clk_0	0x000110a0	0x000110a1	
<input checked="" type="checkbox"/>		ADC_Data	PIO (Parallel I/O)	clk_0	0x00011020	0x0001102f	
<input checked="" type="checkbox"/>		Ch_Select	PIO (Parallel I/O)	clk_0	0x00011000	0x0001100f	
<input checked="" type="checkbox"/>		EOC	PIO (Parallel I/O)	clk_0	0x00011030	0x0001103f	
<input checked="" type="checkbox"/>		ALE_ST	PIO (Parallel I/O)	clk_0	0x00011040	0x0001104f	
<input checked="" type="checkbox"/>		Error_EW	PIO (Parallel I/O)	clk_0	0x00011050	0x0001105f	
<input checked="" type="checkbox"/>		cError_EW	PIO (Parallel I/O)	clk_0	0x00011060	0x0001106f	
<input checked="" type="checkbox"/>		Error_NS	PIO (Parallel I/O)	clk_0	0x00011080	0x0001108f	
<input checked="" type="checkbox"/>		cError_NS	PIO (Parallel I/O)	clk_0	0x00011070	0x0001107f	
<input checked="" type="checkbox"/>		clk_0	Clock Source				
<input checked="" type="checkbox"/>		clk	Clock Output	clk_0			

Figure-6.13 SoPC-based intelligent sun tracking controller optimized in an FPGA.

We construct the embedded SoPC Builder system in the Avalon framework. The construction of the system is accomplished by means of a drag-and-drop style. The required components are dragged and parameterized in the contents page (the central window). The “Module Name” and “Description” columns show the names and interfaces of the configured intellectual property (IP) cores used in the application. The “connections” column in [Figure-6.13](#) is the interconnect logic.

Finally, the beginning and end of the memory addresses of the various components used in the design are shown under “Base” and “End” columns. Because the Nios® II processor maps the I/O peripherals as memory-mapped I/O, then the 32-bit address space is assigned to both the memory component and to the I/O peripherals. In general, to avoid any conflicts for all these memory-mapped components, it is more convenient to automatically assign these unique base addresses.

The ADC interface is implemented with four parallel input-output interface adapters (PIOs) of different dimensions. They are:

**ADC:** The first PIO configured as an 8-bit input port to route the digital data from the converter to the processor when the conversion is completed.

**Channel\_Select:** The second PIO tailored as a 2-bit output port. This output port drives the two least significant address lines of the converter to select any one of the four channels.

**Start\_Conversion:** The third PIO is a 1-bit output port. The processor outputs a positive pulse through this port to accomplish two functions. It latches the address of the selected channel on the positive edge of the pulse and starts the conversion on the negative edge of the pulse.

**EOC:** This last PIO is specified as a 1-bit input port. It is used to route the end-of-conversion output signal of the analog-to-digital converter to be polled by the microprocessor.

The FLC interface also consists of four PIOs. All four are configured as 8-bit parallel output ports. PIOs labeled Error\_EW and cError\_EW are used for to supply the crisp values representing the azimuth angular error and its rate of change as inputs to the azimuth fuzzy-like PD controller. Similarly, PIOs labeled Error\_NS and cError\_NS are used to apply the crisp values representing the elevation angular error and its rate of change as inputs to the elevation fuzzy-like PD controller.

As in any microprocessor-based system, we provided a 32-Kbyte of on-chip RAM to store the firmware code to run the Nios® II processor.

### 3.2.4 Integrating the SoPC and non-SoPC Builder Subsystems in Quartus II Project

Once the required blocks are added and their parameters specified, the memory-map of the Nios® II based system is automatically generated by the SoPC Builder using Auto-Assign Base Addresses. Finally, the SoPC Builder generator program generates the system interconnect fabric and many other output files.

The SoPC Builder generates a graphical Block Symbol File (.bsf) module (a representation of the top-level SoPC Builder system). This block includes the Nios® II core, all peripheral and memory blocks, and the SIF. This symbol is instantiated in the Quartus II project. [Figure-6.14](#) shows the top-level schematic for the FPGA-Based FLC design process for a dual-axis sun tracking system. The large symbol in the Quartus II Block Diagram File (.bdf) project labeled “*Nios\_II\_Based\_System*” is the SoPC Builder system.

We add the custom logic hardware accelerator external to the Nios® II which consists of the fuzzy logic control module with the stepper motors sequence generator block labeled “*FLC*” and the clock divider block labeled “*Clk\_Divider*”.

The input, output, and bi-directional connectors are then added and named. The EP2C35 FPGA target device is selected, the pins assigned and the project file compiled.

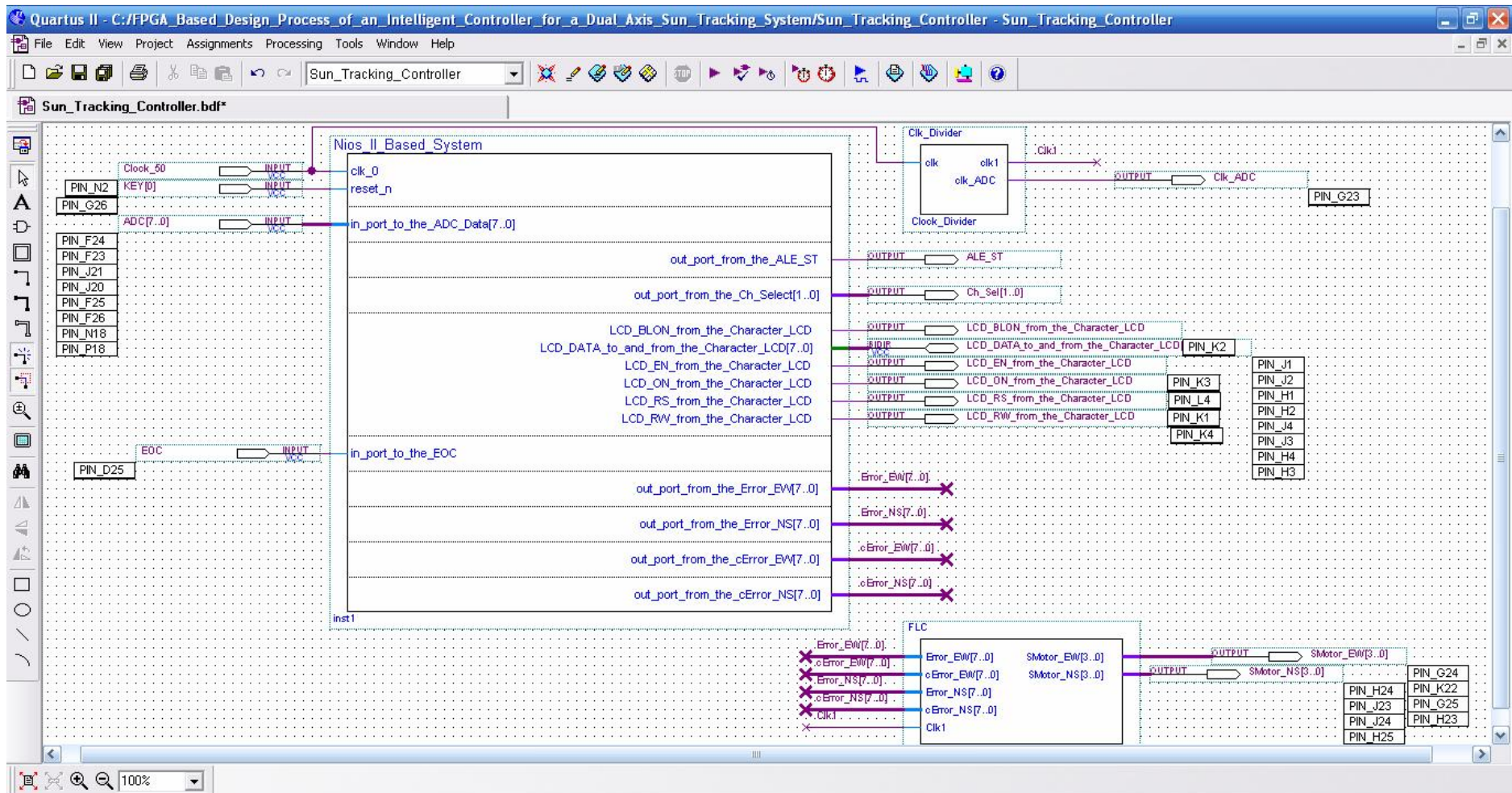


Figure-6.14 Top-Level schematic for the FPGA-Based FLC design process for a dual-axis sun tracking system

Upon successful compilation, the FPGA is ready to be configured with the generated bit stream, a SRAM Object File (.sof) file using the Quartus II Programmer.

### 3.2.5 Firmware Development

Having built, configured the required hardware and downloaded it in the FPGA device, we need to develop the application firmware program to make it run. In order to develop our software code in assembly language (which runs much faster and uses much less memory space compared to that of a similar program written in a high level language), we used the Altera Monitor Program (AMP) development tool. This tool allows the user to assemble, compile and debug the Nios® II assembly language software program, then download it onto the FPGA to run the Nios® II processor. **Figure-6.15** depicts a PC running Quartus II and Altera Monitor Program graphical user interface.

The assembly language code we developed performs the following operations in an infinite loop:

- i- Sequentially gathers raw data from light sensors in digital format.
- ii- Computes the angular errors and their rates of error change

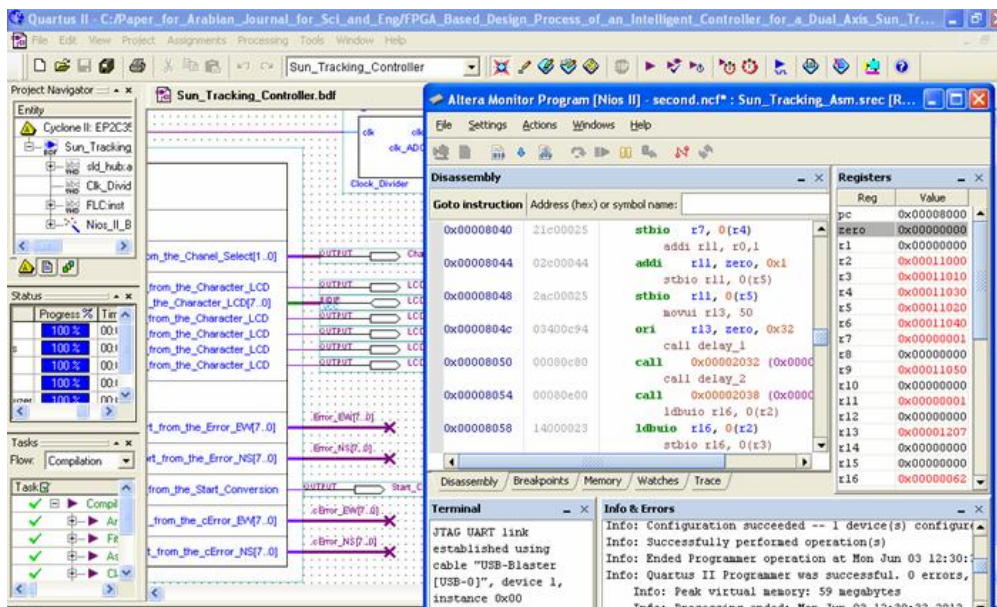


**Figure-6.15.** PC running Quartus II and Altera Monitor Program software

- iii- Feeds the PD-like FLC with the computed data
- iv- Displays system' status on the LCD to provide feedback to the user
- v- Enters into a delay loop, a time during which the FLC determines the action to be carried on to position the solar panel at its optimal posture.
- vi- Repeat.

#### 4 Real-Time Experiment

The overall apparatus of the prototyping platform built in the laboratory for testing and verifying the intelligent dual-axis sun tracking system is illustrated in **Figure-6.16. (a), (b)**. It depicts both the off-chip hardware system on the protoboards and the on-chip hardware/software co-design system on the FPGA board (DE2). The FPGA containing the hardware implementation of the digital controller controls the off-chip hardware circuitry via the board's expansion header. The expansion header provides general-purpose input/output (GPIO) pins. These GPIOs are directly connected to the FPGA device. It is also linked by means of the USB Blaster mechanism to the PC running Altera monitor program and Quartus II software development suite tools. The remaining parts of the prototype consists of a dual-axis tracker platform with a sun finder.

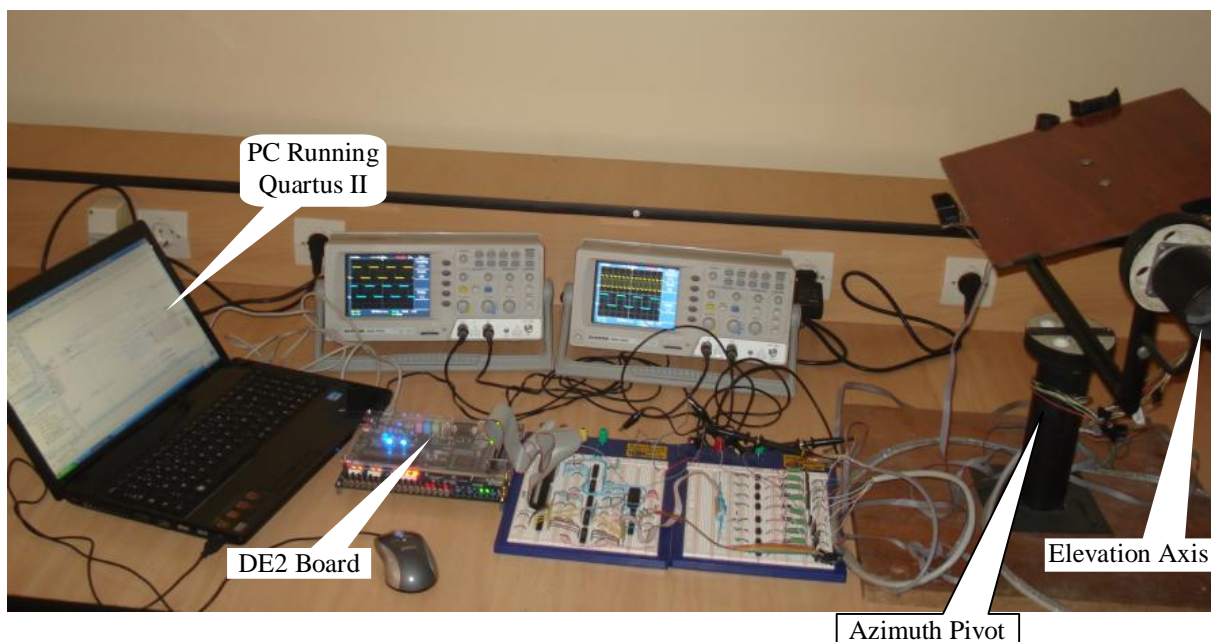


**Figure-6.16. (a).** Hardware setup of the FPGA-based intelligent dual-axis sun tracking system.





**Figure-6.16. (b).** Hardware setup of the FPGA-based intelligent dual-axis sun tracking system.

#### 6.4.1 Operational Cycle Time

The time interval of the operational cycle is 1-sec. **Figure-6.17** depicts the operational cycle time. The cycle begins with the acquisition of the raw data from the sensors via the analog-to-digital converter. This raw data, which represent the position of the sun in the sky with respect to the surface of the solar panel, is processed by the Nios® II based system to calculate the angular errors and the rates of change of these errors to be used by the fuzzy controller module as crisp data inputs. Using these computed data, the fuzzy control module evaluates and determines by how much the solar panel needs to be tuned to minimize its misalignment with respect to the current position of the sun in the sky. These three functions are performed in 0.1 sec.

Also, based on the result of this data manipulation, the Nios® II based system provides the user with the current state of the tracking system by displaying appropriate messages on the LCD of the FPGA platform.

The next stage is the solar panel mechanical adjustment for which we allowed 0.168 sec time interval. During this time interval, the stepper motors may be held idle or rotated by 2, 8 or 16 steps in the appropriate direction depending on the current position of the panel with respect to the optimal posture.

Since the smallest number of steps is 2 which lasts 0.168 sec, we used a clock signal with a frequency of  $1/0.084 = 11.94$  Hz. For the 8 and 16 steps, we used clock signals with frequencies of 47.68 Hz and 95.36 Hz respectively. The remaining time interval is reserved for the solar panel to stabilize before the operational cycle repeats.

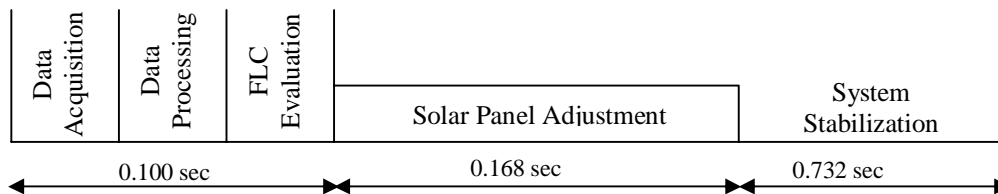


**Figure-6.17** The operational cycle time

## 4.2 Simulation

**Figure-6.18** illustrates a computer simulation timing diagram in the Quartus II simulator.

This window shows the tracking performance and the effectiveness of the proposed controller. We applied several combinations of stimuli coded in hexadecimal for the errors and rates of change of errors and observed the output responses expressed as binary sequences. We notice the response on both driving motors as expected by the tracker.

In the time interval  $0 - 1.33 \mu\text{sec}$ , the azimuth error is  $\$3B$  (NL) and its rate of change is  $\$2C$  (NL). The motor should rotate fast westward. Whereas in the interval  $1.33 \mu\text{sec} - 2.61 \mu\text{sec}$ , the azimuth error is NL but its rate of change is (PS), therefore, to align the panel the motor should be rotated at medium speed westward.

At  $4.48 \mu\text{sec}$ , the simulation window exhibits a case where the sun is tracked. In this case, the azimuth error is NL and its rate of change is PL. The controller need not apply any action. The panel will be aligned normal to the sunlight rays.

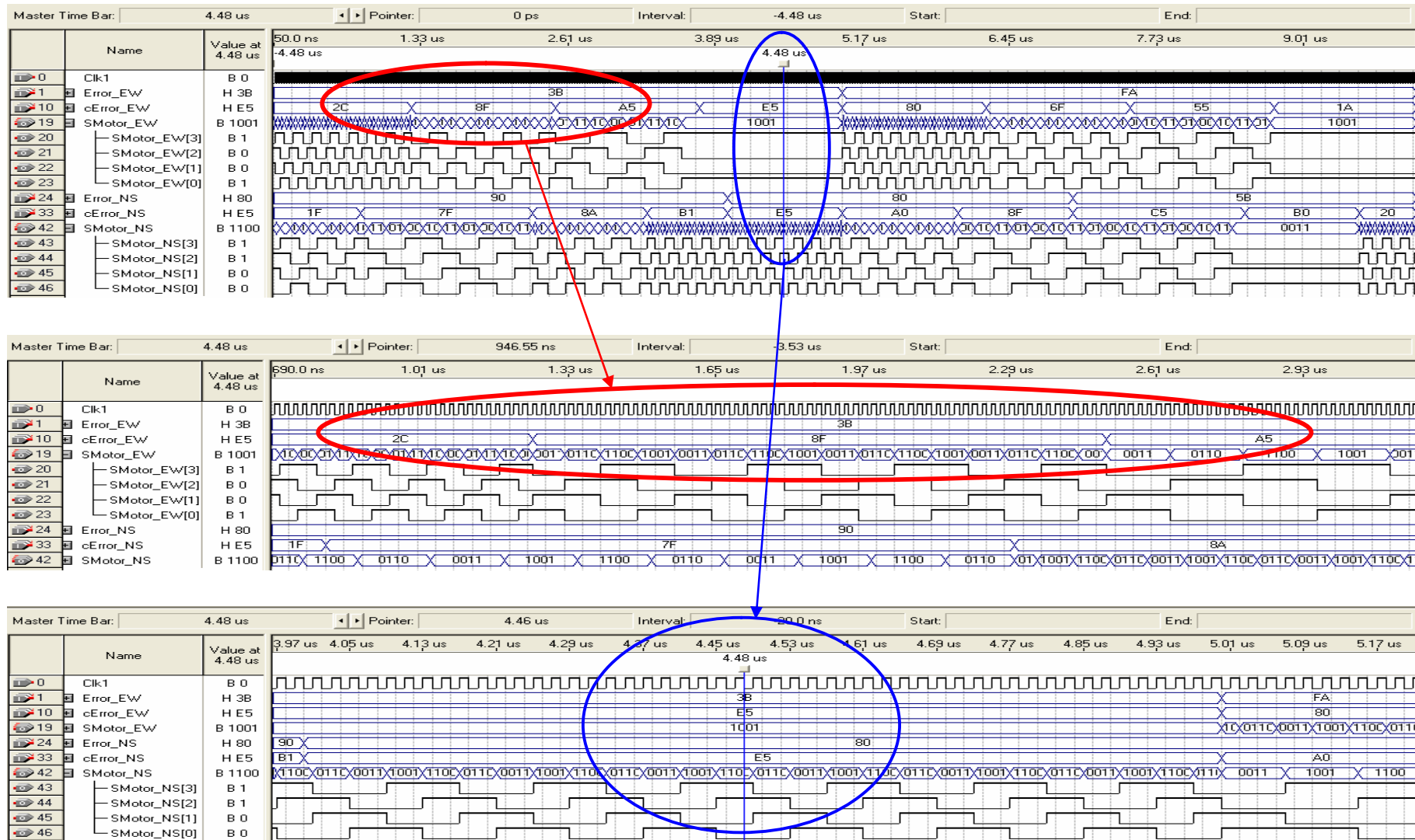


Figure-6.18 Behavioral simulation window in the Quartus II simulator

---

---

**Chapter 7**

---

---

---

---

**Conclusions**

---

---

In this thesis, we presented the design, simulation and implementation processes of a customized FPGA-based (SoPC approach) applied to an intelligent sensor-driven dual-axis sun tracking system in order to maximize power extraction from the solar panel. The goal of using fuzzy control technology is to put human knowledge into engineering systems in a systematic and efficient order. We designed our system with several considerations in mind: autonomy, execution speed and cost, and design complexity. In this regard, the intelligent controller is developed on an FPGA-based heterogeneous computing platform where the overall controller is partitioned between two concurrent modules.

- 1- A fuzzy control module, as a hardware accelerator, implemented on the FPGA fabric using VHDL is utilized to control the steering motors according to the deviation from the desired (optimal) posture of the solar panel.
- 2- A Nios® II based system to acquire the raw data, compute the state variables of the controller and displays in real-time the status of the overall system.

This hardware/software codesign implementation exploits the simplicity of the microprocessor and the massively parallel architecture of the FPGA. This methodology provides a high degree of flexibility in both hardware and software compared to classical

computing platforms. Other reasons why this approach is interesting: It works. It can be applicable to almost all fields.

The SoPC approach has several advantages:

- (1) It allows the use of the exact number of peripherals needed and the parameterization of the peripherals to respond to the application.
- (2) The reconfigurability nature of the FPGA and the short development cycle makes it possible to perform modifications of any component of the system at any stage of the implementation.
- (3) To prevent from obsolescence, the design can be migrated into another larger and more performant FPGA that does not exist yet.
- (4) The ability to integrate an entire system on a single chip at a lower cost compared to the use of off-the-shelf discrete components (MCU, DSP, ASSP, etc) solutions.
- (5) The capability to off-load the computation-intensive functions from the software application running on the soft processor and to implement them as hardware accelerators in the FPGA fabric using VHDL or another design entry.

A common practice to obtain the inputs for the FLC is the use of differential amplifiers and differentiators, in this work these parameters are computed within the FPGA using a digital processing unit. This design greatly enhances system reliability and reduces chip count. Moreover, the robustness of the FLC allows the use of cheaper sensors and low resolution ADCs resulting in reduced implementation cost.

### **Further works**

There are at least two possible directions to work on the way to improve further system performance, design simplicity and flexibility.

- (i) Integrating the fuzzy control module as an intellectual property (IP) component with Avalon interface and connect it to the Avalon Memory Mapped interface.

- (ii) Add custom instructions to the soft-core processor instruction set.

The use of the Nios® II software build tools (SBT) for eclipse to develop the application software code in C, will further improve design productivity and lessen design complexity.

For extremely high speed applications, it is possible to sample all analog data simultaneously using several high speed ADCs, a performance that cannot be achieved with either the microcontroller or the DSP.

In the next generation of FPGAs, where ADCs will be built into the fabric of the FPGA, the proposed computing platform will be more efficient in terms of hardware resources, power consumption and control performance when compared with the standard MCU, DSP solutions.

It is believed that with the significant advancements in materials and technologies combined to the growing awareness concerning environmental problems, renewable energies and solar in particular (with more than 60% annual average growth rate for the past five years) are the future.

---

---

## References

---

---

- [1] Z. Sen, "Solar energy in progress and future research trends." *Progress in Energy and Combustion Science*, 30, pp. 367-416, 2004.
- [2] Saifur. Rahman, "Green Power. Where is it and where can we find it?" *IEEE Power & Energy magazine*, Jan/Feb 2003. pp. 30-37.
- [3] P. Fornasiero, M. Graziani, *Renewable Resources and Renewable Energy: A Global Challenge*, 2<sup>nd</sup> Edition, Taylor & Francis, 2006.
- [4] H. Scheer, *The Solar Economy: Renewable Energy for a Sustainable Global Future*, Earthscan, 2004.
- [5] AIA Research Corporation; "Solar Dwelling Design Concepts". *Washington, DC: U.S. Government Printing Office*, 1976.
- [6] Y. Goswami, F. Kreith, and J. Kreder, "Principle of solar engineering," in *Fundamentals of Solar Radiation*, Philadelphia, PA: Taylor & Francis, 1999.
- [7] S. Seme, G. Stumberger, and J. Vorsic, "Maximum efficiency trajectories of a two-axis sun tracking system determined considering tracking system consumption", *IEEE Trans. On Power Electronics*, Vol. 26, No. 4, April 2011. pp. 1280-1290.
- [8] C.Y. Lee, P. C. Chou, C. M. Chiang, and C.F. Lin, "Sun tracking systems: a review." *Sensors*. 9, pp. 3875-3890, 2009.
- [9] K-K. Chong, C-W. Wong, F-L. Siaw, T-K. Yew, S-S Ng, M-S. Liang, Y-S. Lim and S-L. Lau, "Integration of an On-Axis General Sun-Tracking Formula in the Algorithm of an Open-Loop Sun-Tracking System". *Sensors*, 9, pp. 7849-7865, 2009.
- [10] R. Woods, J. McAllister, G. Lightbody and Ying Yi, *FPGA-based Implementation of signal processing systems*, John Wiley & Sons, Ltd. 2008.
- [11] Ian Grout, *Digital Systems Design with FPGAs and CPLDs*, 2008, Elsevier Ltd. ISBN-13: 978-0-7506-8397-5

- [12] Altera, "Optimize system flexibility by integrating custom microprocessors into FPGAs," *wp-aab090805-1.1*, Feb-2006.  
Available online at [www.altera.com/literature/wp/wp-aab0900805.pdf](http://www.altera.com/literature/wp/wp-aab0900805.pdf)
- [13] Zekai Sen , "Solar energy in progress and future research trends", *Progress in Energy and Combustion Science* 30, 2004, pp. 367–416.
- [14] T. Fazel, S. Zainal and M. A. Shahrin, "FPGA implementation of a single-input fuzzy logic controller for boost converter with the absence of an external analog-to-Digital converter." *IEEE Trans. On. Ind. Electronics*, Vol.59, No.2, pp.1208-1217. Feb 2012.
- [15] Yi Fu, L. Howard and M.E. Kaye, "Hardware/Software codesign for a fuzzy autonomous road-following system." *IEEE Trans. On Systems, Man, and Cyber*, Vol.40, No.6, pp. 690-696. Nov-2010.
- [16] A. H. Zavala and O. C. Nieto, "Fuzzy Hardware: a retrospective and analysis," *IEEE Trans. On Fuzzy Systems*, Vol.20, No. 4, August 2012. pp. 623-635.
- [17] G. Bosque, I. del Campo and J. Echanobe, "Fuzzy systems, neural networks and neuro-fuzzy systems: A vision on their hardware implementation and platforms over two decades" *Engineering App of Artificial Intelligence* 32, 2014, pp.283–331.
- [18] A. Merlaud, M. De Mazière, C. Hermans, and A. Cornet, "Equations for solar tracking." *Sensors*. 12, pp.4074-4090, 2009.
- [19] A. B. Sproul, "Derivation of the solar geometric relationships using vector analysis." *Renewable Energy*. Vol. 32, No. 7, pp. 1187-05, 2007.
- [20] R. H. McFee, "Power collection reduction by mirror surface nonflatness and tracking error for a central receiver solar power system". *Appl. Opt.* 1975, 14, pp. 1493-1502.
- [21] R.P. Semma, and M.S. Imamura, "Sun tracking controller for multi-kW photovoltaic concentrator system.", *In Proceedings of the 3rd International Photovoltaic Sol Energy Conf*, Cannes, France, Oct. pp. 27-31, 1980.
- [22] K.K. Chong and C.W. Wong, "General formula for on-axis sun-tracking system and its application in improving tracking accuracy of solar collector," *Solar Energy* 83, 2009, pp. 298–305



- [23] S. Abdallah, "The effect of using sun tracking systems on the voltage-current characteristics and power generation of flat plate photovoltaics." *Energ. Conversion. Manage.* 2004, 45, pp. 1671-1679.
- [24] R. Grena, "An algorithm for the computation of the solar position." *Solar Energy*. Vol. 82, No. 5, pp. 462-470, 2008.
- [25] M. Blanco-Muriel, D.C. Alarcon-Padilla, T. Lopez-Moratalla, and M. Lara-Coira, "Computing the solar vector." *Solar Energy*. Vol. 70, No. 5. pp. 431-441, 2001.
- [26] I. Reda, and A. Andreas, "Solar position algorithm for solar radiation applications," *Solar Energy*. Vol. 76, No. 5, pp. 577-589. 2004.
- [27] S. Abdallah and S. Nijmeh, "Two axes sun tracking system with PLC control." *Energy Conversion and Management* 45, 2004, pp. 1931–1939.
- [28] F. Duarte, P. D. Gaspar, and L. C. Gonçalves, "Two-axis solar tracker based on solar maps, controlled by a low-power microcontroller." *Proc. of the International Conference on Renewable Energies and Power Quality*. (ICREPQ'10). Granada. Spain. March 23-25, 2010.
- [29] H. Mousazadeh, A. Keyhani, A. Javadi, H. Mobli, K. Abrinia, and A. Sharifi, "A review of principle and sun-tracking methods for maximizing solar systems output." *Renewable and Sustainable Energy Reviews*. 13, pp. 1800-1818, 2009.
- [30] P. Roth, A. Georgiev and H. Boudinov, "Design and construction of a system for sun-tracking." *Renewable Energy*, 2004. 29, pp. 393-402.
- [31] P. Roth, A. Georgiev and H. Boudinov, "Cheap two axis sun following device." *Energy Conversion and Management*, 2005; 46: pp. 1179–1192.
- [32] S.A. Kalogirou, "Design and construction of a one-axis sun-tracking." *Solar Energy*, 1996, 57(6), pp. 465–469.
- [33] Cheng-Dar Lee, Hong-Cheng Huang, Hong-Yih Yeh, "The Development of Sun-Tracking System Using Image Processing." *Sensors* 2013, 13, pp. 5448-5459.
- [34] I. Sefa, M. Demirtas, and I. Colak, "Application of one-axis sun tracking system." *Energy Conversion and Management*, 2009. 50(11), pp. 2709-2718.

- [35] A. Konar, and A. K. Mandal, "Microprocessor based automatic sun tracker." *IEE Proc. Sci., Meas. Technol.*, Vol. 138, No. 4, 1991
- [36] B. Koyuncu, and K. Balasubramanian, "A microprocessor controlled automatic sun tracker." *IEEE Trans. Consumer Electron.* Vol. 37, No. 4, 1991.
- [37] A.K. Saxena, and V.K. Dutta, "A versatile microprocessor based controller for solar tracking." *IEEE. Conf.* Vol. 2, pp.21-25, 1990.
- [38] F.R Rubio, M.G. Ortega, F. Gordillo, and M. Lopez-Martinez, "Application of new control strategy for sun tracking." *Energy. Conversion. And. Management.* Vol. 48, No. 7, July. 2007, pp. 2174-2184.
- [39] Z. Xinhong, W. Zongxian, and Y. Zhengda, "Intelligent solar tracking control system implemented on an FPGA." *Nios II Embedded Processor Design Contest-Outstanding Designs.* 2007.
- [40] M. P. Soares dos Santos and J.A.F. Ferreira, "Novel intelligent real-time position tracking system using FPGA and fuzzy logic." *ISA Transactions: the Journal of Automation.* 53, pp. 402–414. 2014.
- [41] F.M. Al-Naima and B.R. Al-Tae, "An FPGA based stand-alone solar tracking system." *2010 IEEE Inter. Conf. Energy and Exhibition (EnergyCon)*, pp. 513 – 518.
- [42] E. Monmasson, and M.N. Cirstea, "FPGA design methodology for industrial control systems – a review." *IEEE Trans. on Industrial Electronics*, 2007;54(4), pp. 1824-42.
- [43] Chun-Fei Hsu, Pei-Yu Lee and Chih-Hu Wang, "Design of an FPGA-based fuzzy sliding-mode controller for light tracking systems." *International Conference on Machine Learning and Cybernetics (ICMLC)*, 2010, pp. 2782 – 2787.
- [44] S. Cheng, P. Zhao, H. Hongkun, Ji Qianqian and Wei Xu, "An improved design of photo-voltaic solar tracking system based on FPGA." *2010 Inter. Conf. on Artificial Intelligence and Computational Intelligence (AICI)*, 2010, pp. 267- 271.
- [45] W. Aiping, F. Qingqing and L. Yonghua, "Development of multi-axis stepper motion control system based on nios II." *2<sup>nd</sup> Inter. Conf. on Mechanic Automation and Control Engineering (MACE)*, pp. 1230-1232. 2011.
- [46] R. Sharma, G. Singh and M. Kaur, "Development of FPGA-based dual axis solar tracking system." *Am. Trans. on Eng. & Appl. Sci.* Vol 2, No.4, pp. 253-267. 2013.

- Online available at <http://TuEngr.com/ATEAS/V02/253-267.pdf>.
- [47] Qingyi Gu, T. Takaki, and I. Ishii, "Fast FPGA-Based Multiobject Feature Extraction", *IEEE Trans. On. Circuits and Systems for Video Technology*, Vol. 23, No. 1, Jan 2013, pp. 30-45.
- [48] N. A. Ali, S. I. Md Salim, R. Abd Rahim, S. A. Anas, Z. M. Noh, and S. I. Samsudin, "PWM controller design of a hexapod robot using FPGA," *IEEE Inter. Conf. on Control System, Computing and Eng.* 29 Nov-1 Dec. 2013, Penang, Malaysia.
- [49] He-Jin Liu, Ke-Jun Li, Wei-Jen Lee, Hongxia Gao, and Ying Sun, "Development of frequency variable inverter based on SOPC and Nios II.," *IEEE Trans. On Industry Appl.* Vol. 49, No. 5, Sept/Oct, 2013, pp. 2237-2243.
- [50] Chih-Min Lin, Ming-Hung Lin, and Chun-Wen Chen, "SoPC-Based Adaptive PID Control System Design for Magnetic Levitation System", *IEEE Systems Journal*, Vol. 5, No. 2, June 2011 pp. 278-287
- [51] Hsu-Chih Huang, "SoPC-based parallel ACO algorithm and its application to optimal motion controller design for intelligent omnidirectional mobile robots", *IEEE Trans. On. Industrial Informatics*, Vol. 9, No. 4, pp. 1828-1835. Nov 2013.
- [52] Chih-Min Lin, Yu-Lin Liu, and Hsin-Yi Li, "SoPC-Based function-link cerebellar model articulation control system design for magnetic ball levitation systems", *IEEE Trans. On. Industrial. Electronics*, Vol. 61, No. 8, August 2014, pp. 4265-4273.
- [53] H. Sun, Y. Zhang, Z. Wu and J. Xue, "The detecting robot based on SOPC", *Proceedings of IEEE Inter. Conf. on Mechatronics and Automation* August 3 - 6, 2014, Tianjin, China.
- [54] H. Chen, F. Xu and Y. Xi "Field programmable gate array/system on a programmable chip-based implementation of model predictive controller," *IET Control Theory Appl.*, 2012, Vol. 6, Iss. 8, pp. 1055–1063.
- [55] M. Sugeno, "Fuzzy control: Principles, practice and perspectives," *IEEE Inter. Conf. on Fuzzy Systems*, 1992.
- [56] E.H. Mamdani, S. Assilian, "An experiment in linguistic synthesis with a fuzzy logic controller." *Int. J. Man-Machine Studies*. 8, pp. 1-13, 1975.

- [57] H.A. Yousef, "Design and implementation of a fuzzy logic computer-controlled sun tracking system." *Proceeding of the IEEE Inter. Symposium on Industrial Electronics*. Bled, Slovenia, Vol. 3, 1999.
- [58] M. McKenna and B. M. Wilamowski, "Implementing a fuzzy system on a field programmable gate array," *Inter. Joint Conf. on Neural Networks, Proceedings. IJCNN*, Vol.1, 2001.
- [59] Daijin Kim, "An implementation of fuzzy logic controller on the reconfigurable FPGA system," *IEEE Trans. on industrial electronics*. Vol. 47, No. 3, 2000. pp. 703-715.
- [60] S. Poorani, T.V.S. Urmila Priya, K. U. Kumar and S. Renganarayanan, "FPGA based fuzzy logic controller for electric vehicle," *Journal of The Institution of Engineers*, Singapore Vol. 45 Issue 5, 2005.
- [61] Zhou Yan and Zhu Jiaying, "Application of fuzzy logic control approach in a microcontroller-based sun tracking system." *WASE Inter. Conf. on Information Eng. (ICIE)*, 2010, pp. 161-164.
- [62] C-H. Huang, M-R. Lee, B-R. Shih, F-Z. Cai, R. Kang and M-H. Hsieh, "Application of intelligent sun tracking system with fuzzy chip controller," *Inter. Symposium on Computer, Consumer and Control, (IS3C)*, 2014, pp. 43-46.
- [63] N. Al-Rousan, M. Al-Rousan and A. Shareiah, "A fuzzy logic model of a tracking system for solar panels in northern Jordan based on experimental data," *Inter. Conf. on Renewable Energy Research and Appl. (ICRERA)*, 2012. pp. 1-6.
- [64] E. Ataei, R. Afshari, M.A. Pourmina, and M.R. Karimian, "Design and construction of a fuzzy logic dual axis solar tracker based on DSP," *2nd Inter. Conf. on Control, Instr. and Automation (ICCIA)*, 2011. pp. 185-189.
- [65] R-E. Precup and H. Hellendoorn, "A survey on industrial applications of fuzzy control." *Computers in Industry*, 62. 2011. pp. 213-226.
- [66] Gang Feng, "A Survey on analysis and design of model-based fuzzy control systems," *IEEE Trans. On Fuzzy Systems*, Vol. 14, No. 5, October-2006. pp. 676-697.
- [67] Lotfi. A. Zadeh, "Is there a need for fuzzy logic?," *Information sciences, an Inter. Journal*, 178, 2008, pp. 2751-2779.

- [68] S. N. Sivanandam, S. Sumathi and S. N. Deepa, *Book Introduction to fuzzy logic using MATLAB*, Springer-Verlag Berlin Heidelberg, 2007.
- [69] Li-Xin Wang, *A Course in Fuzzy Systems and Control*, Prentice-Hall International, Inc. 1997.
- [70] J. Ross. Timothy, *Fuzzy Logic with Engineering Applications 2<sup>nd</sup> Ed*, John Wiley & Sons, Ltd, 2004.
- [71] C. Grosan and A. Abraham, *Intelligent Systems: A Modern Approach*, Springer-Verlag Berlin Heidelberg, 2011.
- [72] Nazmul Siddique, *Intelligent Control: A Hybrid Approach Based on Fuzzy Logic, Neural Networks and Genetic Algorithms*, Springer International Publishing Switzerland, 2014.
- [73] A. Zilouchian and M. Jamshidi, *Intelligent Control Systems Using Soft Computing Methodologies*, CRC Press LLC, 2001.
- [74] Werner Van Leekwijck, and Etienne E. Kerre, “Defuzzification: criteria and classification”, *Fuzzy Sets and Systems* 108, 1999, pp.159-178
- [75] Oliver Nelles, *Nonlinear system identification: from classical approaches to neural networks and fuzzy models*, Springer-Verlag, 2001.
- [76] R. Woods, J. McAllister, G. Lightbody and Ying Yi, *FPGA-based Implementation of signal processing systems*, John Wiley & Sons, Ltd. 2008.
- [77] N. Mehta, Programmable Logic design, June 2006, Xilinx.
- [78] [www.altera.com/literature/hb/cyc2\\_cii5v1.pdf](http://www.altera.com/literature/hb/cyc2_cii5v1.pdf)
- [79] [www.altera.com/literature/hb/stx5\\_51002.pdf](http://www.altera.com/literature/hb/stx5_51002.pdf)
- [80] [www.altera.com/literature/br/br-soc-fpga.pdf](http://www.altera.com/literature/br/br-soc-fpga.pdf)
- [81] [www.xilinx.com/support/documentation/user\\_guides/ug585-Zynq-7000-TRM.pdf](http://www.xilinx.com/support/documentation/user_guides/ug585-Zynq-7000-TRM.pdf)
- [82] C. MaxField, *FPGAs world class Designs*, 2009, Elsevier. ISBN: 978-1-8561-7-621-7.
- [83] Nios® II Processor Reference Handbook; Altera Corp: San Jose, CA, USA, 2011.
- [84] R. Dubey, *Introduction to Embedded System Design Using Field Programmable Gate Arrays*. Springer-Verlag, 2009.

- 
- [85] [www.altera.com/literature/ug/ug\\_socp\\_builder.pdf](http://www.altera.com/literature/ug/ug_socp_builder.pdf) v.2010
- [86] C. C. Lee., “Fuzzy logic in control systems: fuzzy logic controller –Parts I & II. *IEEE Trans. Syst., Man Cybern.* 20, pp.404-433. 1990.
- [87] N. Sepehri, T. Corbert and P. D. Lawrence, “Fuzzy position control of hydraulic robots with valve deadbands”, *Mechatronics Elsevier Vol. 5*, No. 6, pp623-643, 1995.
- [88] Eva Volna, *Introduction to soft computing*, 1<sup>st</sup> Ed, 2013, eva Volna & bookboon.com.
- [89] I.S. Akkizidis, G.N. Roberts, P. Ridao, and J. Batlle, “Designing a Fuzzy-like PD controller for an underwater robot” *Ctrl Engineering Practice* 11, pp.471–480, 2003.
- [90] A. Benzekri and A. Azrar, “FPGA-Based Design Process of a Fuzzy Logic Controller for a Dual-Axis Sun Tracking System”, *Arab J Sci Eng*, August, 2014, pp. 6109–6123.
- [91] J.G. Tong, I.D.L. Andersan, and M.A.S. Khalid, “Soft-core processors for embedded systems”. *18<sup>th</sup> Int. Conf. on Microelectronics*. pp. 170-173, 2006.
- [92] [http://www.altera.com/literature/ug/ug\\_embedded\\_ip.pdf](http://www.altera.com/literature/ug/ug_embedded_ip.pdf)
- [93] [http://www.altera.com/literature/ug/ug\\_socp\\_builder.pdf](http://www.altera.com/literature/ug/ug_socp_builder.pdf)
- [94] A. Benzeki and L. Refoufi, “Design and implementation of a microprocessor-based interrupt-driven control for an irrigation system”, in *Proceedings of the 1<sup>st</sup> IEEE Inter. Conf. on E-Learning in Industrial Electronics*. Hammamat, Tunisia, Dec-2006.
- [95] A. Benzekri, K. Meghriche and L. Refoufi, “PC-Based automation of a multi-mode control for an irrigation system”, *International Symposium on Industrial Embedded Systems*, 2007, SIES’07, Lisboa, Portugal.
- [96] Pong P. Chu, *Embedded SoPC design with Nios II processor and VHDL examples*, John Wiley & Sons, Inc. 2011.